PONTIFICIA UNIVERSIDAD CATOLICA DEL PERU

ESCUELA DE POSGRADO

Mixed H_2/H_∞ control for infinite dimensional systems

Tesis presentada para optar el grado de:

Magister en

Ingeniería de Control y Automatización

Autor: Matti Noack

Supervisor PUCP: Dr. Antonio Manuel Morán Cárdenas

Supervisor TU-Ilmenau: Prof. Dr.-Ing. Johann Reger

PUCP 2017

Tesis publicada con autorización del autor
No olvide citar esta tesis

Technische Universität Ilmenau

Fakultät für Informatik und Automatisierung

Pontificia Universidad Católica del Perú

Escuela de Posgrado

Master Thesis

Mixed H_2/H_∞ control for infinite dimensional systems

To achieve the degree:

Master of Science (M. Sc.)

---

submitted by:	Matti Noack
date of submission:	03. 05. 2017
date and place of birth:	28. 08. 1989 in Bernau bei Berlin
course of studies:	Technische Kybernetik und Systemtheorie
Supervisor PUCP:	Dr. Antonio Manuel Morán Cárdenas
Supervisor TU-Ilmenau:	Prof. Dr.-Ing. Johann Reger

Tesis publicada con autorización del autor
No olvide citar esta tesis

Special thanks

To everybody reading this! You're awesome ;-)

Tesis publicada con autorización del autor
No olvide citar esta tesis

Abstract

The class of infinite dimensional systems often occurs when dealing with distributed parameter models consisting of partial differential equations. Although forming a comprehensive description, they mainly become manageable by finite dimensional approximations which likely neglect important effects, but underlies a certain structure. In contrast to common techniques for controlling infinite dimensional systems, this work focuses on using robust control methods. Thus, the uncertainty structure that occurs due to the discretization shall be taken into account particularly. Additionally, optimal performance measures can be included into the design process. The mixed H_2/H_∞ control approach handles the inclusion of disturbances and inaccuracies while guaranteeing specified energy or magnitude bounds.

In order to include various of these system requirements, multi-objective robust control techniques based on the linear matrix inequality framework are utilized. This offers great flexibility concerning the formulation of the control task and results in convex optimization problems which can be solved numerically efficient by semi-definite programming.

A flexible robot arm structure serves as the major application example during this work. The model discretization leads to an LTI system of specified order with an uncertainty model which is obtained by considering the concrete approximation impact and frequency domain tests. A structural analysis of the system model relates the neglected dynamics to a robust characterization. For the objective selection, stability shall be ensured under all expected circumstances while the aspects of optimal H_2 performance, passive behavior and optimal measurement output selection are included. The undesirable spillover effect is thoroughly investigated and thus avoided.

Tesis publicada con autorización del autor
No olvide citar esta tesis

Contents

1 Introduction **1**
1.1 Task . . . 2
1.2 Methodology . . . 3
1.3 Document Structure . . . 5

2 Robust Control Basics **7**
2.1 System description . . . 8
2.2 Nominal control & performance . . . 20
2.3 Uncertainty modelling . . . 38
2.4 Robust stability & performance . . . 56

3 Multi-Objective Robust Control **61**
3.1 Introduction to LMI framework . . . 62
3.2 Design specifications with matrix inequalities . . . 64
3.3 Linearizing inertia-preserving transform . . . 72
3.4 Multi-objective controller synthesis . . . 76

4 Flexible Robot Arm **82**
4.1 Modeling & simulation . . . 82
4.2 Control analysis & objectives . . . 107

5 Control Application **114**
5.1 Problem formulation . . . 114
5.2 Simulation setup . . . 122
5.3 Verification . . . 125

6 Conclusion **134**
6.1 Contribution & discussion . . . 134
6.2 Further work . . . 136

Bibliography **137**

Tesis publicada con autorización del autor
No olvide citar esta tesis

List of Figures **142**

List of Tables **144**

Announcement **145**

Tesis publicada con autorización del autor
No olvide citar esta tesis

1 Introduction

In modern control design various influences that have an impact on the actual system are taken into account. Control applications have become increasingly complex due to numerous interconnections and changing plant conditions. Facing these tasks demands a more detailed and specified controller analysis and synthesis.
On the one hand, there is the challenge of uncertain circumstances occurring either from inside the system model or from external sources. Those include measurement noise and physical disturbances as well as reference or excitation signals coming from another user driven system. On the other hand, there are various objectives or tasks that have to be fulfilled at the same time due to high security standards or efficiency requirements. This most frequently results in a multiple-input-multiple-output (MIMO) problem statements, even when considering SISO systems with included signal models and structuring.
Throughout this work, robust control techniques are used for their ability to simultaneously include these considerations into the synthesis process. As one of the most prominent areas in modern systems theory, robust control theory has lead to an extensive theoretical development. This has resulted in a large number of approaches utilizing a wide variety of mathematical tools [DP05]. In addition, there has been notable progress concerning the application of robust design methods to complex problems such as air-craft guidance or process control. That is why its use seems attractive for the challenging type of plant with its respective unsatisfying model description in this work.

In contrast to common linear time-invariant (LTI) systems described by ordinary differential equations (ODE), the class of infinite dimensional systems is mainly described by partial differential equations (PDE) or in functional form [JZ12]. These describe the distributed effects as for example within the field of fluid dynamics, heat transfer, multi-agent networks or flexible structures [Meu13]. The distributed parameter system of a flexible robot arm forms the core application in this work. Several modeling and approximation approaches are discussed and especially the modal discretization is

Tesis publicada con autorización del autor
No olvide citar esta tesis

presented.
The general problem in this case is the resulting infinite dimensional state space as well as the controller realization, which can hardly be implemented. Therefore, mainly two different approaches exist [Rod90]. Either an infinite dimensional control synthesis is performed or the respective optimization problem has to be solved and the result is approximated finite dimensionally, or the whole problem description is approximated by a finite dimensional system first and a conventional implementable controller can be designed with standard techniques. Here, the second approach is dealt with. In particular, the structure of the simplification due to the neglect of high-frequency dynamics shall be included as an uncertainty in terms of the robust control framework. This promotes an analysis of the error and negative effects occurring on account of the approximation.

1.1 Task

The main subject of interest and leading example in this work is the control of flexible robot arm structure with one joint. Especially in the case of long-reach robot arms the effect of flexibility has to be considered. The increasing number of throughput requirements has resulted in the use of lighter motion systems causing the flexible dynamics to become more dominant [Ver09].
This systems can be described in several ways, whether as a distributed parameter system (DPS) or as a lumped parameter system (LPS). The most frequently used form is a linear PDE of fourth order. The resulting infinite dimensional dynamics has to be treated which is mainly done by modal discretization. Due to considering only certain modes and leaving out the most dominant ones, general problems may occur, as the respective dynamics eventually lead to significant vibrations and the potential destabilization of the closed-loop system.
Several works have already been published in connection with robust control. The flexible arm setup used in this work is presented in [METH96]. There a H_∞ control approach without considering structured uncertainties has been developed. A more recent literature study about robust flexible structure control was made by [Ver09]. Especially the impact of the so-called spillover effect is pointed out in detail. It is evident that robust control techniques are an adequate way to achieve a satisfying performance of the controlled robot arm.
Because of the system structure and the planned approximation, a systematic modeling error is expected. This can be included into the robust control synthesis. The closed

Tesis publicada con autorización del autor
No olvide citar esta tesis

loop system shall be stable under these uncertainties and additionally fulfill certain performance goals. Further aspects about optimal approximation order and optimal sensor positioning shall be included as well. Thus, the following control requirements are formulated:

- flexible robot arm description
- system approximation and uncertainty modelling
- assure robust stability (under uncertain conditions)
- guarantee performance objectives (in an energy sense)
- inject damping and avoid spillover effect

In order to achieve these goals, an extensive literature study of robust control theory is required. In particular the combination of several different control objectives has to be realized like for the mixed H_2/H_∞ case introduced in [ZGBD94] and [DZGB94]. This leads to the formulation of convex optimization problems which have to be treated numerically.
In the context of controlling distributed parameter systems like the flexible arm, the current PDE control techniques are investigated. Those are used as a comparison to the techniques used in this work. Accordingly, it is expected to obtain an impression of the connection between these control approaches and to compare the respective results.

1.2 Methodology

Hereinafter some of the common methods to achieve the objectives stated in Section 1.1 shall be presented. Combining the different fields of classic robust control, multi-objective robust control, LMI based optimization via semi-definite programming, modelling and simulation of a distributed system such as the flexible robot arm and conventional control of PDE systems require a large collection of fundamentals and catchy literature. That includes an outline of the most relevant sources used during this work.
The first steps in robust control in the H_2 sense have been made in the 50s with the LQG idea, whereas the H_∞ optimal control theory was introduced in the early 80s by Zames as collected in [ZDG96]. Since then there have been mathematical and numerical problems concerning the standard frequency domain approaches, especially in the

Tesis publicada con autorización del autor
No olvide citar esta tesis

MIMO case. This is why the state-space approach plays the dominant role in robust control since the 70s. The first contributions to the mixed H_2/H_∞ control problem have been made in [ZGBD94] and [DZGB94]. Here the nominal control problem was faced by solving algebraic Riccati equations, well presented for particular problems in [ZD98] or [SPS98]. Additionally the influence of uncertainties and robust performance is considered and finally an analytic solution for the joint problem is obtained.
The foundation of modern system theory is built on the Lyapunov stability theory well presented and explained in [Kha02]. Based on that, simple LMI conditions can already be formulated for guaranteeing stability. An early Riccati inequality approach concerning H_∞ optimal control can be found in [Sch90] where for example the Bounded-Real Lemma was used in LMI form. A collection of further LMI conditions such as the generalized H_2 problem or general quadratic constraints (GQC) was presented by [SGC97]. For linearizing the conditions an inertia preserving transformation of the matrix inequalities is shown. In some terms the resulting controller can be conservative but allows the combination of various specifications.
In [Boy94] an overview of LMI techniques used in control theory was given and the importance and advantages of this framework have been pointed out. Numerically the arising convex optimization problems can be solved linearly with help of semi-definite programs. For these, well-established interior-point methods are utilized. In contrast to that, the recent work of [YYE15] shows the difficulty occurring in mixed H_2/H_∞ control synthesis when no linearizing transformation is applied. There, an exterior-point approach is proposed for solving directly a nonlinear and not convex optimization problem for the simpler state-feedback case. The usefulness of convex optimization in robust control is emphasized in [DP05].

The whole single link flexible robot arm can be modeled as a composition of a distributed parameter system, the flexible structure (hyperbolic type, similar to wave equation), and a lumped parameter system, the actuator system including the controller. Commonly the mechanical model is obtained by applying the Euler-Bernoulli beam principle like in [PRCF05]. This modal decomposition approach is a special and simplified case of the Timochenko beam used in [SC96], but still able to model the system sufficiently well for small stresses and strains. Another modeling idea is built on the use of the finite element method (FEM) [vDL86] with the help of the Lagrange equation. Furthermore FEM can practically be used for simulating the corresponding process adequately.
In [METH96] a robust controller in form of a nominal H_∞ control has been applied

Tesis publicada con autorización del autor
No olvide citar esta tesis

successfully to the robot arm system. A distributed parameter model was used and later discretized modally. Another important issue of the control problem is faced as well, the optimal sensor location. As already stated in [KTLK86] the positioning of the strain gauges is crucial for the detectability of the system. This can be included as an extra optimization scheme.
The literature review [Ver09] illustrates well the robust control problem of more general flexible structures. Especially the challenge of avoiding the spillover effect is pointed out. When the finite approximation is done too roughly some neglected modes may turn out to be dominant and can result in undesirable oscillations or even unstable behavior. Another example of applying robust adaptive control to flexible arm structures was made in [Yos08]. This works follows the idea of designing a finite dimensional control system based on a finite approximation while considering the effect of infinite dimensional modes as external disturbances.
To compare the proposed robust control techniques to conventional methods in the control of distributed systems some basic sources shall be mentioned. The work from [Meu13] builds a comprehensive basis for PDE control techniques. There the general focus lies on flatness based approaches. The class notes from the same author [Meu16] can be considered as an excellent introduction to the field. Another intuitive access to infinite dimensional system theory was made by [JZ12] with the use of the linear Port-Hamiltonian system (PHS) framework, which links to the flexible robot arm example. Additionally PHS take advantage of the physical connection to energetic approaches and can also be characterized as damped or passive systems.
Beside that, infinite dimensional systems can be treated finitely in the structured manner shown in [Rod90]. There a H_∞ model matching problem is introduced and reduced from an infinite dimensional problem to a sequence of finite dimensional ones. This results in the inclusion of the reduced model order into the robust optimization scheme.

1.3 Document Structure

The present work is organized in the following way. First a collection of basic and advanced robust control techniques is given. In the following the system theory of distributed parameter systems is introduced briefly. Based on these impressions the flexible robot arm is considered and the adequate modelling and control design are presented. At the end the control synthesis software is applied to the stated problem and the results are verified simulatively.
For building the basis of applying robust control methods the fundamental concepts

Tesis publicada con autorización del autor
No olvide citar esta tesis

needed for this work are introduced in Chapter 2. There the common notations and system decomposition are presented in Section 2.1. Then nominal specifications in the H_2 and H_∞ sense are reviewed in Section 2.2. This includes basic stability concepts and common Riccati equation approaches. In Section 2.3 it is shown how to include uncertainties into the problem formulation and how they can be structured. With relation to that Section 2.4 introduces the idea of robust performance which considers the system fulfilling certain specifications under those uncertainties. At the end of the chapter common robust control synthesis setups and procedures are presented.
As an extension of robust control the multi-objective problem formulation via LMIs is faced in Chapter 3. After a general introduction to LMIs in Section 3.1 some ways to state different performance measures are presented in Section 3.2. These include internal stability, H_∞ control, generalized H_2 performance, induced passivity and nominal regulation. The resulting optimization problems and inequalities to solve turn out to be nonlinear. Therefore Section 3.3 introduces a linearizing transformation and shows how it is obtained. Based on that Section 3.4 sums up the control synthesis and presents the written software framework (in MATLAB) to solve the problem for a given plant in state-space form. This is explained and verified in Section **??** by illustrating the synthesis and specification process with examples.
The main subject of interest, the flexible robot arm, is analyzed in Chapter 4. First an adequate system model is required which is derived and simulated in Section 4.1. In Section 4.2 the resulting system is characterized in terms of the regulation specifications and with respect to the presented control methods during the former chapters. An optimization approach towards the approximation order determination and the optimal sensor positioning is discussed in Section 4.2.2.
Finally in Chapter 5 the calculation and verification of the controller for the infinite dimensional system of the flexible structure is performed. This starts with stating the control problem properly in Section 5.1. In the following Section 5.2 the application of the control design methods and their simulation is presented. At the end the results are evaluated in Section 5.3.
Chapter 6 closes the work with a conclusion statement on the investigations and considerations made as well as on the obtained results. This is completed by an outlook on possible further steps and improvements.

Tesis publicada con autorización del autor
No olvide citar esta tesis

2 Robust Control Basics

In this chapter the preliminaries and basic techniques of robust control are presented. Feedback control in general is aiming at the regulation of a plant under certain unknown conditions. A system is robust under a well determined class of uncertainties which can be characterized in a dynamical or signal based way. Additionally there can be internal couplings and external influences. In Figure 2.1 a typical system structure and its interconnections are illustrated exemplary. External influences like disturbances can

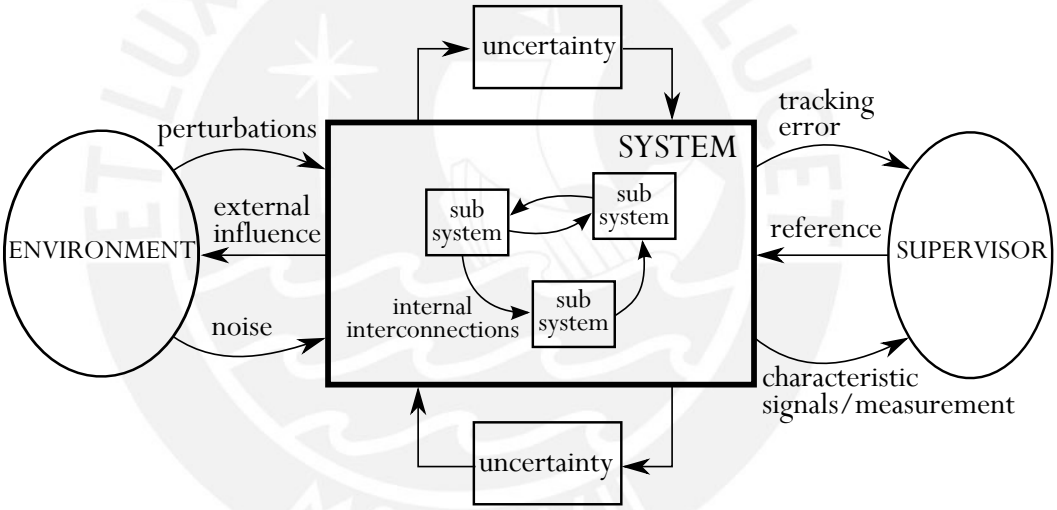

Figure 2.1: General system interconnections [ZD98]

be seen as signals coming from the surrounding environment or the part excluded from the system definition respectively. The coupled uncertainties are considered to be part of system though generating signals from an outside perspective. From an actuator or human point of view the supervisor receives measurement data from the plant and processes, for example, the control calculation, state reconstruction or diagnosis.
There are many different kinds of uncertainties. For this work a specification of the class of not directly known influences is made. The system is considered to be uncertain in the following way [DP05]:

- bad specified or unknown initial conditions,

Tesis publicada con autorización del autor
No olvide citar esta tesis

- the system experiences disturbances from the environment,
- uncertainties occur due to the inaccuracy of system modeling.

The first specification is a common problem faced in all control areas. As it is not possible to model all the physical effects relevant for a process some influences have to be neglected or excluded. These are assumed to be external effects. Internally not all dynamics can be considered, neither can all parameters be determined perfectly. Thus, more or less structured uncertainties dependent on knowledge about the accuracy of the model can be included.
The aim of robust control synthesis is to stabilize the system under the class of considered uncertainties. Additionally certain performance objectives are defined, also with respect to signal transmission and its influence. These objectives shall also be accomplished under the mentioned uncertain conditions.
Therefore, after the introduction of common definitions and nomenclature, nominal control techniques focused on H_2 and H_∞ norm minimization are presented. Then the extraction and modeling of uncertainties is demonstrated and consequences for the controlled system are faced. Finally the overall robust control design is summarized.

2.1 System description

Here the overall subject shall be clarified in form of the common system representation. First the standard linear system formulation for robust control is presented generally and then with an example. Some further aspects like system interconnections and the application to nonlinear systems are discussed.

2.1.1 Linear representation

In this work there is a focus on the state-space based approach. Therefore the considered system is of the following general linear time-invariant (LTI) form:

$$\Sigma_{\text{LTI}} \begin{cases} \dot{x}(t) = Ax(t) + Bu(t)\,,\, x(0) = x_0 \\ y(t) = Cx(t) + Du(t) \end{cases} \tag{2.1}$$

where $A \in \mathbb{R}^{n\times n}$, $B \in \mathbb{R}^{n\times n_u}$, $C \in \mathbb{R}^{n_y\times n}$ and $D \in \mathbb{R}^{n_y\times n_u}$. Correspondingly the signals state x, output y and input u are of respective dimension and are functions of the time $t \in [0, \infty)$. The time dependency is dropped in the following because of convenience.

Tesis publicada con autorización del autor
No olvide citar esta tesis

According to the solution of the ordinary differential equation (ODE) of system Σ_{LTI} the output can be calculated with respect to the input as follows:

$$y(t) = Ce^{At}x_0 + \int_0^t Ce^{A(t-\tau)}Bu(\tau)d\tau + Du(t)\,. \tag{2.2}$$

The transfer behaviour can also be characterized in the Laplace domain by the transfer function G:

$$G(s) = \frac{y(s)}{u(s)} = C(sI - A)^{-1}B + D$$

with homogeneous initial conditions and $y(s)$ and $u(s)$ representing the respective Laplace-transformed signals A common notation used in MIMO and robust control for the transfer function is the following:

$$G(s) = \left[\begin{array}{c|c} A & B \\ \hline C & D \end{array}\right] .$$

Here the matrices A, B, C, D are also called realization of G. For a given G these may not be unique but play an important role for the implementation. Some techniques for obtaining such a realization are presented in Appendix **??**. A realization is called *minimal* if A has minimal dimension. It may be shown that this is the case iff the pair (A, B) is controllable and the pair (A, C) is observable [ZD98]. Minimal realizations obtain the minimal number of possible states n.
In addition to the initial system Σ_{LTI} from Equation (2.1) some extra external input $w(t) \in \mathbb{R}^{n_w}$ and output signal $z(t) \in \mathbb{R}^{n_z}$ are considered. In the following y refers directly to the available measurements and u to the control action. The resulting system has the form:

$$\Sigma_{\text{nom}} \begin{cases} \dot{x} = Ax + B_w w + B_u u\,,\; x(0) = x_0 \\ z = C_z x + D_{zw} w + D_{zu} u \\ y = C_y x + D_{yw} w + D_{yu} u \end{cases} . \tag{2.3}$$

In view of neglecting uncertainties into account the system is called nominal and will be the subject in Section 2.2. With the respective transfer matrix $P(s)$ and the controller $K(s)$ to be designed the following block diagram in Figure 2.2 illustrates the signal partition. In principle the controller K only takes the measurement information y and generates the control signal u dependent on that. Thus in general an output feedback controller is considered (in comparison to state feedback control).

Tesis publicada con autorización del autor
No olvide citar esta tesis

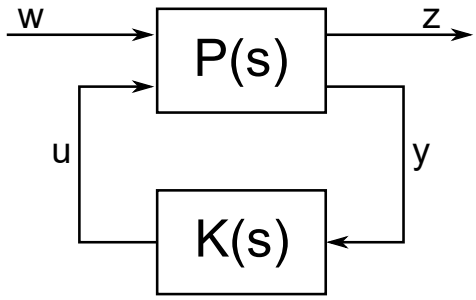

Figure 2.2: Basic system structure with plant and controller

The transfer behaviour can also be written as follows:

$$\begin{pmatrix} z \\ y \end{pmatrix} = P(s) \begin{pmatrix} w \\ u \end{pmatrix}$$

with the transfer function realization

$$P(s) =: \begin{pmatrix} P_{11}(s) & P_{12}(s) \\ P_{21}(s) & P_{22}(s) \end{pmatrix} = \left[\begin{array}{c|cc} A & B_w & B_u \\ \hline C_z & D_{zw} & D_{zu} \\ C_y & D_{yw} & D_{yu} \end{array}\right] . \tag{2.4}$$

Often the control objective is to achieve a certain transfer performance from w to z. So the closed loop transfer behaviour $T_{zw}(s) \in \mathbb{C}^{n_z \times n_w}$ is of interest. It can be stated utilizing the *lower fractional transformation* $\mathcal{F}_l$ (LFT) in the following way:

$$T_{zw}(s) = \mathcal{F}_l(P, K) := P_{11}(s) + P_{12}(s)K(s)\left[I - P_{22}(s)K(s)\right]^{-1} P_{21}(s) .$$

Generally the controller $K(s)$ is also a dynamic system and has its own state space realization. This is important for the optimization process and the implementation itself. The measurement signal y forms the control system input and the generated output is the control action u. In the time domain the following ODE is obtained:

$$\Sigma_K \begin{cases} \dot{x}_K = A_K\, x_K + B_K\, y\,,\, x_K(0) = x_{K,0} \\ u \quad = C_K\, x_K + D_K\, y \end{cases}$$

with the respective realization

$$K(s) = \left[\begin{array}{c|c} A_K & B_K \\ \hline C_K & D_K \end{array}\right] \tag{2.5}$$

Tesis publicada con autorización del autor
No olvide citar esta tesis

where matrices $A_K \in \mathbb{R}^{n_K \times n_K}$, $B \in \mathbb{R}^{n_K \times n_y}$, $C \in \mathbb{R}^{n_u \times n_K}$ and $D \in \mathbb{R}^{n_u \times n_y}$ depend on the control order n_K. Often $n_K = n$ is prescribed for simplicity. But for additional degrees of freedom it is also possible to choose $n_K > n$.

For robust control considerations the dynamic uncertainty structure $\Delta(s)$ is added to the problem formulation. It is introduced in Section 2.3 and its consequences for control are presented in Section 2.4. To distinguish between control, performance and uncertainty channels, as for example realized in [Sch00], consider the following extension of system Σ_{nom} from Equation (2.3):

$$\Sigma_{\text{rob}} \begin{cases} \dot{x} &= Ax + B_\Delta w_\Delta + B_w w + B_u u\,,\; x(0) = x_0 \\ z_\Delta &= C_\Delta x + D_\Delta w_\Delta + D_{\Delta w} w + D_{\Delta u} u \\ z &= C_z x + D_{z\Delta} w_\Delta + D_{zw} w + D_{zu} u \\ y &= C_y x + D_{y\Delta} w_\Delta + D_{yw} w + D_{yu} u \end{cases} \tag{2.6}$$

with uncertainty dimension n_Δ and the equivalent representation:

$$P(s) = \left[\begin{array}{c|ccc} A & B_\Delta & B_w & B_u \\ \hline C_\Delta & D_\Delta & D_{\Delta w} & D_{\Delta u} \\ C_z & D_{z\Delta} & D_{zw} & D_{zu} \\ C_y & D_{y\Delta} & D_{yw} & D_{yu} \end{array}\right].$$

The general system structure with the respective signals is presented in Figure 2.3 (a). It is also possible to maker further signal distinctions. For the purpose of mixed $\mathrm{H}_2/\mathrm{H}_\infty$ control the external input becomes $w = (w_2, w_\infty)^\top$ and the objective output is subdivided into $z = (z_2, z_\infty)^\top$. This is illustrated in Figure 2.3 (b). For this case let $N(s) := \mathcal{F}_l(P, K)$ be the closed control-loop transfer function from $(w_\Delta, w)^\top$ to $(z_\Delta, z)^\top$. The aim is later to guarantee internal stability and performance measures for the whole system while considering a class of the uncertainties Δ. To analyze the overall transfer behaviour the upper fractional transformation $\mathcal{F}_u$ (UFT), similarly to the LFT:

$$T_{zw}^{\Delta}(s) = \mathcal{F}_u(N, \Delta) := N_{22}(s) + N_{21}(s)\Delta(s)\left[I - N_{11}(s)\Delta(s)\right]^{-1} N_{12}(s)\,.$$

Evidently the term $N_{11}\Delta$ plays the decisive role for the system stability and is a major subject in Section 2.4.

Tesis publicada con autorización del autor
No olvide citar esta tesis

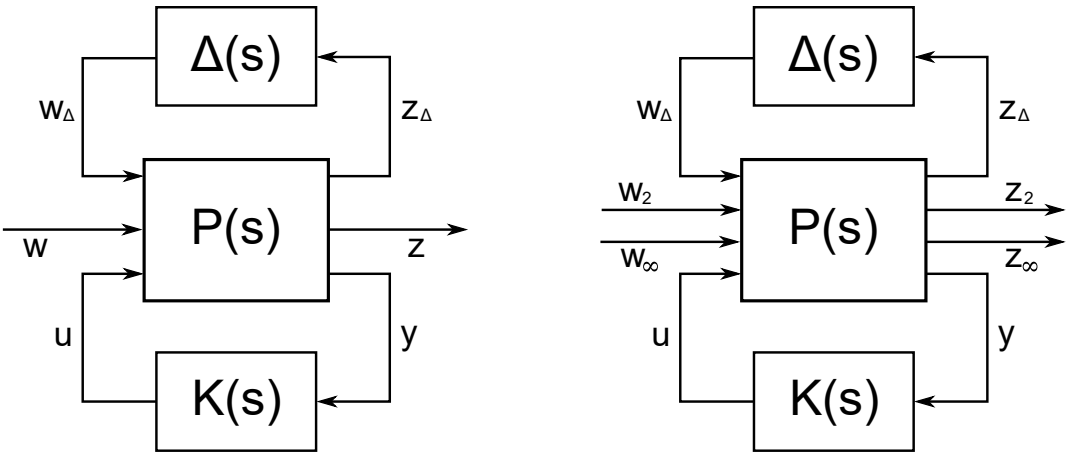

(a) General structure (b) Mixed H_2/H_∞ channel distinction

Figure 2.3: System structures with uncertainty

2.1.2 Formulation example

To demonstrate the problem formulation of a given system in the introduced framework a *mixed-sensitivity* example with additive uncertainty is presented. First the classical SISO (single-input-single-output) control loop composition from Figure 2.4 is considered. The system contains a closed loop with the controller $C(s)$ and the actual

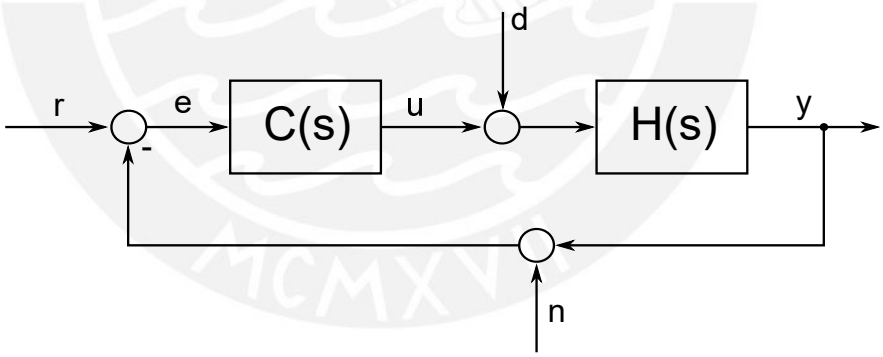

Figure 2.4: Standard feedback control loop

plant $H(s)$. It is driven by an external reference signal r and there is additionally a disturbance on the actuator side d and measurement noise n.
Assume that a plant description $G(s)$ has been obtained by modeling. As all models it contains approximation errors which eventually can be observed by comparing the experimental frequency response $H(j\omega)$ with $G(j\omega)$. The deviation is characterized by the uncertainty structure $\Delta(s) := H(s) - G(s)$. This case taken from [Sch01] is presented more detailed in Section 2.3.

Tesis publicada con autorización del autor
No olvide citar esta tesis

Now the new objective output signal z is defined. After stabilizing the system the main goal is to achieve tracking $r - y =: e \to 0$. Thus e is important to be considered as an objective. Furthermore the control effort u plays an important role for performance and realizability of the control law and is taken into account as well. In Figure 2.5 the system composition of the resulting mixed-sensitivity problem is illustrated. Note that

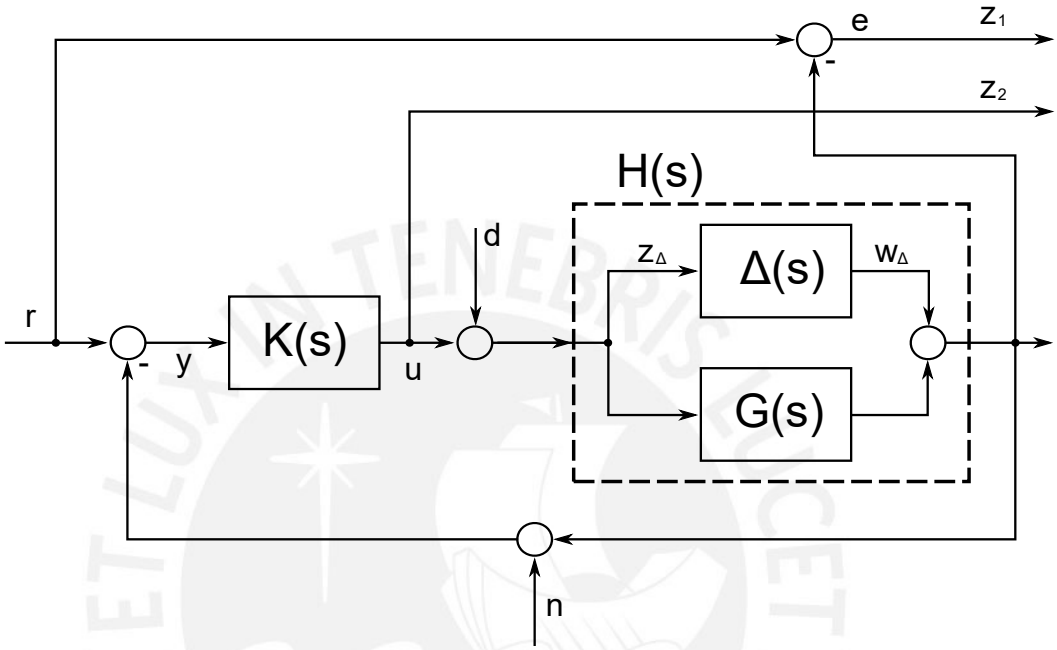

Figure 2.5: Mixed-sensitivity control loop and signal definition

some terms have been redefined to put the system into the form Σ_{rob} from Equation (2.6). Here the controller $K(s)$ converts the measurement y, the error between reference and noisy system output, into the control action u. A general distinction between the following signal classes is made [Sch01]:

- signals effecting the system from outside and cannot be influenced (r, d, n),
- signals characterizing the design objectives (e),
- actuator/control signal (u),
- available measurement (y).

Thus possible signal definitions are:

$$w = \begin{pmatrix} r \\ d \\ n \end{pmatrix}, \; z = \begin{pmatrix} e \\ u \end{pmatrix} .$$

Tesis publicada con autorización del autor
No olvide citar esta tesis

Without including the uncertainty for the moment the overall transfer behavior $P(s)$ from $(w,u)^\top$ to $(z,y)^\top$ like in (2.4) can be stated as:

$$\begin{pmatrix} e \\ u \\ y \end{pmatrix} = \underbrace{\begin{pmatrix} 1 & -G(s) & 0 & -G(s) \\ 0 & 0 & 0 & 1 \\ 1 & -G(s) & -1 & -G(s) \end{pmatrix}}_{=P(s)} \begin{pmatrix} r \\ d \\ n \\ u \end{pmatrix}$$

In practice there are often filters added to the considered signals w and z to weight the performance in a certain frequency range in order to include some signal knowledge within the design. This procedure extends the transfer function $P(s)$ and is explained in Section **??**.

The closed loop transfer function can easily be obtained by using the relation $u = K(s)y$. From the block diagram in Figure 2.5 the auxiliary output $\tilde{y}$ of $G(s)$ is obtained:

$$\tilde{y} = \frac{GK}{1+GK}\, r + \frac{G}{1+GK}\, d - \frac{GK}{1+GK}\, n$$

and due to that:

$$\begin{aligned} e &= \left(1 - \tfrac{GK}{1+GK}\right) r - \tfrac{G}{1+GK}\, d + \tfrac{GK}{1+GK}\, n\,, \\ u &= \tfrac{1}{1+GK}\left(Kr - GKd - Kn\right). \end{aligned}$$

Thus with inputs $w = (r,d,n)^\top$ the objective output $z = (e,u)^\top$ results in:

$$z(s) = \underbrace{\begin{pmatrix} (1+GK)^{-1} & -G(1+GK)^{-1} & GK(1+GK)^{-1} \\ K(1+GK)^{-1} & -GK(1+GK)^{-1} & -K(1+GK)^{-1} \end{pmatrix}}_{=T_{zw}(s)} w(s)\,.$$

With defining the following occurred sensitivities:

- sensitivity: $S = (I+GK)^{-1}$
- complementary sensitivity: $T = GK(I+GK)^{-1}$
- load disturbance sensitivity: $S_d = G(I+GK)^{-1}$
- noise sensitivity: $S_n = K(I+GK)^{-1}$

the closed loop transfer function becomes:

$$T_{zw}(s) = \begin{pmatrix} S(s) & -S_d(s) & T(s) \\ S_n(s) & -T(s) & -S_n(s) \end{pmatrix}.$$

Tesis publicada con autorización del autor
No olvide citar esta tesis

In other cases, like considering output perturbations, more sensitivity functions arise. The relations $e = S(s)r$ and $\tilde{y} = T(s)r$ are pointed out. They play an important role for the internal stability and well-posedness of the closed loop and give inside on particular transfer behaviors.

2.1.3 Interconnecting systems

For the later purpose of considering the connection of plant and controller or extending the system with filters it is necessary to discuss some special interconnection cases like done in [ZD98]. These are characterizing the relation between state space and Laplace domain considerations.
Consider the two transfer functions $G_1(s)$ and $G_2(s)$. Their state space realizations shall be

$$G_1(s) = \left[\begin{array}{c|c} A_1 & B_1 \\ \hline C_1 & D_1 \end{array}\right], G_2(s) = \left[\begin{array}{c|c} A_2 & B_2 \\ \hline C_2 & D_2 \end{array}\right],$$

that is:

$$\Sigma_1 \begin{cases} \dot{x}_1 = A_1 x_1 + B_1 u_1 \\ y_1 = C_1 x_1 + D_1 u_1 \end{cases}, \Sigma_2 \begin{cases} \dot{x}_2 = A_2 x_2 + B_2 u_2 \\ y_2 = C_2 x_2 + D_2 u_2 \end{cases}. \tag{2.7}$$

The state-space representation turns out to be helpful when dealing with cascades of systems. In Figure 2.6 the series interconnection $G_1 G_2$ is shown. Because of the

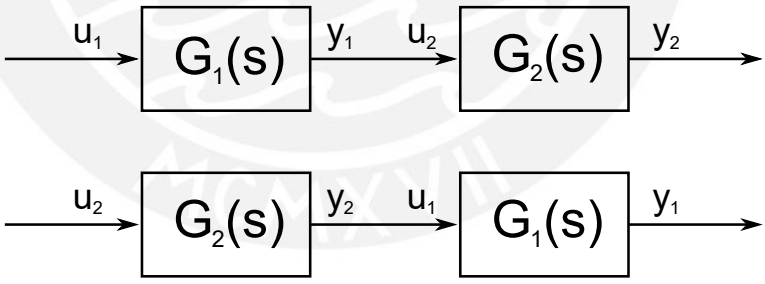

Figure 2.6: Equivalent series interconnection of two systems

concatenation of two scalar linear systems this is equivalent to $G_2 G_1$. For obtaining the state space form of the cascaded system the output of G_1 has to be treated as the input of G_2, thus $y_1 = u_2$ or respectively $y_2 = u_1$. The following result can then be

Tesis publicada con autorización del autor
No olvide citar esta tesis

obtained easily like derived in [ZDG96]:

$$G_1G_2 = G_2G_1 = \left[\begin{array}{c|c} A_2 & B_2 \\ \hline C_2 & D_2 \end{array}\right] \cdot \left[\begin{array}{c|c} A_1 & B_1 \\ \hline C_1 & D_1 \end{array}\right] = \left[\begin{array}{c|c} A_1 & B_1 \\ \hline C_1 & D_1 \end{array}\right] \cdot \left[\begin{array}{c|c} A_2 & B_2 \\ \hline C_2 & D_2 \end{array}\right]$$

$$= \left[\begin{array}{cc|c} A_1 & 0 & B_1 \\ B_2C_1 & A_2 & B_2D_1 \\ \hline D_2C_1 & C_2 & D_2D_1 \end{array}\right] = \left[\begin{array}{cc|c} A_1 & B_1C_2 & B_1D_2 \\ 0 & A_2 & B_2 \\ \hline C_1 & D_1C_2 & D_1D_2 \end{array}\right]$$

The derivation is made by considering the extended system state $\tilde{x} := (x_1, x_2)^\top$. It shows again that the realization itself is not necessarily unique. Both realizations lead to the same combined transfer function and can also be reordered and rewritten in many ways.

Another important interconnection is the parallel structure illustrated in Figure 2.7. Here a much simpler combined realization can be found due to the absence of direct

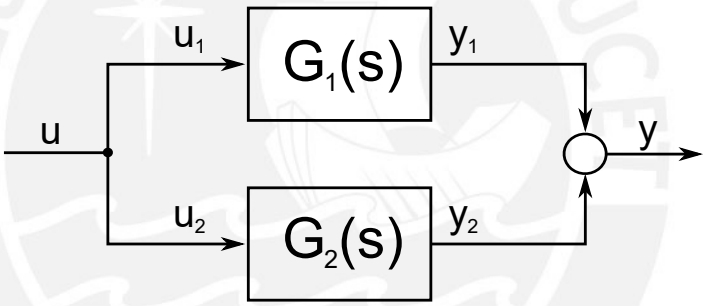

Figure 2.7: Parallel interconnection of two systems

system coupling. The addition of two dynamic systems results in:

$$G_1 + G_2 = \left[\begin{array}{c|c} A_1 & B_1 \\ \hline C_1 & D_1 \end{array}\right] + \left[\begin{array}{c|c} A_2 & B_2 \\ \hline C_2 & D_2 \end{array}\right] = \left[\begin{array}{cc|c} A_1 & 0 & B_1 \\ 0 & A_2 & B_2 \\ \hline C_1 & C_2 & D_1 + D_2 \end{array}\right].$$

After performing some basic connection operations the closed loop interconnection show in Figure 2.2 shall be calculated. Therefore the realizations for $P(s)$ from Equation (2.4) and for $K(s)$ from Equation (2.5) are utilized. For simplicity and practicability the feedthrough $D_{yu} = 0$ is neglected. The resulting closed loop transfer function

Tesis publicada con autorización del autor
No olvide citar esta tesis

then has the form:

$$T_{zw}(s) = \left[\begin{array}{cc|c} A + B_u D_K C_y & B_u C_K & B_w + B_u D_K D_{yw} \\ B_K C_y & A_K & B_K D_{yw} \\ \hline C_z + D_{zu} D_K C_y & D_{zu} C_K & D_{zw} + D_{zu} D_K D_{yw} \end{array}\right]. \tag{2.8}$$

These considerations could also be done for putting certain transfer function in series to just a particular channel, like in the case of input or output filters, but are left out here and applied when needed.

Some other practical relations for MIMO systems can be found by focussing on basic matrix operations. First the *dual system* is defined by the transposed of the transfer matrix $G(s)$.

$$G(s)^\top = \left[\begin{array}{c|c} A & B \\ \hline C & D \end{array}\right]^\top = \left[\begin{array}{c|c} A^\top & C^\top \\ \hline B^\top & D^\top \end{array}\right].$$

The dual system switches the corresponding control and observation problems, which for example can be applied to obtain the dual to the bounded-real lemma, stated in Theorem 2.9 , for solving the Riccati equation in the observer case.
Another important operation is the inversion of a transfer function. Consequently the realization of G changes in the following way:

$$G(s)^{-1} = \left[\begin{array}{c|c} A & B \\ \hline C & D \end{array}\right]^{-1} = \left[\begin{array}{c|c} A - BD^{-1}C & BD^{-1} \\ \hline -D^{-1}C & D^{-1} \end{array}\right].$$

Obviously the feedthrough D has to be a square matrix and non-singular. Inverting the systems means a switch between input and output. The realization can easily be obtained by considering the state space equations and solving the output relation with respect to u.

2.1.4 Nonlinear equation decomposition

After introducing the general formulation framework in terms of LTI systems and getting familiar with the notation one of the main motivations concerning the treatment of more complex systems shall be outlined here. The idea behind the robust control approach is to divide a more complicated problem into a composition of simple problems and perturbations as mentioned in [DP05].

Tesis publicada con autorización del autor
No olvide citar esta tesis

To show the generality of the concept a nonlinear system of the form

$$\Sigma_{\text{NL}} \begin{cases} \dot{x} = f(x,u)\,,\, x(0) = x_0 \\ y = h(x,u) \end{cases} \tag{2.9}$$

with dynamic map $f : \mathbb{R}^n \times \mathbb{R}^{n_u} \to \mathbb{R}^n$ and output map $h : \mathbb{R}^n \times \mathbb{R}^{n_u} \to \mathbb{R}^{n_y}$ sufficiently smooth is considered. Now a decomposition of the system into a linear dynamical and a static nonlinearity part is performed. Therefore the Jacobian linearization around the equilibrium point $(\tilde{x}, \tilde{u}) = (0,0)$ $(f(0,0) = 0)$ is applied and leads to the decomposed following system equivalent to (2.9):

$$\Sigma_{\text{dec}} \begin{cases} \dot{x} = Ax + Bu + \tilde{f}(x,u)\,,\, x(0) = x_0 \\ y = Cx + Du + \tilde{h}(x,u) \end{cases} \tag{2.10}$$

where A, B, C, D represent the linear approximations

$$\begin{aligned} A &= \tfrac{\partial f}{\partial x}\big|_{[0,0]}\,, \quad B = \tfrac{\partial f}{\partial u}\big|_{[0,0]}\,, \\ C &= \tfrac{\partial h}{\partial x}\big|_{[0,0]}\,, \quad D = \tfrac{\partial h}{\partial u}\big|_{[0,0]}\,. \end{aligned}$$

Then the separated nonlinearities have the form:

$$\begin{aligned} \tilde{f}(x,u) &= f(x,u) - Ax - Bu\,, \\ \tilde{h}(x,u) &= h(x,u) - Cx - Du\,. \end{aligned}$$

Clearly Σ_{NL} and Σ_{dec} have equivalent solutions. The system can be further split up into

$$\Sigma_{\text{sNL}} \begin{cases} \dot{x} = Ax + Bu + w_1\,,\, x(0) = x_0 \\ y = Cx + Du + w_2 \end{cases} \tag{2.11}$$

where external signals $w_1 = \tilde{f}(x,u)$ and $w_2 = \tilde{h}(x,u)$ are extracted. Thus system Σ_{sNL} forms the linear mapping:

$$P : (w_1, w_2, u) \mapsto (x, u, y)\,.$$

From the signal substitution the static nonlinear map

$$Q : (x,u) \mapsto (w_1, w_2)$$

Tesis publicada con autorización del autor
No olvide citar esta tesis

is obtained. So resulting structure shown in Figure 2.8 is similar to the the system formulations presented in Figure 2.3 and fits with the former problem perspective. The

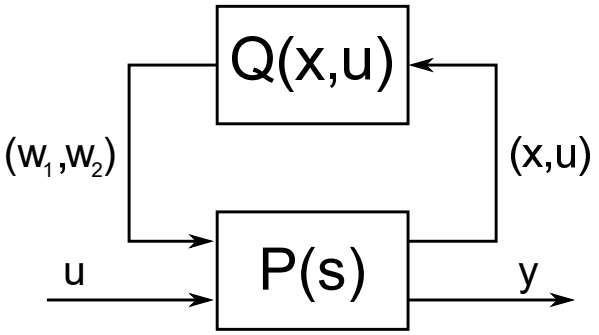

Figure 2.8: Nonlinear system decomposition [DP05]

objective of the consequent uncertainty modelling then is to replace the map Q by a description which is easier to handle. This is part of Section 2.3.
After presenting how to separate the nonlinear part of a system by a static relation the much more difficult task to separate some of the system dynamics shall be introduced. Therefore consider the system partition

$$\Sigma_{\text{part}} \begin{cases} \dot{x}_1 = f_1(x_1, x_2, u)\,,\ x(0) = x_0 \\ \dot{x}_2 = f_2(x_1, x_2, u) \\ y = h(x, u) \end{cases} \tag{2.12}$$

with the decomposed state $x = (x_1, x_2)^\top$. The aim is to neglect the dynamics $\dot{x}_2$. Therefore, similar to decomposition from Equation (2.11), the system is partitioned in the following way. By applying the Jacobian linearization with respect to the first states x_1 the system

$$\Sigma_{\text{dNL}} \begin{cases} \dot{x}_1 = A_1 x_1 + B_1 u + w_1\,,\ x_1(0) = x_{1,0} \\ y \ = C_1 x + D_1 u + w_2 \end{cases} \tag{2.13}$$

is obtained. Then one gets the nonlinear composed system part in the following form:

$$\tilde{\Sigma}_{\text{dNL}} \begin{cases} \dot{x}_2 \qquad = f_2(x_1, x_2, u)\,,\ x_2(0) = x_{2,0} \\ (w_1, w_2) = \left(\tilde{f}_1(x_1, x_2, u), \tilde{h}(x_1, x_2, u)\right) \end{cases} . \tag{2.14}$$

Tesis publicada con autorización del autor
No olvide citar esta tesis

As before the whole system Σ_{part} has been split apart into a linear system $P : (w_1, w_2, u) \mapsto (x_1, u, y)$ formed by Σ_{dNL} and a dynamic nonlinearity $Q : (x_1, u) \mapsto (w_1, w_2)$ based on $\tilde{\Sigma}_{\text{dNL}}$. Thus Q isolates part of the dynamics and the whole system nonlinearity.
The decomposition just seen in both cases often is made up by a low dimensional linear part and a potentially nonlinear part of high dimension [DP05]. It is one of the main ideas of robust control to put the part which is the hardest to model or to describe into another structure outside of the considered system. Then the approach is to capture the behaviour of the Q-part by the set of mappings Δ introduced in Section 2.3. This set can be much larger then the actual uncertainty but is easier to handle.

2.2 Nominal control & performance

Before treating uncertain systems a control scheme for the conventionally modeled plant without any uncertainties, the so-called nominal plant, has to be found. First, a general overview on stability and stabilizing controllers is given. Then performance measures shall be introduced which lead to define the objectives of robust control in a H_2 and H_∞ sense.

2.2.1 Nominal stability & stabilizing controllers

There are many different approaches towards the stability of dynamical systems. Especially of interest is the stable internal behavior of a system composition related to its state space form and stability with respect to the input-output connection. Usually this refers to an equilibrium point. Since the systems considered here are purely linear, this fact is not mentioned frequently.
Here a focus is kept on the stability theory in the sense of Lyapunov. It is extensively presented in [Kha02] and shall not be reintroduced. The common Lyapunov function method is one of the main tools used in this work.
First the general autonomous nonlinear system

$$\Sigma_{\text{aNL}} : \dot{x} = f(x)\,,\ x(0) = x_0 \tag{2.15}$$

shall be considered. In the following the map $f : \mathbb{R}^n \to \mathbb{R}^n$ is assumed to be Lipschitz continuous. Also let $x = 0$ be an equilibrium point of Σ_{aNL}. As a central stability theorem the following one is well-known:

Tesis publicada con autorización del autor
No olvide citar esta tesis

Theorem 2.1 *Lyapunov function & (asymptotic) stability [Kha02]*
Let $D \subset \mathbb{R}^n$ be a domain containing the equilibrium point $x = 0$. The scalar valued function $V : D \to \mathbb{R}$ shall be continuously differentiable such that

$$\begin{aligned} V(0) &= 0\,, \\ V(x) &> 0 \;\forall x \in D \setminus \{0\}\,. \end{aligned} \tag{2.16}$$

Then V is called Lyapunov candidate. If the following holds:

$$\dot{V}(x) = \frac{\partial V(x)}{\partial x} f(x) \leq 0 \;\forall x \in D\,, \tag{2.17}$$

the point $x = 0$ is stable and V is called Lyapunov function. Moreover, if

$$\dot{V}(x) = \frac{\partial V(x)}{\partial x} f(x) < 0 \;\forall x \in D \setminus \{0\}\,, \tag{2.18}$$

then $x = 0$ is an asymptotically stable equilibrium point of Σ_{aNL} and V is called strict Lyapunov function.

From this general stability concept for nonlinear systems a lot of useful implicit results can be found. Here a focus on LTI system Σ_{LTI} from (2.1) is made. In the following the system is considered to be autonomous, thus $u \equiv 0$.
Therefore the following Lyapunov candidate approach is made [Kha02]:

$$V(x) = x^\top X x\,,\; X = X^\top \in \mathbb{R}^{n \times n}\,.$$

Clearly the matrix X has to be positive definite, written $X > 0$, to fulfil the first condition (2.16) from Theorem 2.1. From that the following idea leads to condition (2.18):

$$\dot{V}(x) = \dot{x}^\top X x + x^\top X \dot{x} = x^\top \underbrace{\left(A^\top X + X A\right)}_{=:-Q} x \overset{!}{<} 0$$

This results in the so called *Lyapunov equation*

$$A^\top X + X A + Q = 0 \tag{2.19}$$

where $Q = Q^\top > 0$ is some given real matrix of dimension $n \times n$. The solution of this equation can easily be obtained by calculating [DP05]:

$$X = \int_0^\infty e^{A^\top \tau} Q e^{A\tau} d\tau\,.$$

Tesis publicada con autorización del autor
No olvide citar esta tesis

So for LTI systems the task of finding a Lyapunov function for proofing stability is reduced to calculate a square matrix X from an algebraic equation. This is summarized by the following theorem statement.

Theorem 2.2 *Lyapunov equation & inequality [DP05]*
For autonomous LTI system part of Σ_{LTI} the following two stability statements hold:

(i) Let $Q = Q^\top > 0$. Then A is Hurwitz if and only if there exists a solution $X = X^\top > 0$ to the Lyapunov equation (2.19).

(ii) The matrix A is Hurwitz if and only if there exists $X > 0$ satisfying

$$A^\top X + XA < 0\,. \tag{2.20}$$

The statement *(ii)* can directly be derived from *(i)* and forms the first and one of the most important LMIs in this work as it guarantees the stability of the closed loop system. Actually the correspondence of LMI techniques to the state space realization makes these time domain stability considerations so important.

On the other hand the switch between the time and frequency domain perspective is characteristic for the robust control framework. That is why the connection between these domains in terms of stability shall be made and some basic frequency domain tools are revisited.
Now the system Σ_{LTI} is not considered to be autonomous for the characterization of input-output behavior in the following. Therefore the nominal system Σ_{nom} with in- and outputs from (2.3) shown in Figure 2.2 is of interest. From the interconnection studies resulting in the closed loop transfer function realization presented in (2.8) it becomes obvious that the matrix

$$A_{\text{CL}} := \begin{pmatrix} A + B_u D_K C_y & B_u C_K \\ B_K C_y & A_K \end{pmatrix}$$

describes the entire dynamics of the closed control loop system. In fact it can be stated that the controller $K(s)$ stabilizes the internal system dynamics asymptotically if $\text{eig}(A_{\text{CL}}) \subset \mathbb{C}^-$ or if a $X > 0$ can be found fulfilling Theorem 2.2. This connects the state space theory with the transfer function realization of the system.
After using the state space description, now the input-output description in form of transfer functions is considered. First some new terms have to be introduced referring to aspects like the physical realizability of $K(s)$.

Tesis publicada con autorización del autor
No olvide citar esta tesis

Definition 2.3 *Proper transfer matrix & well-posedness [ZD98]*

(i) Let $G(s)$ be a transfer matrix. If $G(s)$ is a rational polynomial matrix and can be decomposed as

$$G(s) = G(\infty) + \tilde{G}(s)$$

where, with defining $d(s) = s^r + a_1 s^{r-1} + \ldots + a_{r-1}s + a_r$ as the least common denominator polynomial of the entries of $G(s)$:

$$\tilde{G}(s) = \frac{1}{d(s)} N(s) = \frac{1}{d(s)} \left(N_1 s^{r-1} + \ldots + N_{r-1}s + N_r \right),$$

it is proper and strictly proper in case $G(\infty) = 0$. A proper transfer function is also referred to as realizable. Usually it occurs that $r = n_y$.

(ii) A feedback interconnection like shown in Figure 2.4 is said to be well-posed if the closed loop transfer matrices of all sensitivity functions are well-defined and proper.

With these characterizations now the closed loop interconnection Σ_{nom} is considered again. As a recapitulation the closed loop transfer function is calculated by the LFT:

$$z(s) = \left(P_{11}(s) + P_{12}(s)K(s) \left[I - P_{22}(s)K(s) \right]^{-1} P_{21}(s) \right) w(s) .$$

Obviously the existence of a proper inverse of $I - P_{22}(s)K(s)$ is substantial for obtaining a stable system. Therefore the stability is investigated by looking at Figure 2.9, which is an augmented version of the system in Figure 2.2 containing all the relevant transfer functions that have to be tested. The reason for this extended consideration is that an obtained stable transfer matrix T_{zw} is not necessarily implying a stabilizable or detectable closed control loop realization [Sch01]. It turns out that with the auxiliary signals v, v_1, v_2 the following can be stated:

$$\begin{aligned} \begin{pmatrix} z \\ y \end{pmatrix} &= P \begin{pmatrix} w \\ u \end{pmatrix}, u = Kv + v_1, v = y + v_2 \\ \Leftrightarrow \begin{pmatrix} z \\ v_1 \\ v_2 \end{pmatrix} &= \begin{pmatrix} P_{11} & P_{12} & 0 \\ 0 & I & -K \\ -P_{21} & -P_{22} & I \end{pmatrix} \begin{pmatrix} w \\ u \\ v \end{pmatrix} . \end{aligned} \tag{2.21}$$

Tesis publicada con autorización del autor
No olvide citar esta tesis

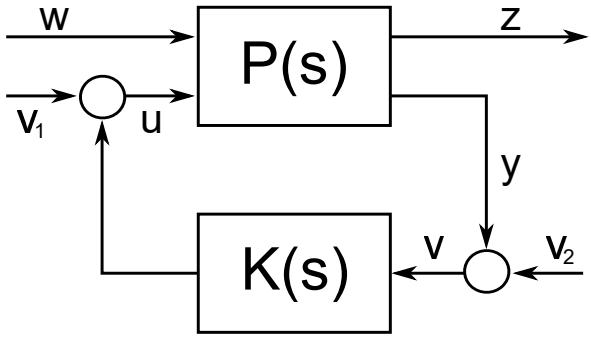

Figure 2.9: Control loop for stability considerations [Sch01]

The system results to be well-posed in case $I - P_{22}(\infty)K(\infty)$ is non singular. This result is derived from the lower right block matrix which relates the internal and augmented signals, $(u, v)^\top \to (v_1, v_2)^\top$. In particular the condition means that $I - D_{yu}D_K$ has to be invertible. Most practical systems without any in beforehand installed proportional control action, as the one considered in this work, do not contain a control feedthrough, $D_{yu} = 0$. Thus the relevant system interconnection is always well-posed in that context.
Another important statement concerning the depicted system structure is the following:

Theorem 2.4 *Stabilizing controller [Sch01]*
The controller $K(s)$ stabilizes $P(s)$ in the control loop from Figure 2.9 if and only if the interconnecting system (2.21) *defines a proper transfer matrix*

$$\big(w, v_1, v_2\big)^\top \to \big(z, u, v\big)^\top$$

and is stable.

So the augmented system seems to be the adequate object of investigating stability for the input-output system. Referring again to internal stability, like discussed at the end of the formulation example in Section 2.1, the following statements are summarized:

Theorem 2.5 *Internal stability [ZD98]*
The system (2.21) *from Figure 2.9 is said to be internally stable if the characteristic transfer matrix*

$$\begin{pmatrix} I & -K \\ -P_{22} & I \end{pmatrix}^{-1} = \begin{pmatrix} (I - KP_{22})^{-1} & K(I - KP_{22})^{-1} \\ P_{22}(I - KP_{22})^{-1} & (I - KP_{22})^{-1} \end{pmatrix}$$

from (v_1, v_2) to (u, v) belongs to $\mathcal{RH}_\infty$ (strictly proper and stable).

Tesis publicada con autorización del autor
No olvide citar esta tesis

It is interesting to observe that similar important sensitivity functions occur here in the MIMO case as they did in the SISO case during the formulation example. The internal stability guarantees all signals in the system to be bounded provided that the injected signals are bounded (BIBO stable). To state the necessity of avoiding unstable pole-zero cancellations the following generalization can be found.

Theorem 2.6 *Unstable pole-zero cancellation [ZD98] Let m_K be the number of open right-half plane (rhp) poles of $K(s)$ and m_P be the number of open rhp poles of $P_{22}(s)$. Then the system is internally stable if and only if it is well-posed and*

(i) the number of open rhp poles of $P_{22}(s)K(s)$ and $K(s)P_{22}(s)$ equals $m_K + m_P$,

(ii) $(I - KP_{22})^{-1}$ is stable.

The previous theorem requires just to check one sensitivity function instead of all to proof internal stability. This makes it convenient to use.
Clearly as one of the basic necessary and sufficient conditions for the existence of an internally stabilizing controller for the system Σ_{nom} is that (A, B_u) is stabilizable and (A, C_y) is detectable [DP05].

2.2.2 Performance measures & analysis

After discussing the issue of nominal stability, the term of nominal performance shall be clarified here. It is common in control applications to formulate some objectives beside the stabilization itself. Usual specification examples are the rise time or overshoot concerning the step response. Here the techniques used refer to norm specifications.
The performance specifications shall be done for a transfer connection of the form:

$$z = G(s)w\,.$$

Clearly the transfer function $G(s)$ could be seen as the closed loop transfer function already including the controller and further weighting filter extensions. This corresponds to $G = T_{zw}$ for system Σ_{nom} from Equation (2.3). The objective is to determine and analyze the induced specifications of the transfer behavior with respect to the class of transferred signals. The following part shall motivate the utilized signal classes. Here

Tesis publicada con autorización del autor
No olvide citar esta tesis

are some exemplary scalar signal types with physical context [SP01]:

$$\begin{aligned}
\text{Power:} \quad \mathcal{BP} &= \left\{ w \;\middle|\; \lim_{T\to\infty} \frac{1}{2T} \int_{-T}^{T} |w(t)|^2 dt \leq 1 \right\}, \\
\text{Energie:} \quad \mathcal{B}L_2 &= \left\{ w \;\middle|\; \|w\|_2^2 = \int_{-\infty}^{\infty} |w(t)|^2 dt \leq 1 \right\}, \\
\text{Magnitude:} \quad \mathcal{B}L_\infty &= \left\{ w \;\middle|\; \|w\|_\infty = \operatorname{ess\,sup}_t |w(t)| \leq 1 \right\}.
\end{aligned}$$

The prefix $\mathcal{B}$ indicates the unit boundedness. In fact these are signal types indicating a bounded power or energy level, or simply a restriction on the magnitude. These are of practical interest because energy consumption and maximal impact amplitude are mattering performance factors.
General important signal norms in the time domain, or L norms, are defined over scalar signals $x(t) \in \mathbb{C}, t \in (-\infty, \infty)$:

$$\|x(\cdot)\|_p = \left(\int_{-\infty}^{\infty} |x(t)|^2 dt \right)^{1/p},$$

or also as frequency domain norms for $x(s) \in \mathbb{C}$:

$$\|x(\cdot)\|_p = \left(\frac{1}{2\pi} \int_{-\infty}^{\infty} |x(j\omega)|^2 d\omega \right)^{1/p}.$$

These norms form Banach spaces notated by

$$L_p = \left\{ x(\cdot) \;\middle|\; \|x\|_p < \infty \right\}$$

and expressing the characteristic signal classes. For relating the signal attributes to the respective transfer matrix, inner product spaces can also be defined for matrix valued functions. Two famous examples in relation with complex-valued matrices $X : \mathcal{C} \to \mathbb{C}^{n\times m}$:

$$\begin{aligned}
\mathcal{L}_2(j\mathbb{R}) &= \left\{ X(j\omega) \;\middle|\; \frac{1}{2\pi} \sqrt{\int_{-\infty}^{\infty} \operatorname{trace}\left(X(j\omega)^* X(j\omega) \right) d\omega} < \infty \right\}, \\
\mathcal{L}_\infty(j\mathbb{R}) &= \left\{ X(j\omega) \;\middle|\; \operatorname{ess\,sup}_t \sigma_{\max}\Big(X(j\omega) \Big) < \infty \right\}.
\end{aligned}$$

These will lead to the Hardy spaces $\mathcal{H}_2$ and $\mathcal{H}_\infty$ in the following subsections where some of the expressions are explained in detail. Especially in the context of realizable transfer matrices it makes sense to restrict the spaces:

Tesis publicada con autorización del autor
No olvide citar esta tesis

- $\mathcal{RL}_2 \subset \mathcal{L}_2$: real, rational, strictly proper transfer function with no poles on $j\mathbb{R}$
- $\mathcal{RL}_\infty \subset \mathcal{L}_\infty$: real, rational transfer functions with no poles on $j\mathbb{R}$

Other useful matrix norms not explained here are for example the Frobenius norm, the sum norm, the maximum column or row norm.
Now the question of norm induction occurs. More precise this objective can be formulated like this:

$$\|z\|_\alpha \leq 1 \, \forall \|w\|_\beta \leq 1 \Leftrightarrow \|G\|_? \leq 1 \,,$$

meaning "Which output signal specification holds for a certain input signal class equivalently to the wanted transfer matrix norm?". This formulation transfers the signal performance definition the transfer matrix construction which can actually be manipulated by the control algorithm.
The Table 2.1 sums up sum of the mentioned induced norm relations: For some com-

	Power $w \in \mathcal{BP}$	Energy $w \in \mathcal{B}L_2$	Magnitude $w \in \mathcal{B}L_\infty$	Sinusoidal $w = \sin(\omega t)$	Impulse $w = \delta(t)$
$\|z\|_P$	$\|G\|_\infty$	0	$\leq \|G\|_\infty$	$\frac{1}{\sqrt{2}}\|G\|_\infty$	0
$\|z\|_2$	∞	$\|\boldsymbol{G}\|_\infty$	∞	∞	$\|G\|_2$
$\|z\|_\infty$	∞	$\|G\|_2$	$\|g(t)\|_1$	$\|G\|_\infty$	$\|g(t)\|_\infty$

Table 2.1: Signal transmission and induced norms

binations there does not exist a characterization. In the table g refers to the impulse response for describing the system in the time domain. In this work mainly L_2 signals are of interest and it is one of the main tasks to determine the corresponding closed loop system realization.

Another commonly used tool for the performance measuring of a transfer matrix are its maximal and minimal singular values [ZD98]. They can be used as a good measure of the gain of a transfer matrix in terms of generalizing the gain concept of SISO systems. In comparison with eigenvalues they have the advantages to be applicable to non squared systems and are not restricted to its eigenvector components [SP01].
Firstly the singular value for the matrix $X \in \mathbb{C}^{n \times m}$ is defined as:

$$\sigma_i(X) := \sqrt{\lambda_i\left(X^* X\right)} \,.$$

By the *singular value decomposition* (SVD) the matrix X can be split into two unitary matrices and a matrix containing the singular values. This point of view allows a

Tesis publicada con autorización del autor
No olvide citar esta tesis

geometric interpretation of the concept. Any complex matrix X may be factorized into a SVD:

$$X = U\Sigma V^* \tag{2.22}$$

with $U \in \mathbb{C}^{n\times n}$ and $V \in \mathbb{C}^{m\times m}$ being unitary, meaning $U^* = U^{-1}$ and $V^* = V^{-1}$. Furthermore there is the matrix $\Sigma \in \mathbb{C}^{n\times m}$ containing a diagonal matrix $\tilde{\Sigma} = \mathrm{diag}(\sigma_1, \ldots, \sigma_{\min(n,m)})$ where the $\sigma_i \geq 0$ are arranged in descending order, thus $\bar{\sigma} = \sigma_1$ and $\underline{\sigma} = \sigma_{\min(n,m)}$. Its form then is:

$$\Sigma = \begin{cases} \begin{bmatrix} \tilde{\Sigma} \\ 0 \end{bmatrix} & : n > m \\ \tilde{\Sigma} & : n = m \\ \begin{bmatrix} \tilde{\Sigma} & 0 \end{bmatrix} & : n < m \end{cases}$$

It appears that the unitary matrices U and V form orthonormal bases for the column space (output) and the row space (input) of respectively. That is why the columns of U are called output singular vectors (left) and the column vectors of V input singular vectors (right).

There are further interesting properties and special cases are mentioned in [SP01]. Interestingly the rank of a general non-squared matrix is equivalent to the number of non-zero singular values. They also help to define the condition number $\gamma(X) := \bar{\sigma}/\underline{\sigma}$ which is important concerning numerical issues.

For control application and performance measuring its practicability comes directly from the geometric interpretation. Supposing v_i and u_i being the respective column vectors of V and U with unit norm scaling $\|v_i\|_2 = \|u_i\|_2 = 1$ it follows from Equation (2.22):

$$XV = U\Sigma \Leftrightarrow Xv_i = \sigma_i u_i \,.$$

This means considering inputs in the direction v_i the output results to be in the direction u_i. Because of the unit scaling the singular value σ_i gives directly the matrix gain in this direction:

$$\sigma_i(X) = \|Gv_i\|_2 = \frac{\|Gv_i\|_2}{\|v_i\|_2} \,.$$

Beside the adequate gain characterization of a MIMO transfer function the singular value has the advantage to obtain orthogonal plant directions by the SVD. For the minimum and maximum singular values $\underline{\sigma}$ and $\bar{\sigma}$ it is clear that the corresponding

Tesis publicada con autorización del autor
No olvide citar esta tesis

directions have some significance as well [Rai10]. For example $v_1 = \bar{v}$ corresponds to the input with the largest amplification and $u_1 = \bar{u}$ is the output direction in which inputs are most effective. These refer to the high-gain directions.
The maximum singular values plays an important role for frequency domain performance and robustness measure [ZD98]. Considering the sensitivity function, for example $S = (I - KP_{22})^{-1}$ from Theorem 2.5, the relation e/r can be characterized where e the output error and r the control reference. Then, based on the former discussion, the following bounds can be found:

$$\underline{\sigma}\Big(S(j\omega)\Big) \leq \frac{\|e(\omega)\|_2}{\|r(\omega)\|_2} \leq \bar{\sigma}\Big(S(j\omega)\Big)\,.$$

For the performance it is seems reasonable to demand a small ratio $\|e(\omega)\|_2/\|r(\omega)\|_2$, even for the worst case scenario (high-gain direction). To accomplish that a performance weight $W_P(j\omega)$ is introduced whose inverse shall represent the maximum allowed amplitude of $\|e\|_2/\|r\|_2$. In other terms the requirement is formulated as:

$$\begin{aligned} & \bar{\sigma}\Big(S(j\omega)\Big) \overset{!}{<} \frac{1}{W_P(j\omega)}\,\forall\omega \\ \Leftrightarrow\quad & \bar{\sigma}\Big(W_P(j\omega)S(j\omega)\Big) < 1\,\forall\omega \\ \Leftrightarrow\quad & \|W_P S\|_\infty < 1\,. \end{aligned}$$

Here the used H_∞ norm is explained more detailed in the following subsection. The objective of this technique is to design a controller fulfilling the the bound given in form of the performance filter W_P. This also allows to define a bandwidth for MIMO systems.
On the other hand there can be complementary design specifications. Other requirements for sensitivities could be to make $\bar{\sigma}(K(I + P_{22}K)^{-1})$ relatively small for a disturbance compensation at the plant output [ZD98]. That can be achieved by similar techniques. These procedures are called loop-shaping methods and represent an own field of control design.
In this part a introduction to nominal performance measures has been given. Specification characteristics for MIMO transfer matrices have been given in form of induced norms and the singular value approach. They connect signal transfer properties directly to the transfer function structure and its design.

Tesis publicada con autorización del autor
No olvide citar esta tesis

2.2.3 H_2 optimal performance

After introducing more general performance concepts in the former subsection, here the H_2 norm shall be focused on for signal evaluation. The system structure considered in this case has the form:

$$G(s) = \left[\begin{array}{c|c} A & B \\ \hline C & 0 \end{array}\right] ,$$

which means not allowing a feedthrough, $D = 0$ explicitly. This for example corresponds to the system Σ_{nom} form Equation (2.3) in a closed control loop with no direct relation between the input w and output z, thus $D_{zw} = 0$. The following definition formulates the basis of the H_2 analysis.

Definition 2.7 *H_2 norm and the space $\mathcal{H}_2$ [ZD98]*
For the transfer function $G(s)$ the H_2 norm is defined as:

$$\|G\|_2 := \sqrt{\frac{1}{2\pi} \int_{-\infty}^{\infty} trace\Big(G(j\omega)^* G(j\omega)\Big) d\omega} .$$

The corresponding space $\mathcal{H}_2$ is a Hilbert space of the complex matrix functions $G(\cdot)$ declared on $j\mathbb{R}$ in the following way:

$$\mathcal{H}_2 := \Big\{ G : \mathbb{C} \to \mathbb{C}^{n \times m} \,\Big|\, G(s) \text{ analytic } \forall s : Re(s) > 0 \,,\, \|G\|_2 < \infty \Big\} .$$

For $G_1, G_2 \in \mathcal{H}_2$ the inner product is given by

$$\langle G_1, G_2 \rangle = \frac{1}{2\pi} \int_{-\infty}^{\infty} trace\Big(G_1(j\omega)^* G_2(j\omega)\Big) d\omega .$$

Obviously in comparison to the former discussion one can state $\mathcal{H}_2 \subset \mathcal{L}_2(j\omega)$. So the connection to the transfered signal energy is one of the major motivation of using the H_2 framework. These specifications lead to the respective desired transfer matrix class:

$$\mathcal{RH}_2 = \{ G \in \mathcal{H}_2 \,|\, G(s) \text{ real rational, strictly proper, stable} \} .$$

For further characterization of the H_2 norm some basic system properties are revisited. First, instead of representing the transfer behaviour by the transfer function, alternatively the impulse response is can be used. It is obtained by applying the impulse input $u(t) = [\delta_1(t), \ldots, \delta_{n_u}(t)]^\top$ to the system Σ_{LTI}. Assuming the initial condition to vanish $x = 0$ and because of the integral property of the delta distribution $\delta_i(\cdot)$ the

Tesis publicada con autorización del autor
No olvide citar esta tesis

impulse response has the form:

$$y_{ij}(t) = \begin{cases} C_i e^{At} B_j & : t > 0 \\ 0 & : t \leq 0 \end{cases} \quad \Rightarrow \quad g(t) := \begin{pmatrix} y_{11}(t) & \cdots & y_{1n_u}(t) \\ \vdots & \ddots & \vdots \\ y_{n_y 1}(t) & \cdots & y_{n_y n_u}(t) \end{pmatrix},$$

where C_i describes the i-th row of C and B_j represents the j-th column of B. This can be derived using the analytic system solution (2.2).
To motivate the H_2 norm formulation the following special Lyapunov equations are considered:

$$AZ + ZA^\top + BB^\top = 0 \Rightarrow Z = \int_0^\infty e^{At} BB^\top e^{A^\top t} dt\,, \tag{2.23}$$

$$A^\top Y + YA + C^\top C = 0 \Rightarrow Y = \int_0^\infty e^{A^\top t} C^\top C e^{At} dt\,. \tag{2.24}$$

The solution Z from Equation (2.23) is referred to as *Controllability Gramian* and the solution Y from Equation (2.24) is called *Observability Gramian*. They play an important role in general control theory. Most significantly, Z has full rank iff (A, B) controllable, Y is of full rank iff (A, C) observable. Further explanation concerning the Gramians can be found in Appendix **??** in the context of the Hankel operator.
Now using the Parseval theorem for signal $x(t)$ with its Fourier transformed $X(j\omega)$

$$\int_{-\infty}^{\infty} |x(t)|^2 dx = \frac{1}{2\pi} \int_{-\infty}^{\infty} |X(j\omega)|^2 d\omega$$

the following holds:

$$\begin{aligned} \|G\|_2^2 &= \frac{1}{2\pi} \int_{-\infty}^{\infty} trace\Big(G(j\omega) G(j\omega)^*\Big) d\omega \\ &\overset{\text{Parseval}}{=} \int_0^\infty trace\left(g(t) g(t)^\top\right) dt \\ &\overset{\text{solution}}{=} \int_0^\infty trace\left[C e^{At} B B^\top e^{A^\top t} C^\top\right] dt \\ &\overset{\text{Gramian}}{=} trace(CZC^\top) \\ &\overset{\text{transpose}}{=} trace(B^\top Y B)\,. \end{aligned} \tag{2.25}$$

This gives the capability to directly compute the H_2 norm of the signal transmission from u to y just depending on the transfer system realization A, B, C. Here the formulation of Equation (2.25) is used mainly, as well as the corresponding Equation (2.23).

Tesis publicada con autorización del autor
No olvide citar esta tesis

Now for guaranteeing a certain bound on the H_2 performance the Lyapunov equation for the Gramian is truncated to a Lyapunov inequality [DP05]. It can be seen that a matrix $X = X^\top \in \mathbb{R}^{n\times n}$ satisfying

$$AX + XA^\top + BB^\top < 0 \tag{2.26}$$

also fulfills $X > Z$. This implies the following important relation for the H_2 norm bound of the system $G(s)$ for a given $\nu > 0$:

$$G(s)\,\text{stable}\,,\ \|G\|_2 < \sqrt{\nu} \quad \Leftrightarrow \quad \exists X = X^\top > 0 : (2.26) \wedge \operatorname{trace}(CXC^\top) < \nu\,.$$

Thus a LMI condition on the system could be formulated in terms of H_2 performance. To formulate a more convenient LMI on this the following idea is sketched by using the Schur complement presented in Appendix **??**. Introducing the auxiliary variable $W = W^\top \in \mathbb{R}^{n_y\times n_y}$ defined as

$$\begin{aligned} & W := CXC^\top + \varepsilon I\,,\ \varepsilon > 0 \\ \Leftrightarrow \quad & W - CXC^\top > 0 \\ \Leftrightarrow \quad & W - CXX^{-1}XC^\top > 0 \\ \Leftrightarrow \quad & \begin{pmatrix} W & CX \\ XC & X \end{pmatrix} > 0\,. \end{aligned}$$

This also implies $\operatorname{trace}(W) = \operatorname{trace}(CXC^\top) + n_y\varepsilon$. With $\varepsilon \to 0$ the equivalent H_2 norm characterization

$$\begin{aligned} & \begin{pmatrix} AX + XA^\top & B \\ B^\top & -I \end{pmatrix} < 0\,, \\ & \begin{pmatrix} W & CX \\ XC^\top & X \end{pmatrix} > 0\,,\ \operatorname{trace}(W) < \nu \end{aligned} \tag{2.27}$$

can be stated. Note that the derivation idea here only demonstrates the necessity of this equivalence. Often the inverse Lyapunov variable $\tilde{X} := X^{-1}$ is used as well. The optimality refers to minimize the bound ν.

Like mentioned in [ZDG96] a direct connection between the H_2 control problem of minimizing ν and the LQG problem can be found. This also gives a stochastic interpretation of the H_2 performance. It means that in the presence of Gaussian type white noise a H_2 controller guarantees optimal performance. That is why it is an important part of the control procedure in this work. Its energy related measure and the

Tesis publicada con autorización del autor
No olvide citar esta tesis

compatibility with other robust control techniques make it an excellent choice for a performance characterization.
Nevertheless, the H_2 optimal control minimizes the effect of random and thus unstructured disturbances. Accordingly it does not seem to be appropriate to deal with higher order terms as they tend to be structured.

2.2.4 H_∞ suboptimal performance

The other important performance measure in this work is the H_∞ norm. As discussed at the beginning of this section the maximal transmission of the gain induced by an input signal can be characterized in a L_2 sense. This can be done by using the singular value to lower maximum gain bounds and trying to make error signals small. It is of great interest for the controller design to weaken the influence of external perturbations on the objectives. Another important application is to guarantee the amplification of a coupled uncertain system part to be beneath a certain threshold.
Here the LTI system $G(s)$ with realization A, B, C, D of the following form shall be considered:

$$G(s) = \left[\begin{array}{c|c} A & B \\ \hline C & D \end{array}\right].$$

In this case a feedthrough $D \neq 0$ is allowed. For the system Σ_{nom} this refers to $D_{zw} \neq 0$, which for example could directly describe the influence of the reference input to the regulation error. The following definition concretes the respective desired transfer function class.

Definition 2.8 *H_∞ norm and the space $\mathcal{H}_\infty$ [ZD98]*
For the transfer behaviour $z = G(s)w$ the H_∞ norm is defined as:

$$\begin{aligned}\|G\|_\infty &:= \sup_{w \in L_2} \frac{\|z\|_2}{\|w\|_2} \\ &= \sup_{\omega \in \mathbb{R}} \overline{\sigma}\Big(G(j\omega)\Big) = \sup_{\omega \in \mathbb{R}} \sqrt{\lambda_{\max}\Big(G(j\omega)^* G(j\omega)\Big)}\,.\end{aligned}$$

The corresponding space $\mathcal{H}_\infty$ is a Banach space of the complex matrix functions $G(\cdot)$ declared on $j\mathbb{R}$ in the following way:

$$\begin{aligned}\mathcal{H}_\infty := \Big\{ G : \mathbb{C} \to \mathbb{C}^{n \times m} \,\Big|\, & G(s) \text{ analytic } \forall s : Re(s) > 0\,, \\ & G(s) \text{ bounded } \forall s : Re(s) = 0\,,\ \|G\|_\infty < \infty \Big\}.\end{aligned}$$

Tesis publicada con autorización del autor
No olvide citar esta tesis

As in the H_2 case one can also state $\mathcal{H}_\infty \subset \mathcal{L}_\infty(j\omega)$. Similarly the desired realizable transfer functions are expected to be in the set

$$\mathcal{RH}_\infty = \{G \in \mathcal{H}_\infty \,|\, G(s) \text{ real rational, proper, stable}\} \,.$$

The properness property of the functions contained in $\mathcal{H}_\infty$ guarantees componentwise boundedness of $G(s)$ as $s \to \infty$.
Finding conditions and computation methods for the H_∞ characterization is often connected to tools like the *Bounded-Real Lemma* (BRL) or the *Kalman-Yakubovich-Popov Lemma* [DP05]. In the LTI case this mainly results in *Algebraic Riccati Equation* (ARE) or *Algebraic Riccati Inequality* (ARI) problems respectively which can be treated numerically efficient [Sch90].
Because of the many existing forms and derivation approaches for these results only some ideas behind the concepts shall be shown instead of presenting entire proofs. Beside the objective of stabilizing the system $G(s)$ it is aimed for minimizing the maximum induced gain $\|G\|_\infty$, thus the worst case scenario. As the optimal performance achievement often turns out to be a difficult task and a rather extreme solution, the suboptimal H_∞ problem is addressed here, namely to find the solution for a given norm bound. Later that bound is objective to a minimization problem. This can be formulated in the following manner for a given $\gamma > 0$:

$$\begin{aligned}
& \forall w \in L_2 : \quad \|z\|_2 \overset{!}{\leq} \gamma \, \|w\|_2 \\
\Leftrightarrow \quad & \forall w \in L_2 : \quad -\|z\|_2^2 + \gamma^2 \|w\|_2^2 \geq 0 \\
\Leftrightarrow \quad & \forall w \in L_2 : \quad \int_0^\infty \Big(-(Cx+Dw)^\top (Cx+Dw) + \gamma^2 w^\top w \Big) dt \geq 0 \\
\Leftrightarrow \quad & \inf_{w \in L_2} \int_0^\infty \begin{pmatrix} x \\ w \end{pmatrix}^\top \begin{pmatrix} -C^\top C & -C^\top D \\ -D^\top C & \gamma^2 I - D^\top D \end{pmatrix} \begin{pmatrix} x \\ w \end{pmatrix} dt \geq 0 \,. \qquad (2.28)
\end{aligned}$$

So it is a necessary condition for the bound requirement if the matrix occurring in the center of the integral in (2.28) would be positive definite. This formulation with including stability also leads to a variant of the LQP problem as shown in [Sch90]. Now it is also clear that since $G(\infty) = D$ the restriction $\|G\|_\infty \geq \bar{\sigma}(D)$ holds.
One of the major results can be derived by using the theory of dissipative systems, well introduced in [van96]. Like proven in [DP05] the following storage function can

Tesis publicada con autorización del autor
No olvide citar esta tesis

be used:

$$V(x) := x^\top X x\,, \quad 0 < X = X^\top \in \mathbb{R}^{n\times n}$$

with the corresponding dissipation inequality

$$\dot{V}(x) < \gamma\|w\|^2 - \|z\|^2\,.$$

If this inequality would be fulfilled internal stability could be guaranteed and then, due to a vanishing V as $t \to \infty$ the desired relation $\|z\|^2 \leq \gamma\|w\|^2$ would be accomplished (integration over inequality). Plugging the system definition into the dissipation inequality and separating a quadratic form with respect to $(x, w)^\top$ results in:

$$\begin{aligned}
& \dot{x}^\top X x + x^\top X \dot{x} + (Cx + Dw)^\top (Cx + Dw) - \gamma^2 w^\top w < 0 \\
\Leftrightarrow \quad & x^\top (A^\top X + XA + C^\top C)x + 2w^\top (B^\top X + D^\top C)x + w^\top(-\gamma^2 I + D^\top D)w < 0 \\
\Leftrightarrow \quad & \begin{pmatrix} C^\top \\ D^\top \end{pmatrix} \begin{pmatrix} C & D \end{pmatrix} + \begin{pmatrix} A^\top X + XA & XB \\ B^\top X & -\gamma^2 I \end{pmatrix} < 0\,.
\end{aligned}$$

With this idea of constructing matrix inequalities out of norm relations and advanced stability concepts like dissipativity the H_∞ norm characterization can be performed. The preceding sketch can not serve as an entire proof which can be found in the respective source of the following theorem.

Theorem 2.9 *Bounded real lemma [DP05]*
Taking the dynamic system $G(s)$ with realization A, B, C, D into account, the following conditions are equivalent:

(i) The matrix A is Hurwitz and

$$\|G\|_\infty < \gamma\,,$$

(ii) $\exists X = X^\top > 0$ such that

$$\begin{pmatrix} C^\top \\ D^\top \end{pmatrix} \begin{pmatrix} C & D \end{pmatrix} + \begin{pmatrix} A^\top X + XA & XB \\ B^\top X & -\gamma^2 I \end{pmatrix} < 0\,,$$

(iii) $\exists X = X^\top > 0$ such that

$$\begin{pmatrix} A^\top X + XA & XB & C^\top \\ B^\top X & -\gamma I & D^\top \\ C & D & -\gamma I \end{pmatrix} < 0\,.$$

Tesis publicada con autorización del autor
No olvide citar esta tesis

The equivalence to *(iii)* can be obtained by utilizing the Schur complement from Appendix **??**. This theorem is a powerful condition on a dynamic system to be in $\mathcal{H}_\infty$ with a desired energy amplification bound γ.
To clarify the relation between the H_∞ norm of a system $G(s)$ with its realization, the norm calculation in terms of the matrices A, B, C, D is an important point. When dealing with the H_∞ control synthesis one frequently is confronted with Riccati equation solving problems (Appendix **??**). Directly connected to the Riccati equation solution is the so called Hamiltonian matrix [Sch90]. Similarly this auxiliary matrix can be used for computing the H_∞ norm. Therefore the following major result and defining the Hamiltonian of interest is needed.

Theorem 2.10 *H_∞ norm and Hamiltonian [ZD98]*
Let $\gamma > 0$ and $G(s) \in \mathcal{RH}_\infty$. Defining the matrix

$$H := \begin{pmatrix} A + BR^{-1}D^\top C & BR^{-1}B^\top \\ -C^\top(I + DR^{-1}D^\top)C & -(A + BR^{-1}D^\top C)^\top \end{pmatrix}$$

with $R = \gamma^2 I - D^\top D$, the following conditions are equivalent:

(i) $\|G\|_\infty < \gamma$,

(ii) $\bar{\sigma}(D) < \gamma$ *and* $eig(H) \cap j\mathbb{R} = \emptyset$,

(iii) $\bar{\sigma}(D) < \gamma$ *and* $H \in dom(Ric)$ *and* $Ric(H) \geq 0$ $\Big(Ric(H) > 0$ *if* (A, C) *observable*$\Big)$.

Here another way of characterizing the H_∞ sub-optimality is found, in a very similar way to the BRL from Theorem 2.9. Especially the last point *(iii)*, introducing the connection to the Riccati framework notationally, gives the connection with the Lyapunov variable $X = \mathrm{Ric}(H)$ for stabilizing solutions.
The idea behind Theorem 2.10 can be given easily by considering the case with $D = 0$. Correspondingly the Riccati equation for this example would be of the form:

$$A^\top X + XA + C^\top C + \frac{1}{\gamma^2} XBB^\top X = 0\,.$$

Let an auxiliary system $\Phi(s)$ be the following transfer matrix:

$$\Phi(s) := \gamma^2 I - G(-s)^\top G(s) = \left[\begin{array}{cc|c} A & 0 & -B \\ -C^\top C & -A^\top & 0 \\ \hline 0 & B^\top & \gamma^2 I \end{array}\right].$$

Tesis publicada con autorización del autor
No olvide citar esta tesis

By using the techniques for interconnecting systems (addition and multiplication) presented in Section 2.1 the obtained realization is explained. The expression $G(-s)^\top$ is called the para-Hermitian conjugate or conjugate system and refers to the complex conjugate case [DP05]. Additionally, performing an inversion operation on $\Phi(s)$ leads to

$$\Phi(s)^{-1} = \left[\begin{array}{cc|c} A & \frac{1}{\gamma^2} BB^\top & \frac{1}{\gamma^2} B \\ -C^\top C & -A^\top & 0 \\ \hline 0 & \frac{1}{\gamma^2} B^\top & \frac{1}{\gamma^2} I \end{array}\right].$$

One can find the following relation:

$$\|G\|_\infty < \gamma \quad \Leftrightarrow \quad \Phi(j\omega) > 0 \, \forall \omega \in \mathbb{R} \quad \Leftrightarrow \quad \Phi(j\omega)^{-1} \text{ has no poles on } j\mathbb{R}\,.$$

The firs equivalence directly comes from the H_∞ norm Definition 2.8 and its relation to the singular value. Due to $\Phi(\infty) > 0$ and since $\Phi(\cdot)$ is a continuous function, the second equivalence between $\Phi(j\omega) > 0 \, \forall \omega$ and $\Phi(j\omega)$ nonsingular $\forall \omega$, or $\Phi(j\omega)$ has no imaginary axis zero ("zero crossing") respectively, is valid. This is then directly related to the poles of the inverse of $\Phi(j\omega)$.
In the extensive case with $D \neq 0$ the derivation can be drawn similarly but with more expanded calculations being avoided in this work. Here the property of $\Phi(\infty) = R > 0$ and the assumption $\bar{\sigma}(D) < \gamma$ are the crucial difference. Additionally the unobservable modes are of rather technical concerns.
Thus the connection between the Hamiltonian H, which forms the dynamics of the auxiliary system $\Phi(s)^{-1}$, and the norm calculation is clear. The whole proof can be found in [ZD98].
For computational issues the Hamiltonian checking tool on the H_∞ norm can be used in form of an iterative algorithm. A classical bisection can be applied in the following way:

Algorithm:

1. **INIT:** Choose bounds $\gamma_l \leq \|G\|_\infty \leq \gamma_u$ and tolerance $\varepsilon > 0$
2. **IF** $\frac{\gamma_u - \gamma_l}{\gamma_u} \leq \varepsilon$ **THEN** $\|G\|_\infty := \frac{\gamma_u + \gamma_l}{2}$; **RETURN**;
   ELSE $\gamma := \frac{\gamma_u + \gamma_l}{2}$;
3. **IF** $\mathrm{eig}(H) \cap j\mathbb{R} = \emptyset$ **THEN** $\gamma_u := \gamma$; *//check* $\|G\|_\infty < \gamma$
   ELSE $\gamma_l := \gamma$;
4. **GO TO** step 2

Tesis publicada con autorización del autor
No olvide citar esta tesis

Here the condition on H containing imaginary eigenvalues is used to check the validity of the current iteration step bound. Dependent on that the bound is increased or lowered in a mean way. The termination criteria depends on the chosen approximation tolerance ε.
In this subsection the H_∞ norm has been characterized by several criterion mainly stated in Theorem 2.9 and 2.10. It is an important performance measure for evaluating the worst case amplification of a system and thus also plays an important role on describing the influence of uncertainties. Furthermore an algorithmic way of calculating the norm is presented.

2.3 Uncertainty modelling

For the robustness analysis and treatment the description of a possible uncertainty class turns out to be the core requirement. It is actually the key feature of robust control in comparison with other control approaches to guarantee a working system under concretely specified circumstances of the unknown conditions. Accordingly this specification shall be addressed in this section. As it can be seen as part of the mathematical system modelling task, formulating uncertainties is a difficult task and in general requires skill and experience.
That is why in the following part a bunch of exemplary uncertainty structures are motivated and presented. The relation to the physical origin and effects is essential for putting those perturbations into a systematic context. In the end of the modelling process the aim is to obtain system interconnection reformulation like shown in Figure 2.10. Here the known system part in the center of the loop can be thought of as a

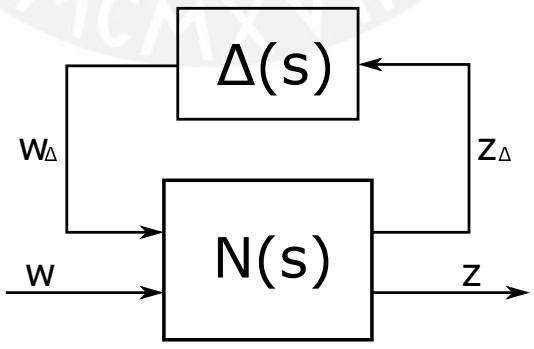

Figure 2.10: General system $N(s)$ with separated uncertainty structure $\Delta(s)$

modelled system $P(s)$ combined with the controller $K(s)$, thus $N(s) = \mathcal{F}_l(P, K)$. The procedure of separating the system is also referred to as pulling out the uncertainty.

Tesis publicada con autorización del autor
No olvide citar esta tesis

Rather than modelling a concrete transfer function for $\Delta(s)$ it is desired to find a system class $\mathbf{\Delta}$ with later considering the closed loop $\mathcal{F}_u(N, \Delta)\,\forall\Delta \in \mathbf{\Delta}$. While $\mathbf{\Delta}$ classifies all possible uncertainty transfer structures, the set $\mathbf{\Delta}_c$ contains the corresponding complex values these transfer matrices can obtain. Thus a better problem transformation is made possible and with additional normalization the sets can be handled in a unified manner. They are defined as from [Sch01] in the following way:

$$\begin{aligned} \mathbf{\Delta}_c &:= \left\{\Delta_c \in \mathbb{C}^{n_\Delta \times n_\Delta} \,\middle|\, \|\Delta_c\| < 1\right\} \\ \mathbf{\Delta} &:= \left\{\Delta(\cdot) \in \mathcal{RH}_\infty \,\middle|\, \Delta(j\omega) \in \mathbf{\Delta}_c\, \forall\omega \in \mathbb{R} \cup \{\infty\}\right\} \end{aligned} \tag{2.29}$$

Note that equivalently $\mathbf{\Delta} = \{\Delta(\cdot) \in \mathcal{RH}_\infty \,|\, \|\Delta\|_\infty < 1\}$. Now the task is to characterize these sets of interest with respect to the relation $w_\Delta = \Delta(s) z_\Delta$ for concrete application problems. A big challenge during this process is to really focus on important and realistic uncertainty conditions to include. If the system is forced to handle too many models which are even senseless it loses a lot of flexibility. This problem is referred to as *conservatism*.

2.3.1 Dynamic modeling errors

Continuing the motivating formulation example from Section 2.1 there was the following problem setup taken from [Sch01]. The SISO example faces the task of controlling a real plant $H(s)$ with a slightly inaccurate model $G(s)$. A mathematical model can only be an approximation of the real system behavior and thus always errors are made. This approach relies on frequency domain considerations.
Assuming the plant to be stable and of minimum phase the frequency response magnitude characterizes the system fully. For example sweep experiments can be made and the magnitude plot seen in Figure 2.11 (absolute values) can be obtained. For direct comparison the corresponding plot of the model is shown as well. It can be observed that the system model is sufficiently accurate for low frequencies but has a high deviation in the high frequency region. This is an actual practical issue and therefore of interest. Easily it can be seen that the overall magnitude error is always smaller the one, so the following characterization holds:

$$|H(j\omega) - G(j\omega)| < 1\,\forall\omega \in \mathbb{R} \cup \{\infty\}\,.$$

Tesis publicada con autorización del autor
No olvide citar esta tesis

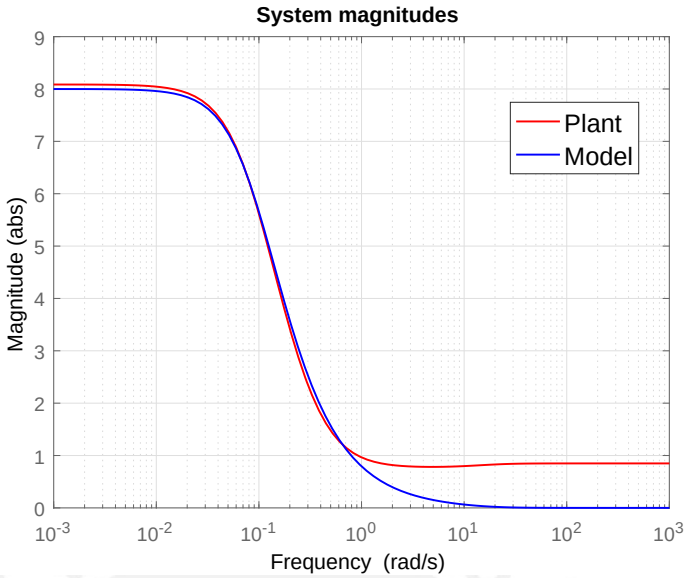

Figure 2.11: Magnitude comparison of experimental plant $H(s)$ and system model $G(s)$

This motivates the introduction of the modelling error $\Delta(s)$:

$$\Delta(s) := H(s) - G(s) \quad \Rightarrow \quad |\Delta(j\omega)| < 1 \, \forall \omega \in \mathbb{R} \cup \{\infty\} \, .$$

Because of the generally unknown characteristics of the plant the error set $\mathbf{\Delta}$ shall be used. A controller synthesis would be aiming for stabilizing the closed-loop system for all possible uncertainties $\Delta \in \mathbf{\Delta}$. In Figure 2.12 some compatible uncertainty examples (a) and their corresponding plant frequencies responses (b) are presented. It

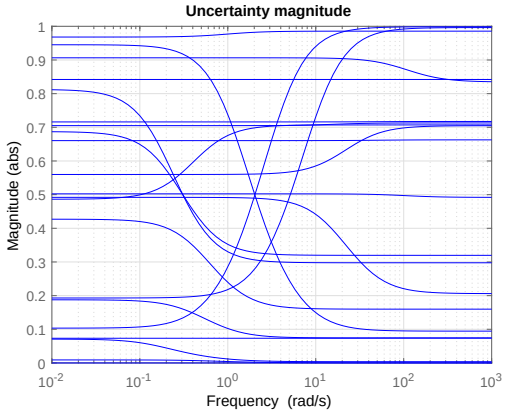

(a) Unit uncertainties $\Delta(s)$

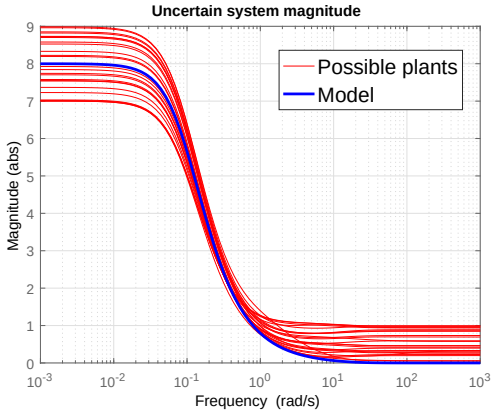

(b) Possible uncertain plants

Figure 2.12: Magnitude plots for uncertainty distribution

Tesis publicada con autorización del autor
No olvide citar esta tesis

demonstrates the wide range of considered plants a controller has to be designed for. One can get an impression of the overestimation of possible systems done by that. In the low frequency range huge deviations occur which change the nature of the system significantly. One can imagine that treating all those different and mostly unreasonable possible plants at once leads to the earlier mentioned phenomenon of conservative solutions. This especially forms a problem in MIMO systems where numerous internal couplings exist. That is why in practice weighting filters $W_\Delta(s)$ are used for evaluate the frequency dependency of the expected uncertainty which. Here a high-pass filter would be reasonable. The filter design problem, one of the core designing tasks in robust control, is focused on later in Section **??**.
The uncertainty fitting with this kind of modeling inaccuracy is clearly additive and can be reformulated in the following way to pull out the uncertainty structure:

$$z = G_\Delta w = (G + \Delta)w \quad \Leftrightarrow \quad \begin{pmatrix} z_\Delta \\ z \end{pmatrix} = \begin{pmatrix} 0 & I \\ I & G \end{pmatrix} \begin{pmatrix} w_\Delta \\ w \end{pmatrix}, \; w_\Delta = \Delta z_\Delta \, .$$

To analyze the uncertain control loop consider the block diagram drawn in Figure 2.13 with the introduced plant model $G(s)$ and controller $C(s)$. It is assumed that

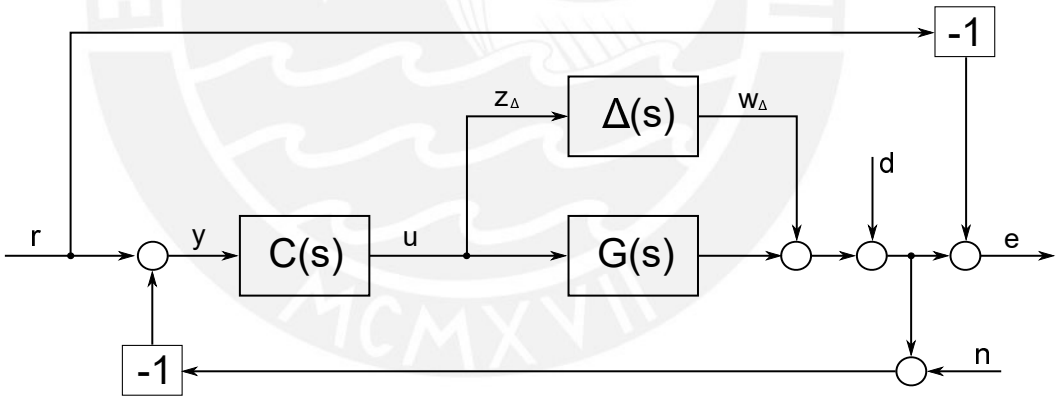

Figure 2.13: Closed loop interconnections with additive uncertainty

a controller stabilizing the nominal closed loop has already been found. As sketched in the formulating example standard loop structure with uncertainty has now to be decomposed into the form Σ_{rob} from Equation (2.6). The aim is to find the transfer matrix $N(s)$ introduced in Figure 2.10 in the following way:

$$\begin{pmatrix} z_\Delta \\ z \end{pmatrix} = N(s) \begin{pmatrix} w_\Delta \\ w \end{pmatrix} \text{ with } N(s) =: \begin{pmatrix} M(s) & N_{12}(s) \\ N_{21}(s) & N_{22}(s) \end{pmatrix} .$$

Tesis publicada con autorización del autor
No olvide citar esta tesis

In this example the objective output is the tracking error $z = e$ and the external inputs $w = (r, d, n)^\top$ contain the control reference, the disturbance (not on input side here) and measurement noise. The upper left block $M(s)$ is of special interest because it relates w_Δ to z_Δ and considering the closed loop

$$\mathcal{F}_u(N, \Delta) = N_{22}(s) + N_{21}(s)\Delta(s)\Big[I - M(s)\Delta(s)\Big]^{-1} N_{12}(s)$$

it is evident that it determines the stability of the total system. Analyzing the block diagram 2.13 one can find these relations:

$$\begin{aligned} z_\Delta &= C(s)\Big(r - n - d - w_\Delta - G(s)z_\Delta\Big) \\ \Leftrightarrow \quad z_\Delta &= \Big(I + C(s)G(s)\Big)^{-1} C(s)\left(r - n - d - w_\Delta\right). \end{aligned}$$

Thus the decisive system part is $M = -(1 + CG)^{-1}C$. A further block diagram consideration yields

$$e = -r + \Big(I + G(s)C(s)\Big)^{-1}\Big(d + w_\Delta + G(s)C(s)(r - n)\Big).$$

Thus the system composition can be expressed with the following transfer function:

$$N(s) = \begin{pmatrix} -(\mathbf{I} + \mathbf{CG})^{-\mathbf{1}}\mathbf{C} & (I + CG)^{-1}C & -(I + CG)^{-1}C & -(I + CG)^{-1}C \\ (I + GC)^{-1} & -(I + GC)^{-1} & (I + GC)^{-1} & -(I + GC)^{-1}GC \end{pmatrix}.$$

After formulating the problem structure a stability analysis shall be made. This is done by applying the Nyquist criterion presented for the general case in Appendix **??** to the inverted term $I - M\Delta$. Due to the fact that $C(s)$ is stabilizing M is a stable transfer function, as well as $\Delta(s)$. Then a necessary condition for closed loop stability is if the curve $-M(j\omega)\Delta(j\omega)$ does not encircle the point -1. This is certainly true if $\forall\omega \in \mathbb{R} \cup \{\infty\}$:

$$\begin{aligned} & |M(j\omega)\Delta(j\omega)| < 1 \\ \overset{|\Delta|\leq 1}{\Rightarrow} \quad & \Big|\Big(I + C(j\omega)G(j\omega)\Big)^{-1} C(j\omega)\Big| \leq 1\,. \end{aligned} \tag{2.30}$$

So there is a simple condition on checking the stability of the system under all uncertainties $\Delta \in \mathbf{\Delta}$. This is referred to as robust stability which is introduced formally in Section 2.4. To apply this to a concrete control example a internally stabilizing controller has to be found primarily for the nominal system. Without mentioning any

Tesis publicada con autorización del autor
No olvide citar esta tesis

numerical details Figure 2.14 (a) provides the Nyquist plot for the open loop corresponding to an adequate controller $C(s)$. It can be seen that there are no encirclements of -1 which means for the stable plant $G(s)$ that the closed loop system is stable in the nominal case. Even the phase margin of $\Phi_m = 60.9°$ and a gain margin $K_m = 27\text{dB}$ seem to be sophisticating in terms of robustness expectations.
Now the robust stability test obtained in (2.30) is applied to the respective transfer functions. The second part of Figure 2.14 in (b) illustrates the magnitude plot $|M(j\omega)|$. Additionally the critical magnitude of $1\hat{=}0\text{dB}$ is indicated by a dashed line. Unfortunately for some frequencies holds $|M(j\omega)| > 1$ and thus the condition is violated. So stability for all $\Delta \in \mathbf{\Delta}$ cannot be guaranteed. Although this seems to be a negative result it still gives important information on the robustness of the system. First one can observe that the magnitude remains below $1.5\hat{\approx}3.5\text{dB}$, thus $|M(j\omega)| < \frac{3}{2}\,\forall\omega$. That means that robust stability still holds unrestrictedly for all uncertainties with $|\Delta(j\omega)| < \frac{2}{3} \approx 0.7\,\forall\omega$. Actually this largest validity bound for still guaranteeing stability can be characterized in general as $\|M\|_\infty^{-1}$.
On the other hand the magnitude information especially of the violated area can be used for constructing a concrete destabilizing uncertainty like shown in [Sch01].

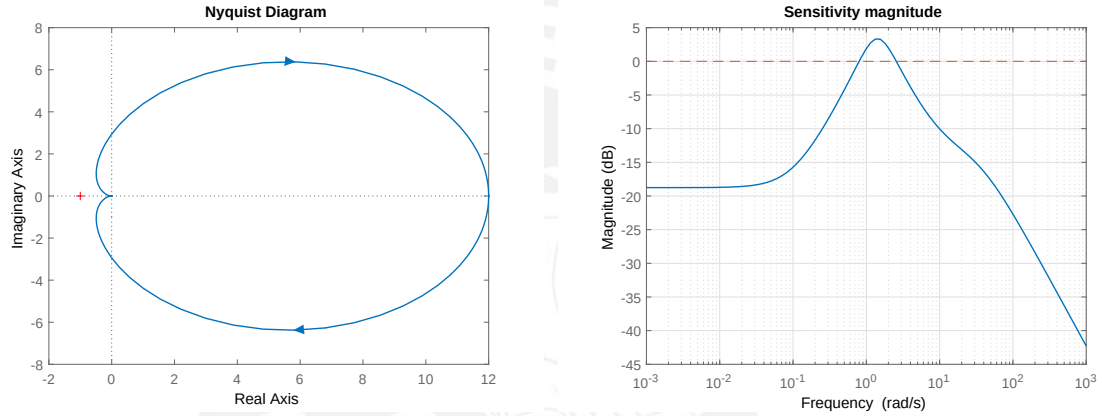

(a) Nyquist plot of nominal open loop GC (b) Robust stability condition check (2.30)

Figure 2.14: Closed loop system robust analysis for additive uncertainty

Summarizing the general procedure for dynamic uncertainties characterized by the frequency response one can state that in practice plants are treated which are mainly determined in the frequency domain. Let $\mathcal{H}(\omega)$ denote a set of complex number for every frequency ω corresponding to taken measurements or expected characteristics. This experiment leads to the conclusion that proper models $H(s)$ satisfying $H(j\omega) \in \mathcal{H}(\omega)$

Tesis publicada con autorización del autor
No olvide citar esta tesis

are appropriate models for the underlying plant.
Since frequency experiments can only be performed at a finite number of points the description $\mathcal{H}(\omega)$ turns out to be difficult to use. This dilemma leads to the idea of robust control to cover uncertain sets or system conditions with a broader class of transfer behavior much easier to handle. Therefore the following relation is shall be achieved:

$$\mathcal{H}(\omega) \subset G(j\omega) + W(j\omega)\mathbf{\Delta}_c \; \forall \omega \in \mathbb{R} \cup \{\infty\}$$

where $G(s)$ is a real rational proper transfer matrix, $W(s)$ is a real rational weighting filter and the open set $\mathbf{\Delta}_c$ as defined in Equation (2.29). Graphically this introduces a disk with the center $G(j\omega)$ and radius $|W(j\omega)|$ containing all the elements of $\mathcal{H}(\omega)$. The weight $W(s)$ captures the variance of the uncertainty with respect to the frequency. As shown in the example most models are not good for high frequencies so often a high-pass filter is used.
The actual set of possible dynamic uncertainties $\mathbf{\Delta}$ has also been introduced in (2.29). Finally, the resulting uncertain system is described by $G_\Delta := G + W\Delta$ with $\Delta \in \mathbf{\Delta}$. So a set of systems has been obtained, parameterized by the transfer functions in $\mathbf{\Delta}$, which include the real expected uncertainty. Again one has to pay attention to not making this class too big, resulting in a loss of flexibility and obtaining conservative solutions.

2.3.2 Parametric uncertainties

After the introductory example for motivating the different uncertainty aspects more model related techniques shall be presented in the following. It is well known that during the modelling process errors in depicting the right parameters often occur [SP01]. On the one hand this simply comes from parameters of the linear model only known approximately within a certain range. Furthermore there is the appearance of varying parameters in the linear model due to the impact of nonlinearities or changing operating conditions.
These parametric uncertainties may occur in various forms. For example from a state space perspective it makes a big difference if they are part of the dynamic matrix A or lie in the input or output channel respectively. That is why two major examples shall be discussed in this part.

Tesis publicada con autorización del autor
No olvide citar esta tesis

Input matrix uncertainty

A modern example taken from satellite control concerning uncertainties on the actuator sight in the MIMO case is presented here [Sch01]. So consider the following system realization:

$$G(s) = \left[\begin{array}{cc|cc} 0 & a & 1 & 0 \\ -a & 0 & 0 & 1 \\ \hline 1 & a & 0 & 0 \\ -a & 1 & 0 & 0 \end{array}\right] = \frac{1}{s^2+a^2}\begin{pmatrix} s-a^2 & a(s+1) \\ -a(s+1) & s-a^2 \end{pmatrix}.$$

Here $a > 0$ is a known parameter. The uncertainty comes into play when looking at the actuator where certain tolerances have to be taken into account. Accordingly the input matrix takes the form:

$$B_\Delta = \begin{pmatrix} 1+\delta_1 & 0 \\ 0 & 1+\delta_2 \end{pmatrix},$$

where $\delta_1, \delta_2 \in \mathbb{R}$ unknown, but within the range of $|\delta_1| < r, |\delta_2| < r$ for a known $r > 0$. Then the following relation holds because of $D = 0$:

$$\begin{aligned} G_\Delta(s) &= C(sI-A)B_\Delta = C(sI-A)(B+\Delta) \\ &= \frac{1}{s^2+a^2}\begin{pmatrix} s-a^2 & a(s+1) \\ -a(s+1) & s-a^2 \end{pmatrix}\left(I + \begin{pmatrix} \delta_1 & 0 \\ 0 & \delta_2 \end{pmatrix}\right) \\ &= G(s)\Big(I+\Delta\Big), \end{aligned}$$

with the uncertainty structure $\Delta := \mathrm{diag}(\delta_1, \delta_2)$. The real plant $H(s)$ thus is represented by the system class $G_\Delta(s)$. In comparison to the former example, where the uncertainty occurred additively, Δ appears multiplicatively from the Laplace domain point of view. In this case the uncertainty can be pulled out by redefining channels:

$$z = G_\Delta w = G(I+\Delta)w \quad \Leftrightarrow \quad \begin{pmatrix} z_\Delta \\ z \end{pmatrix} = \begin{pmatrix} 0 & I \\ G & G \end{pmatrix}\begin{pmatrix} w_\Delta \\ w \end{pmatrix}, \; w_\Delta = \Delta z_\Delta .$$

For demonstrating the analysis of a control loop a simple controller $C(s) = I$ is taken here. The system composition is illustrated in the block diagram of Figure 2.15. Now the system shall be reformulated to obtain the structure of Σ_{rob} and finally the transfer behaviour $N(s)$ shown in Figure 2.10. This results again in finding the relation

Tesis publicada con autorización del autor
No olvide citar esta tesis

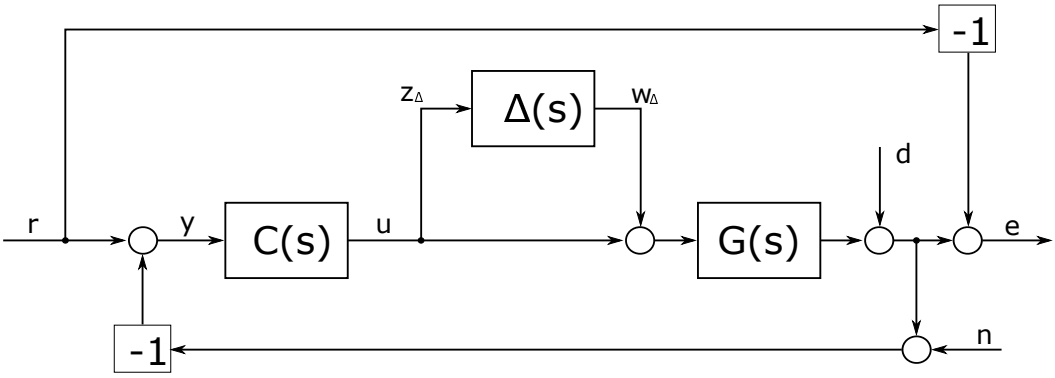

Figure 2.15: Closed loop interconnections with input multiplicative uncertainty

$z_\Delta = M(s)w_\Delta$ determining the stability of the uncertain system. From the block diagram analysis one obtains:

$$z_\Delta = C(s)\Big(r - n - d - G(s)(w_\Delta + z_\Delta)\Big)$$

$$\Leftrightarrow \quad z_\Delta = \underbrace{-\Big(I + C(s)G(s)\Big)^{-1}C(s)G(s)}_{=:M(s)}\, w_\Delta + \Big(I + C(s)G(s)\Big)^{-1}(r - d - n)\,.$$

Plugging in the system definition the transfer matrix $M(s)$ is given by:

$$M(s) = \frac{1}{s+1}\begin{pmatrix} -1 & -a \\ a & -1 \end{pmatrix}.$$

As in the former example for stability it has to be checked whether $I - M\Delta$ has a stable and proper inverse for all possible Δ. According to [Sch01] (Lemma 2) this is the case iff $I - M(\infty)\Delta(\infty)$ is non-singular and $\det(I - M(s)\Delta(s))$ has no zeros in $\mathbb{C}^+$. The determinant of

$$I - M(s)\Delta = \begin{pmatrix} 1 + \frac{\delta_1}{s+1} & \frac{a\delta_2}{s+1} \\ \frac{-a\delta_1}{s+1} & 1 + \frac{\delta_2}{s+1} \end{pmatrix}$$

can be calculated as

$$\det\Big(I - M(s)\Delta\Big) = \frac{1}{(s+1)^2}\Big(s^2 + (2 + \delta_1 + \delta_2)s + 1 + \delta_1 + \delta_2 + (a^2+1)\delta_1\delta_2\Big)\,.$$

Tesis publicada con autorización del autor
No olvide citar esta tesis

There are no zeros at ∞ and using the Hurwitz criterion for a polynomial of second order results in the following stability condition:

$$2 + \delta_1 + \delta_2 > 0\,,$$
$$1 + \delta_1 + \delta_2 + (a^2 + 1)\delta_1\delta_2 > 0\,.$$

In Figure 2.16 the respective contour of the region where the condition is violated is illustrated for the parameter $a = 10$. Various conclusions can be drawn from analyzing

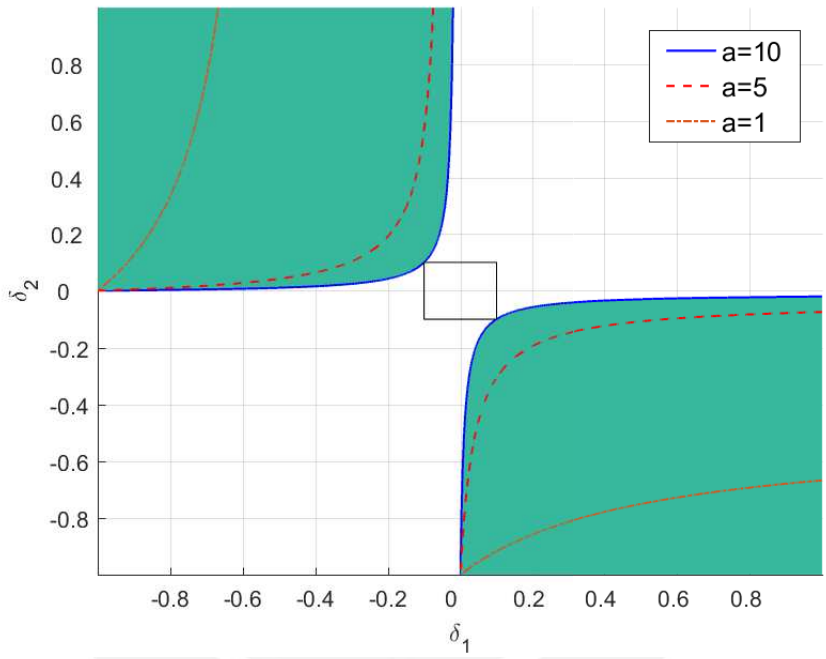

Figure 2.16: Region of destabilizing parameters (contoured)

this plot. First consider the stability condition for the uncertain parameter $\delta_2 = 0$. Then the system would be stable for $\delta_1 \in (-1, \infty)$ and vise versa for the flipped case. This makes clear that considering the stability region for only one parameter without taking the other into account misleads to false impressions. That is why for robustness analysis especially in MIMO systems the region of common variations plays an important role. For the parameter $a = 10$ the common bound $r = 0.1$ can be found. One can suspect from the other plotted contours $a \in \{1, 5\}$ that this bound will decrease with increasing a.

During the presented procedure the decomposition of a system with input multiplicative uncertainty has been explained. For the output case with including C_Δ a very

Tesis publicada con autorización del autor
No olvide citar esta tesis

similar methodology can be applied. From the transfer function perspective, gain uncertainties can also easily be brought into this form [SP01].
The presented example is a very special constructed case where such an explicit analysis of the stability region is possible. In general this will fairly never be the case. Therefore more universal tools have to be developed for determining robust stability and performance. These results are presented in Section 2.4.

Dynamic parameterization

Before going into state space form type of parameter description consider firstly a SISO transfer function with uncertainties regarding the time constants [Rai10]. Considering the typical mass-spring-damper system of second order

$$m\ddot{x} + d\dot{x} + cx = u \leftrightarrow G(s) = \frac{1}{ms^2 + ds + c}$$

with positive uncertain parameters $m \in (m_1, m_2), d \in (d_1, d_2), c \in (c_1, c_2)$ within their tolerances. Selecting the respective nominal value as $m_0 := \frac{m_1+m_2}{2}$ a scaled error can be introduced:

$$\Delta_m := \frac{m - m_0}{m_2 - m_0}\,,\ \Delta_d := \frac{d - d_0}{d_2 - d_0}\,,\ \Delta_c := \frac{c - c_0}{c_2 - c_0}\,.$$

Clearly $\Delta_m, \Delta_d, \Delta_c \in \mathbf{\Delta}$ holds. With defining the respective weights $W_m := m_2 - m_0$ the frequency domain description of the uncertain plant is obtained by

$$G_\Delta(s) = \frac{1}{(m_0 + W_m\Delta_m)s^2 + (d_0 + W_d\Delta_d)s + (c_0 + W_c\Delta_c)}$$

Thus a whole set of uncertain functions could be found parameterized by the uncertainties $\Delta_m, \Delta_d, \Delta_c$. Another perspective can be chosen from the time constant point of view like done in [SP01]. In this form the time constants appear multiplicatively in the transfer function so consider a single uncertain term exemplary given by

$$G_\Delta(s) = \frac{1}{\tau s + 1} G_0(s)\,,\ \tau_{\min} \leq \tau \leq \tau_{\max}\,.$$

Again with rewriting $\tau = \tau_0(1 + r\Delta)$ where $\Delta \in \mathbf{\Delta}_c$ the model class is converted to

$$G_\Delta(s) = \frac{G_0(s)}{1 + \tau_0 s + r\tau_0 s\Delta} = \underbrace{\frac{G_0(s)}{1 + \tau_0 s}}_{=:G(s)} \cdot \frac{1}{1 + W(s)\Delta}\,,\quad W(s) := \frac{r\tau_0 s}{1 + \tau_0 s}\,.$$

Tesis publicada con autorización del autor
No olvide citar esta tesis

With this system decomposition a multiplicative uncertainty structure could be pulled out of transfer function due to the multiplicative nature of the time constant form. Physically it does not make sense for τ to change sign, otherwise that would correspond to a pole at infinity.
For a more general parameter uncertainty case from the state space perspective a linear dependency on the parameters is assumed [SP01]. Here system of the following form is considered:

$$\begin{cases} \dot{x} = A_\Delta x + B_\Delta u \\ y = C_\Delta x + D_\Delta u \end{cases} \Rightarrow G_\Delta(s) = C_\Delta(sI - A_\Delta)^{-1}B_\Delta + D_\Delta$$

where the cause of uncertainty is characterized by some parameters $\delta_i \in \mathbb{R}$ (e.g. temperature, mass, etc.). Then the system matrices can be rewritten into

$$A_\Delta = A + \sum \delta_i A_i \,,\; B_\Delta = B + \sum \delta_i B_i \,,\; C_\Delta = C + \sum \delta_i C_i \,,\; D_\Delta = D + \sum \delta_i D_i \,,$$

where A, B, C, D belong to the nominal system model. The corresponding perturbations can be collected in the matrix Δ containing δ_i along its diagonal. For example taking the matrix A_Δ:

$$A_\Delta = A + \sum \delta_i A_i = A + W_2 \Delta W_1$$

with the weight matrices $W_{1,2}$ for generating the diagonal structure of Δ. With the auxiliary matrix function $\Psi(s) := (sI - A)^{-1}$ the central part of the transfer function $G_\Delta(s)$ can be expressed as

$$(sI - A_\Delta)^{-1} = (sI - A - W_2 \Delta W_1)^{-1} = (I - \Psi(s) W_2 \Delta W_1)^{-1} \Psi(s).$$

This is a common technique to pull known structures out of uncertain compositions. The resulting uncertainty has the form of an inverse additive interconnection like presented in Figure 2.17. With this procedure and using the linear fractional transformation introduced in Section 2.1 uncertainties in all system matrices can be handled. The challenge then is to pull the uncertainties into a common Δ structure which can be technically difficult. A good example for extracting various parametric uncertainties at the same time can be found in [SP01] (p.287).
One interesting idea of obtaining a direct uncertainty extraction can be obtained by

Tesis publicada con autorización del autor
No olvide citar esta tesis

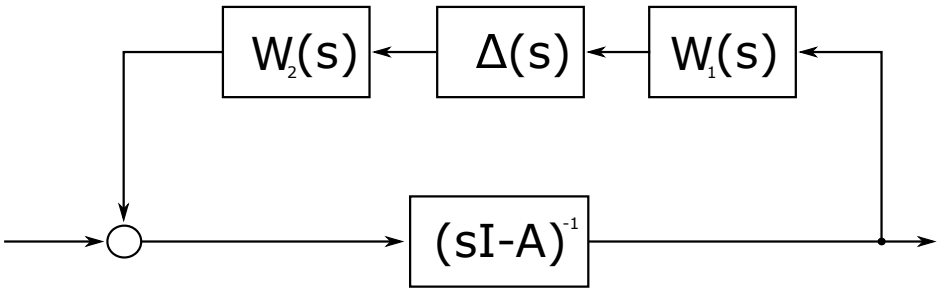

Figure 2.17: Inverse additive uncertainty structure from parametric uncertainties

factorization[Sch01].With the notation from above one can state:

$$\begin{pmatrix} A_\Delta & B_\Delta \\ C_\Delta & D_\Delta \end{pmatrix} = \begin{pmatrix} A & B \\ C & D \end{pmatrix} + \sum_i \delta_i \begin{pmatrix} A_i & B_i \\ C_i & D_i \end{pmatrix} .$$

Then determine the following factorization:

$$\begin{pmatrix} A_i & B_i \\ C_i & D_i \end{pmatrix} =: \begin{pmatrix} L_i^1 \\ L_i^2 \end{pmatrix} \begin{pmatrix} R_i^1 & R_i^2 \end{pmatrix}$$

where the matrices $(L_i^1, L_i^2)^\top$ and (R_i^1, R_i^2) have full column and row rank respectively. If one is successful to find such a decomposition the uncertain system can be rewritten in the form:

$$\begin{pmatrix} \dot{x} \\ z \\ z_1 \\ \vdots \\ z_k \end{pmatrix} = \left[\begin{array}{cc|ccc} A & B & L_1^1 & \cdots & L_k^1 \\ C & D & L_1^2 & \cdots & L_k^2 \\ \hline R_1^1 & R_1^2 & 0 & & \\ \vdots & \vdots & & \ddots & \\ R_k^1 & R_k^2 & & & 0 \end{array}\right] \begin{pmatrix} x \\ w \\ w_1 \\ \vdots \\ w_k \end{pmatrix}, \quad \begin{pmatrix} w_1 \\ \vdots \\ w_k \end{pmatrix} = \begin{pmatrix} \delta_1 I & & \\ & \ddots & \\ & & \delta_k I \end{pmatrix} \begin{pmatrix} z_1 \\ \vdots \\ z_k \end{pmatrix}$$

with uncertainty index numbering $i = 1, \ldots, k$. Note that the identity matrices in connection with their respective δ_i are of different dimension. This form can easily be transferred into the system form Σ_{rob}. It is desired to achieve factorization with a minimal numbers of columns and rows respectively. Thus the size of the identity blocks in the uncertainty results to be minimal as well. Arbitrary size factorizations are possible but turn out to be inefficient.

All the presented cases of parametric uncertainties can be put into a H_∞ framework. However, it is often avoided to introduce parametric uncertainties directly because of several reasons [SP01]:

Tesis publicada con autorización del autor
No olvide citar esta tesis

- large effort of modelling parametric uncertainties (usually),
- deceiving in the sense that parametric uncertainty models provide a detailed description, even though the underlying assumptions concerning the model can be much less exact,
- exact model structure required (unmodelled dynamics not suitable),
- real perturbations required.

That is why usually more general complex perturbation from the class $\mathbf{\Delta}$ although this might introduce more conservatism to the system. Thus the often "disk-shaped" uncertainty structure already used in the introductory example turns out to be adequate for capturing this type of uncertainty as well.

2.3.3 Nonlinearities & higher dynamics

In the Section 2.1 the decomposition of nonlinear systems has been discussed. Following these ideas concrete uncertainty structures shall be found for the cases of dealing with nonlinearities and respective neglected dynamics [DP05].
Formerly a nonlinear structure Q has been separated from the system to obtain an isolated LTI part. The requirement on the structure class $\mathbf{\Delta}$ constructed to capture the nonlinear behavior is the following:

$$\exists p : \; q = Q(p) \;\Rightarrow\; \exists \Delta \in \mathbf{\Delta} : \; q = \Delta p \,.$$

This means that for every input-output pairing there exists an uncertainty element generating the same relation. These elements tend to be of much simpler dynamical structure and are practicable treatable by linear tool, although a quiet huge object of probable circumstances is generated.
Finally $\mathbf{\Delta}$ will contain more elements than required to describe Q so that

$$\Big\{(p,q) \,|\, q = Q(p)\Big\} \subset \Big\{(p,q) \,|\, \exists \Delta \in \mathbf{\Delta} : \; q = \Delta p\Big\}$$

which then allows to treat the closed loop $\mathcal{F}_u(G,Q)$ with using $\mathcal{F}_u(G,\Delta)$ instead while guaranteeing to capture the same input-output relations. Generally speaking the degree of closeness of these sets determines the level of conservatism introduced by the replacement.

Tesis publicada con autorización del autor
No olvide citar esta tesis

Static nonlinearity

In a first step by using a linearization approach the general nonlinear system Σ_{NL} from Equation (2.9) could be split up into a linear part Σ_{aNL} depending on two external signals $w_1 = f(x,u) - Ax - Bu$ and $w_2 = h(x,u) - Cx - Du$ representing static nonlinearities. Suppose the separated nonlinear functions fulfill the sector condition

$$\begin{aligned} \|w_1(t)\| &\leq k_{11}x(t) + k_{12}u(t)\,, \\ \|w_2(t)\| &\leq k_{21}x(t) + k_{22}u(t)\,, \end{aligned}$$

with constants $k_{ij} > 0$. These parameters can for example be chosen by selecting the Lipschitz constants of f and g with respect to the corresponding variable locally. However, this might be a rough sector approximation, so if there is more knowledge available it should be involved. Then the nonlinearity $(w_1, w_2)^\top = Q(x,u)$ like shown in Figure 2.8 can be stated in the form

$$\begin{aligned} w_1(t) &= \delta_{11}x(t) + \delta_{12}u(t)\,, \\ w_2(t) &= \delta_{21}x(t) + \delta_{22}u(t)\,, \end{aligned} \tag{2.31}$$

where the functions of time $\delta_{ij}(\cdot)$ satisfying $\delta_{ij}(t) \in [-k_{ij}, k_{ij}]\,\forall t \geq 0$. Based on that the uncertainty structure Δ can defined as:

$$\Delta = \begin{pmatrix} \delta_{11} & \delta_{12} \\ \delta_{21} & \delta_{22} \end{pmatrix}$$

with $|\delta_{ij}(t)| \leq 0\,\forall t \geq 0$. Thus the more complex nonlinear structure could be captured by a class of linear ones which can be considered within the stability analysis and robust control synthesis. After some normalization a class $\mathbf{\Delta}$ can be found with the property that for any given input-output pair satisfying $(w_1, w_2)^\top = Q(x,u)$ there exists one particular uncertainty $\Delta \in \mathbf{\Delta}$ to meet the relation (2.31).

Neglecting higher dynamics

Another more complicated case occurs when not only separating the nonlinear part of the system, but whole dynamics is neglected like done for the system Σ_{part} from (2.12) with decomposing into (2.13) and (2.14). This results in a dynamic extraction Q with $(w_1, w_2)^\top = Q(x_1, u)$ and where Q contains of the internal states x_2.

Tesis publicada con autorización del autor
No olvide citar esta tesis

Assume for example that the following rather strong energy inequality holds:

$$\int_0^\infty \|w_1(t)\|^2 dt \leq k_1 \left(\int_0^\infty \|x_1(t)\|^2 dt + \int_0^\infty \|u(t)\|^2 dt \right),$$
$$\int_0^\infty \|w_2(t)\|^2 dt \leq k_2 \left(\int_0^\infty \|x_1(t)\|^2 dt + \int_0^\infty \|u(t)\|^2 dt \right),$$

which is well defined if all the signals are from L_2. Then, according to [DP05] an object $\mathbf{\Delta}$ can be defined which consists of linear mappings $\Delta : (x_1, u)^\top \mapsto (w_1, w_2)^\top$ satisfying the above inequalities for all suitable functions x_1, u. It is possible to show that if $(w_1, w_2)^\top = Q(x_1, u)$, for some bounded energy functions x_1 and u, then there exists a mapping $\Delta \in \mathbf{\Delta}$ such that $(w_1, w_2)^\top = \Delta(x_1, u)^\top$. Thus $\mathbf{\Delta}$ can generate any behavior of Q. With this kind of approach the initial condition of the internal state x_2 can be neglected. So there is the requirement of stability in high-order dynamics that can be isolated in this way.

2.3.4 Structured and unstructured uncertainties

Another and more general perspective on uncertainty objects can be made by dividing them with regards to their structure. This faces the contradiction between two important aspects in uncertainty modelling [Rai10]:

- the more structured an uncertainty the more complex results the corresponding perturbation class to be,
- the less structured an uncertainty the less close the approximative system captures the real behaviour (conservatism).

So there is obviously a trade of to make between the accuracy of an uncertainty object and its manageability. Well structured uncertainties form a very precise description of the underlying perturbation, whereas unstructured error models can be integrated more easily into the control design process.
In the following this distinction is explained more detailed and the former uncertainty examples are classified. These ideas then help to introduce certain robust analysis tools presented in Section 2.4.

Unstructured uncertainties

In this general case there does not exist information about concrete perturbation influences rather then an overall impression of the nature of uncertainty. For MIMO

Tesis publicada con autorización del autor
No olvide citar esta tesis

systems this for example can be the case when there is just the knowledge about a good model for low frequency and an inaccurate one for high frequencies, like presented in first example (additive SISO dynamic uncertainty). The corresponding MIMO representation in the frequency domain is [Sch01]:

$$G_\Delta(j\omega) = G + W(j\omega)\Delta_c\,,\ \Delta_c = \begin{pmatrix} \Delta_{11} & \Delta_{12} & \cdots \\ \Delta_{21} & \Delta_{22} & \cdots \\ \vdots & \vdots & \ddots \end{pmatrix}$$

with $\|\Delta_c\| = \bar{\sigma}(\Delta_c) < 1$ and thus clearly $\Delta_c \in \mathbf{\Delta}_c$, which then can be related to $\mathbf{\Delta}$. So the uncertainty is not expected to have any particular structure. In the exemplary case the filter $W(s)$ would simply be a high-pass filter. Characteristic for unstructured uncertainties is the use of one unified filter for all uncertainty components without structural distinction. This occurs due to the lack of specific information.
Like stated in [Rai10] also the multiplicative uncertainty type is often introduced in an unstructured way. Another characterization can be done by the so-called factorized modeling errors. This is based on a (left-) coprime factorization of the plant model into a nominator and denominator part resulting in a system form:

$$G = \tilde{M}^{-1}\tilde{N} \rightarrow G_\Delta = (\tilde{M} + \Delta_M)^{-1}(\tilde{N} + \Delta_N)\,.$$

Here the transfer form is made up by a simple additive and an inverse additive part in the end. Then the aim is again to bring the system into the form shown in Figure 2.10.
Generally these unstructured uncertainties are mainly characterized by their maximum singular value which is an useful tool in some sense but can also produce very strict results, especially if the considered perturbation class is too conservative. Therefore in Section 2.4 a more practical characterization in form of the structured singular value is introduced.

Structured uncertainties

On the other hand with some insight of the plant uncertainty models can be formulated precisely. Like shown in the former examples this is often motivated physically. The conversion to transfer matrices then usually leads to complicated feasible regions. These include parametric or particular additive uncertainties like shown before.
The following two dimensional MIMO example from [Sch01] illustrates the typical

Tesis publicada con autorización del autor
No olvide citar esta tesis

structured framework. Consider the uncertain system

$$G_\Delta(j\omega) = G(j\omega) + \begin{pmatrix} W_1 1(j\omega)\Delta_{11} & W_1 2(j\omega)\Delta_{12} \\ W_2 1(j\omega)\Delta_{21} & W_2 2(j\omega)\Delta_{22} \end{pmatrix}$$
$$= G + \begin{pmatrix} W_{11}(j\omega) & 0 & W_{12}(j\omega) & 0 \\ 0 & W_{21}(j\omega) & 0 & W_{22}(j\omega) \end{pmatrix} \underbrace{\begin{pmatrix} \Delta_{11} & & & \\ & \Delta_{21} & & \\ & & \Delta_{12} & \\ & & & \Delta_{22} \end{pmatrix}}_{=\Delta_c} \begin{pmatrix} 1 & 0 \\ 1 & 0 \\ 0 & 1 \\ 0 & 1 \end{pmatrix},$$

where $|\Delta_{ij}| < 1$ with the consequence of $\|\Delta_c\| < 1$ and the filters $W_{ij} \in \mathcal{RH}_\infty$. The big difference to the unstructured additive example is the fact that there are specific structural weights for each uncertainty separately.
This motivates to describe the set $\mathbf{\Delta}$ generally in a block-diagonal uncertainty form. Thus the set $\mathbf{\Delta}$ from Equation 2.29 is given by specifying the complex valued set $\mathbf{\Delta}_c$ in the following way:

$$\mathbf{\Delta}_c = \left\{ \Delta_c = \begin{pmatrix} \delta_1 I_{n_1} & & & & \\ & \ddots & & & \\ & & \delta_r I_{n_r} & & \\ & & & \Delta_1 & \\ & & & & \ddots \\ & & & & & \Delta_f \end{pmatrix} \middle| \, \delta_i \in \mathbb{R}, \Delta_i \in \mathbb{C}^{n_\Delta \times m_\Delta}, \|\Delta_c\| < 1 \right\}.$$

The upper blocks are distinguished into the real δ parts, corresponding for example to parametric uncertainties, and the complex Δ parts, related to dynamic uncertainties. Then many systems can be decomposed into the form

$$G_\Delta = G + W_2 \Delta W_2$$

with $\Delta \in \mathbf{\Delta}$ and and weighting matrices $W_1, W_2 \in \mathcal{RH}_\infty$ capturing the frequency dependency of the specific perturbation blocks.
Finally this illustrates the flexibility choosing this type of uncertainty model offers. It depends a lot on the requirements on refinement with respect to the mentioned modeling contradiction.

Tesis publicada con autorización del autor
No olvide citar esta tesis

2.4 Robust stability & performance

The objective of this part is, who to include the uncertainty structures from Section 2.3 into the control design, show for the nominal case in Section 2.2. It is desired to guarantee certain performance specifications considering the uncertain system under $\Delta \in \mathbf{\Delta}$. For the closed control-loop $\mathcal{F}_l(P, K) = N(s)$ a transfer distinction is made:

$$N(s) =: \begin{pmatrix} M & N_{12} \\ N_{21} & N_{22} \end{pmatrix}$$

where the transfer matrix M closes the loop with the internal uncertainty due to $z_\Delta = M(s)w_\Delta$. In comparison to Figure 2.10 the structure presented in Figure 2.18 is obtained. Then, the resulting closed-loop behavior of the controlled uncertain system

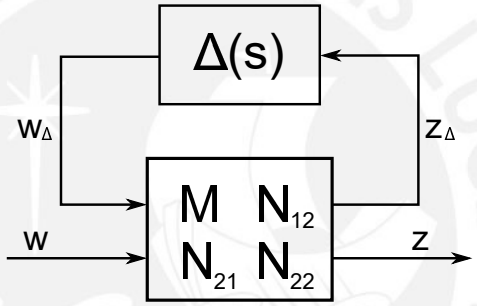

Figure 2.18: Closed control loop structure with uncertainty $\Delta(s)$

can be expressed as:

$$T_{zw}(s) = \mathcal{F}_u(N, \Delta) = N_{22} + N_{12}\Delta(I - M\Delta)^{-1}N_{21}$$

by using the LFT. The following introduction to the topic of robust stability and performance and the respective theorems are taken from the comprehensive explanation in [DP05]. It is assumed that the controller $K(s)$ nominally stabilizes $N(s)$.

2.4.1 Well-connectedness & unstructured uncertainty

The stability of $T_{zw}(s)$ clearly depends on the term $(I - M\Delta)^{-1}$ and its invertability. If for a given operator M and a set $\mathbf{\Delta}$ holds that $(I - M\Delta)^{-1}$ is nonsingular $\forall \Delta \in \mathbf{\Delta}$, the interconnection from Figure 2.18 are called *robustly well-connected*. Often, this property is referred to the pair $(M, \mathbf{\Delta})$ is equivalent to robust stability.
Intuitively, the property of robust well-connectedness causes a bounded transfer map

Tesis publicada con autorización del autor
No olvide citar esta tesis

between w and z. As it turns out, this characterization is the central interest in robustness analysis and design. Even a lot of important problems can be reduced to that. The application of this concept highly depends on the structuring of the uncertainty, which was motivated and introduced at the end of Section 2.3.
The first simple case is to consider the general unstructured uncertainty class of $\mathbf{\Delta} = \{\Delta \in \mathcal{RH}_\infty \,|\, \|\Delta\|_\infty \leq 1\}$.

Theorem 2.11 *Unstructured small gain theorem [DP05]*
Let M be an operator and $\mathbf{\Delta} = \{\Delta \in \mathcal{RH}_\infty \,|\, \|\Delta\|_\infty \leq 1\}$. Then, $I - M\Delta$ is nonsingular $\forall \Delta \in \mathbf{\Delta}$ if and only if:

$$\|M\|_\infty < 1 \,.$$

Note, that this task then can be treated as a suboptimal H_∞ problem for the bound $\gamma = 1$ with respect to the LTI system $M(s)$. Although the robust stability analysis problem is simple in the unstructured case, there are several reasons adding a certain structure to the problem. This is discussed in the following part.
In addition to a robustly well-connected $(M, \mathbf{\Delta})$ it is desired to keep some performance measure. Consider the following closed-loop system requirement:

$$\|\mathcal{F}_u(N, \Delta)\|\infty < 1 \quad \forall \Delta \in \mathbf{\Delta} \,.$$

With the prerequisite of robust stability, the term of robust performance can be introduced as such a desired norm bound on the total closed-loop system. The following result shows, how this can be related to the well-connectedness of the interconnection.

Theorem 2.12 *Problem reduction with additional structure [DP05]*
For a set $\mathbf{\Delta}$ define the auxiliary perturbation set:

$$\mathbf{\Delta}_p := \{\Delta = diag(\Delta_u, \Delta_p) \,|\, \Delta_u \in \mathbf{\Delta} \,,\, \Delta_p \in \mathcal{RH}\infty : \|\Delta_p\|_\infty \leq 1\} \,.$$

Then $(M, \mathbf{\Delta})$ is robustly well connected and $\|\mathcal{F}_u(N, \Delta_u)\|_\infty < 1 \, \forall \Delta_u \in \mathbf{\Delta}$ if and only if $I - N\Delta$ is nonsingular $\forall \Delta \in \mathbf{\Delta}_p$.

This proposition demonstrates the transformation of a combined robust stability and performance problem to the H_∞ condition of $\|N\|_\infty < 1$. Nevertheless, this usually leads to very conservative solutions and is the major motivation for considering structured uncertainties and derive equivalent conditions for them.

Tesis publicada con autorización del autor
No olvide citar esta tesis

2.4.2 Block-structured uncertainty

In addition to the former motivation of reducing the conservatism is that when modeling the interconnection of different systems, the uncertainties turn out to be naturally of block-diagonal structure. Like motivated before, an arbitrarily block-structured uncertainty set of the form:

$$\mathbf{\Delta}_a = \{\mathrm{diag}(\Delta_1, \ldots, \Delta_d) \,|\, \Delta_i \in \mathcal{RH}_\infty : \|\Delta_i\|_\infty \leq 1\}$$

is utilized. Note, that every block can be of different dimension. For this special subset, the general small gain condition $\|N\|_\infty < 1$ turns out to be very conservative. The basic idea to reduce conservatism is the introduction of commuting operators Θ with respect to the perturbations. For example, a commutant of the set $\mathbf{\Delta}_a$ is defined by:

$$\Theta_a = \{\Theta \in \mathcal{RH}_\infty \,|\, \Theta \text{ invertible}, \Theta\Delta = \Delta\Theta \; \forall \Delta \in \mathbf{\Delta}_a\} \; .$$

For $\Delta \in \mathbf{\Delta}_a$ and $\Theta \in \Theta_a$, this leads directly to:

$$\begin{aligned} &\Theta(I - N\Delta)\Theta^{-1} = I - (\Theta N \Theta^{-1})\Delta \\ \Rightarrow &\Big[\; I - N\Delta \text{ singular} \quad \Leftrightarrow \quad I - (\Theta N \Theta^{-1})\Delta \text{ singular} \; \Big] . \end{aligned}$$

Thus, it can be concluded that if there exists a commutant Θ such that:

$$\|\Theta N \Theta^{-1}\|_\infty < 1 \, ,$$

the robust well-connectedness of $(N, \mathbf{\Delta}_a)$ is guaranteed. It can be shown that [DP05]:

$$\Theta \in \Theta_a \quad \Leftrightarrow \quad \Theta = \mathrm{diag}(\theta_1 I, \ldots, \theta_d I)$$

with constants $\theta_i \in \mathbb{C} \setminus \{0\}$. These constant matrices are also referred to as scalings. Often, the set of positive scalings $\Theta_a^+ := \{\Theta = \mathrm{diag}(\theta_1 I, \ldots, \theta_d I) \,|\, \theta_i \in \mathbb{R}, \, \theta_i > 0\}$ is of interest. These results are summarized in the following theorem.

Tesis publicada con autorización del autor
No olvide citar esta tesis

Theorem 2.13 *Scaled small gain test [DP05]*
For an LTI system N with the realization $N = \left[\begin{array}{c|c} A & B \\ \hline C & D \end{array}\right]$ and with A Hurwitz, the following statements are equivalent:

(i) $(N, \mathbf{\Delta}_a)$ *is robustly well-connected,*

(ii) $\exists\, \Theta \in \Theta_a : \|\Theta N \Theta^{-1}\|_\infty < 1$,

(iii) $\exists\, \Theta \in \Theta_a^+$ *and* $\exists X = X^\top > 0$*:*

$$\begin{pmatrix} C^\top \\ D^\top \end{pmatrix} \Theta \begin{pmatrix} C & D \end{pmatrix} + \begin{pmatrix} A^\top X + XA & XB \\ B^\top X & -\Theta \end{pmatrix} < 0\,.$$

The scaled small gain condition turns out to be necessary and sufficient and thus, eliminates the majority of the conservatism. Additionally, the former theorem offers an LMI condition for the computation of the scaling $\Theta \in \Theta_a^+$ and accordingly, on robust stability and performance.

2.4.3 Robust synthesis sketch & further tools

These results form the basis of finding a controller $K(s)$ which stabilizes the system $N(s) = \mathcal{F}_l(P, K)$ nominally and guarantees robustness in the form of $\|\mathcal{F}_u(N(K), \Delta)\|_\infty < 1$ for $\Delta \in \mathbf{\Delta}$. The procedure contains briefly of these two major steps:

- for a fixed scaling $\Theta \in \Theta_a$ the nominal control problem is solved (see Section 2.2 or more specifically Chapter 3),
- for the fixed controller K the robustness analysis over $\mathbf{\Delta}_a$ is performed by utilizing *(iii)* from Theorem 2.13

In general, this is a difficult task and cannot be solved commonly. There are iterative algorithms aiming for a approximative solution. As those go to far for the setting of this work, this shall form a brief overview on the topic.
Further approaches, like shown in the collection [EN00a], make use of uncertainty multipliers, which can be used for LMI based optimization. There, several ideas for robust H_2 design are proposed. Most commonly, the structured singular value is utilized for robust control synthesis [ZD98]. It turns out to be a useful characterization and most frequently leads to the D/K algorithm (scaling/controller iteration). Other

Tesis publicada con autorización del autor
No olvide citar esta tesis

approaches, like in [SP01], aim for robust loop-shaping which consider the respective sensitivity functions directly.

Tesis publicada con autorización del autor
No olvide citar esta tesis

3 Multi-Objective Robust Control

The formulation and solution of robust control tasks is generally complicated. As pointed out in Chapter 2 one of the most common tools to solve classical H_2 or H_∞ problems are Riccati equations. During the last few decades linear matrix inequalities (LMIs) have become a common technique for numerous control applications [Boy94]. These inequalities have also been introduced in the previous chapter for simple performance specifications.

In the work [Sch90] a focus on Riccati inequalities already has been made and developed further. Then the aim is to reformulate those into LMIs because of the resulting convex optimization problems which are relatively easy to solve. Especially with interior-point methods the corresponding semi-definite programs (SDPs) can be treated efficiently [BV09] and it turns out to be an advantage to formulate a task in terms of LMIs.

In addition to the numerical preferences the LMI framework gives a certain flexibility in the way problems can be stated. This leads to the term of multi-objective robust control because of the combination of several conditions on the system performance at the same instance. Thus for example guaranteeing a certain H_2 or H_∞ gain, robust stability and regional pole restrictions at once becomes possible. Even the mixture of time- and frequency-domain specifications can be realized [SGC97].

An attempt to solve the H_2/H_∞ problem was made first in [ZGBD94] considering robust stability and in [DZGB94] continuing with optimal performance. Here a Riccati equation solution could be found requiring a rather complicated computation. In contrast to such closed form solutions, the LMI approach seems to be easier to obtain but often produces quite conservative results dependent on the accuracy of the respective problem formulation.

The book [EN00a] forms a great collection on modern LMI techniques and their application. It presents deep theoretical aspects as well as practical implementation issues. Especially in terms of robust performance analysis via LMIs, advanced results are explained extensively. During its introduction chapter [EN00b] the main advantages of this approach are the combination of classical control, such as PID, with modern ideas,

Tesis publicada con autorización del autor
No olvide citar esta tesis

like H_2 and LQG. Thus it is referred to as "postmodern" control. Furthermore LMI techniques are capable of reducing the number of parameters, simplifying the numerical solutions and providing design guarantees for even competing specifications.
Note that here the control design shall be focused on the output-feedback case, as pure state-feedback does not seem to fit to the application of this work.

3.1 Introduction to LMI framework

In the book [Boy94] the subject is introduced and presented in context with several problems. The application summary [VB00] also provides an insight on basic LMI techniques. An LMI can briefly be defined in the form:

$$F(x) = F_0 + \sum_{i=1}^{m} x_i F_i > 0 \tag{3.1}$$

with the variable $x \in \mathbb{R}^m$ and symmetric matrices $F_i = F_i^\top \in \mathbb{R}^{n \times n}$. The inequality (3.1) notation means positive definiteness of $F(x)$, being equivalent to $z^\top F(x) z > 0 \, \forall z \in \mathbb{R}^n \setminus \{0\}$. This can also be expressed as n polynomial inequalities because of the leading principle minors of $F(x)$ having to be positive.
Here only strict matrix inequalities are considered. The LMI (3.1) forms a convex constraint as the set $\{x \,|\, F(x) > 0\}$ is convex. This is a big advantage for formulating convex optimization problems such as linear and quadratic inequalities, matrix norm inequalities or Lyapunov inequalities [Boy94].
An important property is that multiple LMIs can easily be expressed as a single LMI by using one block-diagonal structure. Thus there is no distinction made between a set of LMIs and a single one. Another useful relation is the Schur complement. It allows to convert nonlinear convex inequalities into LMI form. The basic form is given by:

$$\begin{aligned} & R(x) > 0\,, \quad Q(x) - S(x) R(x)^{-1} S(x)^\top > 0 \\ \Leftrightarrow \quad & \begin{bmatrix} Q(x) & S(x) \\ S(x)^\top & R(x) \end{bmatrix} > 0 \end{aligned}$$

with matrices $R(x) = R(x)^\top$, $Q(x) = Q(x)^\top$ and $S(x)$ of appropriate dimensions. This is an important technique for transforming characteristic equations into LMI expressions.
Here we encounter problems containing matrix variables as in the Lyapunov inequality

Tesis publicada con autorización del autor
No olvide citar esta tesis

case or the more general example:

$$A^\top P + PA + PBR^{-1}B^\top P + Q < 0$$

where $A, B, Q = Q^\top, R = R^\top$ are given and $P = P^\top > 0$ is the variable. Using the Schur complement this can be transformed into:

$$\begin{bmatrix} -A^\top P - PA - Q & PB \\ B^\top P^\top & R \end{bmatrix} > 0$$

Due to the matrix variable this still is not of the form (3.1). For saving notation and efficient computation there is no further transformation made (which can be done by selecting a proper matrix basis) and the condensed LMI form is used.
A bunch of standard problems can be found in [Boy94]. The basics concerning optimality and the numerical treatment are explained in [BV09].

Before presenting the important LMI conditions for the control design another system representation has to be introduced. For the multi-objectivity different input-output-channels are needed to be characterized for applying the respective specification. The system for the mixed H_2/H_∞ robust control has the structure shown in Figure 3.1. Here a channel distinction is made by construction as in the case of system Σ_{rob} from

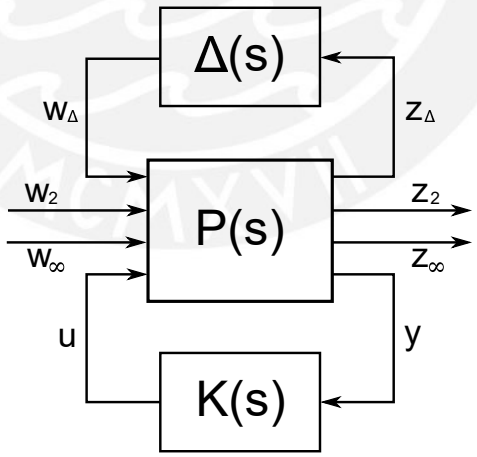

Figure 3.1: Mixed H_2/H_∞ system setup

Tesis publicada con autorización del autor
No olvide citar esta tesis

Equation (2.6). First the LTI system Σ is considered:

$$\Sigma \begin{cases} \dot{x} = Ax + B_w w + B_u u\,,\; x(0) = x_0 \\ z = C_z x + D_{zw} w + D_{zu} u \\ y = C_y x + D_{yw} w \end{cases} . \tag{3.2}$$

This is quiet similar to the definitions from Section 2.1. Considering a controller $K(s) = \left[\begin{array}{c|c} A_K & B_K \\ \hline C_K & D_K \end{array}\right]$ one obtains the closed-loop realization from Equation (2.8). Now the particular performance channels between input w and output z are distinguished. Therefor different channels are marked by the index $j \in \{1, \ldots, N\}$. Using the notation from [SGC97] input and output selection matrices R_j and L_j are chosen in the way:

$$T_j(s) := L_j T_{zw}(s) R_j = \left[\begin{array}{cc|c} A + B_u D_K C_y & B_u C_K & B_j + B_u D_K F_j \\ B_K C_y & A_K & B_K F_j \\ \hline C_j + E_j D_K C_y & E_j C_K & D_j + E_j D_K F_j \end{array}\right] =: \left[\begin{array}{c|c} A_{\mathrm{cl}} & B_{\mathrm{cl}}^j \\ \hline C_{\mathrm{cl}}^j & D_{\mathrm{cl}}^j \end{array}\right]$$

where $B_j := B_w R_j$, $C_j := L_j C_z$, $D_j := L_j D_{zw} R_j$, $E_j := L_j D_{yw}$ and $F_j := D_{zu} R_j$. This simplifies the problem formulation a lot as input-output pairs can be stated as $(w_j, z_j) = (R_j^{-1} w, L_j z)$.

3.2 Design specifications with matrix inequalities

Like already mentioned during the previous chapter there are several ways of formulating matrix norm specifications utilizing LMIs. In this work, for the closed loop system the following properties shall be fulfilled:

- internal stability
- H_2 optimal performance
- suboptimal H_∞ gain (disturbance)
- passive behavior
- no remaining tracking error
- stability under uncertainties

Tesis publicada con autorización del autor
No olvide citar esta tesis

Guaranteeing all the objectives fully at the same instance turns out to be quiet ambitious and most probably leads to conservative results. The aim is to investigate the combination of these goals and make use of the LMI framework advantage to realize flexible problem formulations. It adds lots of degrees of freedoms allowing a precise tuning of complex control synthesis tasks.
The following LMI criteria are based on the extensive listing and explanation from the work [SGC97].

3.2.1 Internal stability

It is the prior task for the controller to stabilize the closed loop system internally. This does not necessarily mean that the controller $K(s)$ itself is described by a stable system. A standard quadratic Lyapunov function ansatz for the homogeneous system part with:

$$V(x) := x^\top X x\,,\; X = X^\top > 0\,,$$

where x determines the compound closed-loop system state and X the Lyapunov variable, leads to the necessary condition:

$$\dot{V}(x) = x^\top \left(A_{\mathrm{cl}}^\top X + X A_{\mathrm{cl}}\right) x \overset{!}{<} 0 \;\Leftrightarrow\; A_{\mathrm{cl}}^\top X + X A_{\mathrm{cl}} < 0\,.$$

This expresses an additional constraint which is included in every LMI optimization problem for ensuring the stability. Note that A_{cl} contains the control parameters to be found, but remains independent of the respective channel selections $T_j(s)$.

3.2.2 H_2 performance and generalization

During the part 2.2.3 already a derivation for an LMI condition on the H_2 norm minimization has been made. Here, in terms of the j-th channel choice to be the respective H_2 one, the following optimization problem similar to statement (2.27) is obtained:

$$\min \|T_j\|_2^2 \quad \rightarrow \quad \min_{\nu,W,X} \nu \quad \text{s.t.:} \quad \mathrm{trace}(W) < \nu$$

$$\begin{pmatrix} A_{\mathrm{cl}}^\top X + X A_{\mathrm{cl}} & X B_{\mathrm{cl}}^j \\ (B_{\mathrm{cl}}^j)^\top X & -I \end{pmatrix} < 0\,,\; \begin{pmatrix} X & (C_{\mathrm{cl}}^j)^\top \\ C_{\mathrm{cl}}^j & W \end{pmatrix} > 0\,,\; D_{\mathrm{cl}}^j = 0\,,\; X > 0$$

Note that again there is no feedthrough on the H_2 channel allowed, which if possible can be obtained by an appropriate controller choice of D_K. The optimization problem

Tesis publicada con autorización del autor
No olvide citar esta tesis

contains of the variables $\nu > 0$, $X = X^\top$, $W = W^\top$. Because of the linear cost function $J(\nu, X, W) = \nu$ with LMI restrictions $F(\nu, X, W) > 0$ it is an excellent SDP example. Classically the H_2 norm minimization guarantees optimality in presence of Gaussian type disturbances and thus obtains good performance. An extension to this concept has bee made in [Rot93] by introducing the generalized H_2 norm in the form:

$$\|T_j\|_g := \sup \left\{ \|z_j(\tau)\| \,\middle|\, x(0) = 0,\, \tau > 0,\, \int_0^\tau \|w_j(t)\|_2^2 \, dt \leq 1 \right\}.$$

Minimizing this norm can be interpreted as keeping the peak amplitude of the output z_j over an unit-energy input w_j. It can also be referred to the loop gain from L_2 to L_∞ being below some specified level. A characterization is obtained by considering the following approach based on the Lyapunov function $V(x) = x^\top X x, X = X^\top > 0$. Supposing the following inequalities hold $\forall \tau \geq 0$ for a given $\alpha > 0$:

$$\|z_j(\tau)\|_2^2 \leq \alpha V(x(\tau)) \quad \wedge \quad V(x(\tau)) < \int_0^\tau \|w_j(t)\|_2^2 \, dt$$

the desired relation of $\|z_j(\tau)\|_2^2 < \alpha$ for $\|w_j\|_{L_2}^2 \leq 1$ is obtained and thus $\|T_j\|_g < \sqrt{\alpha}$. Minimizing α then leads to the minimal output peak amplitude.
The auxiliary step makes it easy to obtain an LMI characterization in the following manner. By integrating over

$$\begin{aligned} \dot{V}(x) < w_j^\top w_j \quad &\Leftrightarrow \quad x^\top \left(A_{\text{cl}}^\top X + X A_{\text{cl}} \right) x + x^\top X B_{\text{cl}}^j w_j + w_j^\top (B_{\text{cl}}^j)^\top X x - w_j^\top I w_j < 0 \\ &\Leftrightarrow \quad \begin{pmatrix} A_{\text{cl}}^\top X + X A_{\text{cl}} & X B_{\text{cl}}^j \\ (B_{\text{cl}}^j)^\top X & -I \end{pmatrix} < 0 \end{aligned}$$

the second inequality is obtained using $x(0) = 0$. The firs relation can be written as:

$$\begin{aligned} z_j(\tau)^\top z_j(\tau) \leq \alpha V(x(\tau)) \quad &\Leftrightarrow \quad 0 \leq x^\top \left(X - (C_{\text{cl}}^j)^\top \left(\frac{1}{\alpha} I \right) C_{\text{cl}}^j \right) x \\ &\Leftarrow \quad \begin{pmatrix} X & (C_{\text{cl}}^j)^\top \\ C_{\text{cl}}^j & \alpha I \end{pmatrix} > 0 \end{aligned}$$

which utilizes the Schur complement and requires $D_{\text{cl}}^j = 0$. Finally a similar optimization problem as in the H_2 case is found. Note that it is a special case with $W = \alpha I$ allowing an interpretation of the resulting optimization parameter α and creating a further restriction of the LMI bounds. Thus the generalized H_2 norm minimization is

Tesis publicada con autorización del autor
No olvide citar esta tesis

summarized as:

$$\min \|T_j\|_g^2 \quad \rightarrow \quad \min_{\alpha,X} \alpha \quad \text{s.t.} :$$
$$\begin{pmatrix} A_{\text{cl}}^\top X + X A_{\text{cl}} & X B_{\text{cl}}^j \\ (B_{\text{cl}}^j)^\top X & -I \end{pmatrix} < 0 \,, \begin{pmatrix} X & (C_{\text{cl}}^j)^\top \\ C_{\text{cl}}^j & \alpha I \end{pmatrix} > 0 \,, \, D_{\text{cl}}^j = 0 \,, \, X > 0$$

Again it can be computed as an SDP using less variables than in the usual H_2 case.

3.2.3 H_∞ performance

In comparison to the generalized H_2 norm, the H_∞ norm considers both, input w_j and output z_j, to be measured in the L_2 norm. It has been introduced in part 2.2.4 where the bounded real lemma is sketched in Theorem 2.9. This lead to the following LMI constrained for a given $\gamma > 0$:

$$\begin{pmatrix} A_{\text{cl}}^\top X + X A_{\text{cl}} & X B_{\text{cl}}^j & (C_{\text{cl}}^j)^\top \\ (B_{\text{cl}}^j)^\top X & -\gamma I & (D_{\text{cl}}^j)^\top \\ C_{\text{cl}}^j & D_{\text{cl}}^j & -\gamma I \end{pmatrix} < 0 \,, \quad X > 0$$

with the matrix variable $X = X^\top$. It has been derived by using passive concepts and can thus be related to general quadratic constraints presented in the following part 3.2.4. The H_∞ norm characterization is also crucial for robust stability guaranteeing shown in the part 3.2.6.

The upper LMI condition ensures the constraint $\|T_j\|_\infty < \gamma$ to be fulfilled if feasible. It can be minimized over γ and X for obtaining the optimal H_∞ norm. This results in a so called eigenvalue problem [Boy94]. Nevertheless, often it is not desirable to get the minimal norm bound because of eventual bad performance or control response, and in many cases it is simply hard to compute.

That is why most frequently the suboptimal H_∞ problem is approached to. This means to solve the LMI constraints for a specified value of γ obtained by previous considerations. One possibility is to calculate the optimal gain and take this as a point of orientation for selecting a bound with satisfying performance. Another choice can be made by depicting a mixed cost function different robust objectives are combined and weighted.

Tesis publicada con autorización del autor
No olvide citar esta tesis

3.2.4 Passivity

The concept of passive and dissipative control is extensively explained in [van96]. Its advantage is the occurrence of passive behavior in many physical systems, such as electrical networks or Lagrangian type mechanical systems, which can be connected to the Hamiltonian framework. There is a strong link to general energy considerations as passivity makes use of stored internal energy and supply rates.
This concept also has a close relation to the Lyapunov theory and can be seen as an extension. In the following passivity is defined briefly just utilizing the most important terminology for this work.

Definition 3.1 *Passive system [Kha02]*
A general nonlinear system Σ_{NL} from Equation (2.9) with $n_y = n_u$ is said to be passive if there exists a positive semidefinite function $V \in \mathcal{C}^1(\mathbb{R}^{n\times n}, \mathbb{R})$, called storage function, such that:

$$\dot{V}(x) = \frac{\partial V}{\partial x} f(x,u) \leq u^\top y\,, \quad \forall (x,u) \in \mathbb{R}^n \times \mathbb{R}^{n_u}\,.$$

Moreover, it is said to be strictly passive if there exists a positive definite function Ψ such that:

$$\dot{V}(x) \leq u^\top y - \Psi(x)\,.$$

The bound on the time derivative of the storage function V is referred to as supply rate.

For the LTI system in this case, using the passivity channel j with $n_{z_j} = n_{w_j}$, the standard storage function approach $V(x) := x^\top X x, X = X^\top > 0$ as in the former cases is made. Then the following LMI condition for a system to be passive can easily be derived by plugging in the system matrices:

$$\dot{V}(x) \leq w_j^\top z_j \quad \Rightarrow \quad \begin{pmatrix} A_{\mathrm{CL}}^\top X + X A_{\mathrm{CL}} & X B_{\mathrm{CL}}^j - (C_{\mathrm{CL}}^j)^\top \\ (B_{\mathrm{CL}}^j)^\top X - C_{\mathrm{CL}}^j & -\left((D_{\mathrm{CL}}^j)^\top + D_{\mathrm{CL}}^j\right) \end{pmatrix} \leq 0$$

Another point of view on passive systems can be made from the frequency domain. For the closed loop transfer function $T_j(s)$ being positive real, meaning $T_j(s) + T_j(s)* > 0\, \forall s : \mathrm{Re}(s) > 0$, is equivalent to a passive transfer behavior. This frequency domain property can be shown by using the positive real lemma (PRL), proven in [Kha02]. An extension to strict positive realness and thus a strict passive system is obtained with help of the Kalman-Yakubovich-Popov lemma. The strictness is important because it is equivalent to asymptotic stability of the system equilibrium.
Interestingly passivity this can be considered as a special case of a general quadratic

Tesis publicada con autorización del autor
No olvide citar esta tesis

constraint on w_j and z_j [SGC97]. These are of the form:

$$\int_0^\tau \begin{pmatrix} z_j(t) \\ w_j(t) \end{pmatrix}^\top \begin{pmatrix} U_j & W_j \\ W_j^\top & V_j \end{pmatrix} \begin{pmatrix} z_j(t) \\ w_j(t) \end{pmatrix} dt < 0$$

with problem dependent fixed matrices $U_j \geq 0$, $V_j = V_j^\top$ and W_j. Here, strict passivity corresponds to $U_j = 0$, $V_j = 0$, $W_j = -I$ which directly results in the integral form of the passive definition.
The H_∞ problem also forms a particular case of quadratic constraint choosing $U_j = \gamma^{-1} I$, $U_j = -\gamma I$, $W_j = 0$. Because of these two objectives being closely related, there are several common approaches to passive and H_∞ control. In [BL07] this forms the basis of a strategy constructing LMI conditions for this type of mixed objective task. Especially in this work including passivity into the control design is of interest. The approach is often used for flexible structures, such as the robot arm presented in Chapter 4, because it is comparable to a damping injection. This yields a good "natural" performance and guarantees certain robustness.

3.2.5 Nominal regulation

An important objective for control in general is reference tracking. This shall be achieved by regulating the channel j such that $\lim_{t\to\infty} z_j(t) = 0 \, \forall w_j \in \mathcal{W}_j$. It is required to know the dynamic system class generating the input signal:

$$\mathcal{W}_j = \left\{ w_j(\cdot) \,\middle|\, \dot{w}_j(t) = S w_j(t) \,,\, S \in \mathbb{R}^{n_{w_j} \times n_{w_j}} \right\}$$

The method of nominal regulation is based on [Fra76] and follows the *internal model principle*. Note that in this case no LMI is formulated but an extension of the controller structure is made, resulting in a higher order controller $K(s)$. This means that the disturbance model is included into controller estimate its ... and reject it from the output z_j.
The following assumptions are made to ensure the solubility of the regulation problem:

- $C_j = L_j C_z \stackrel{!}{=} C_y$,
- $D_j = L_j D_{zw} R_j \stackrel{!}{=} F_j = D_{yw} R_j$,
- $E_j = L_j D_{zu} \stackrel{!}{=} 0$,
- the pair $\left(\begin{pmatrix} A & B_j \\ 0 & S \end{pmatrix}, \begin{pmatrix} C_y & F_j \end{pmatrix} \right)$ is detectable.

Tesis publicada con autorización del autor
No olvide citar esta tesis

Clearly the first three requirements state that $z_j \equiv y$ and the last one is necessary for being able to track the disturbance asymptotically as part of an extended system. In the case of $\sigma(S) \subset \mathbb{C}^-$ the input decays naturally $\lim_{t\to\infty} w_j(t) = 0$ and thus no real regulation occurs.
First the control structure is composed into the following parts as shown in [SGC97]:

$$u = \left[\begin{array}{c|cc} S & 0 & I \\ \hline V & I & 0 \end{array}\right] \begin{pmatrix} v_1 \\ v_2 \end{pmatrix}, \quad \begin{pmatrix} v_1 \\ v_2 \end{pmatrix} = \left[\begin{array}{c|c} A_K & B_K \\ \hline \begin{matrix} C_{K1} \\ C_{K2} \end{matrix} & \begin{matrix} D_{K1} \\ D_{K2} \end{matrix} \end{array}\right] y =: \tilde{K}(s)\, y\,.$$

Thus the two auxiliary signals v_1, v_2 generated by a conventional control structure feed the extended control system which can be seen as an estimator of the input w_j. This system has the form:

$$\Sigma_{\hat{w}} \begin{cases} \dot{\hat{w}}_j = S\hat{w}_j + v_2\,,\ \hat{w}_j(0) = \hat{w}_{j,0} \\ u = v_1 + V\hat{w}_j \end{cases}.$$

It can be interpreted as an input observer which clarifies the detectability requirement. To determine the output matrix V of the internal model consider the following idea for constructing a system of equations. The regulation objective with respect to the augmented system for a pseudo-stationary state $\bar{x}$ is:

$$z_j = C_j\bar{x} + F_j w_j \stackrel{!}{=} 0\,.$$

For ensuring the existence of a solution to the regulation problem $\bar{x}$ is assumed have a linear relation to w_j:

$$\bar{x} =: -Uw_j \quad \Rightarrow \quad (-C_j + F_j)w_j = 0\,.$$

Now this is related to the pseudo-stationary dynamic plugging in $\dot{w}_j = Sw_j$ and $B_w w = B_j w_j$:

$$\dot{\bar{x}} = A\bar{x} + B_u(V\bar{w}_j + v_1) + B_w w \Rightarrow (AU - US)w_j = B_u V\bar{w}_j + B_j w_j + B_u v_1\,.$$

Tesis publicada con autorización del autor
No olvide citar esta tesis

The compensation goal is obtained for $\hat{w}_j = w_j$. In total this leads solving the linear system equations:

$$\begin{aligned} AU + B_u V - US &= B_j \\ C_y U &= F_j \end{aligned}$$

with matrix variables $U \in \mathbb{R}^{n \times n_{w_j}}$ and $V \in \mathbb{R}^{n_u \times n_{w_j}}$ for concluding the internal model approach. Here, we just apply this procedure in case there exists a unique solution to the problem. If there is an infinite number of solutions, the transformation applied in Section 3.3 is more difficult to be adapted because of a nonlinear problem arising [SGC97].
Now consider the extended plant structure including the disturbance model:

$$\begin{pmatrix} z \\ y \end{pmatrix} = \left[\begin{array}{cc|ccc} A & B_u V & B_w & B_u & 0 \\ 0 & S & 0 & 0 & I \\ \hline C_z & D_{zu} V & D_{zw} & D_{zu} & 0 \\ C_y & 0 & D_{yw} & 0 & 0 \end{array}\right] \begin{pmatrix} w \\ v_1 \\ v_2 \end{pmatrix} .$$

The auxiliary control structure $\tilde{K}(s)$ is designed and such that the extended system is stabilized and subject to the original design specifications. This guarantees the nominal regulation criterion to be fulfilled.
A special case which appears commonly in control problems is reference tracking using integral action. Thus for constant reference signals $w_j = r = \text{const.}$ the dynamics clearly are described by $S = 0$.
There is also the opportunity of extending this concept to robust regulation like mentioned in [SGC97]. It is a quiet interesting approach which is going too far for the application case treated in this work.

3.2.6 Robust stability

As already mentioned in the former part 2.2.4 regarding the H_∞ LMI characterization, it can be used for integrating robust stability into the design procedure. To do so, recapitulate the small-gain theorem from Section 2.4. The considered uncertainty $\Delta \in \mathbf{\Delta}$ is assumed to fulfill $\|\Delta\|_\infty \leq 1$. Then, for the closed loop system robust stability is assured if $\|M\|_\infty < 1$ with $z_\Delta = M(s) w_\Delta$.
In terms of the channel distinction in this chapter for channel j the following LMI

Tesis publicada con autorización del autor
No olvide citar esta tesis

condition is formulated:

$$\begin{pmatrix} A_{\mathrm{cl}}^{\top}X + XA_{\mathrm{cl}} & XB_{\mathrm{cl}}^{j} & (C_{\mathrm{cl}}^{j})^{\top} \\ (B_{\mathrm{cl}}^{j})^{\top}X & -I & (D_{\mathrm{cl}}^{j})^{\top} \\ C_{\mathrm{cl}}^{j} & D_{\mathrm{cl}}^{j} & -I \end{pmatrix} < 0\,, \quad X > 0\,.$$

Clearly this is a special form of the H_∞ criterion applied for $\gamma = 1$. This procedure is highly dependent on uncertainty modeling and the respective filter choice for normalization.
There are also several approaches to include robust performance as an LMI formulation. In the work from [YHF00] a robust H_2 performance synthesis method is presented. It makes use of linear multipliers to compute LMI bounds on the uncertainty.

3.3 Linearizing inertia-preserving transform

After characterizing the control specifications for the closed-loop system in form of matrix inequality, the actual optimization parameters have to be taken into account. Considering one common Lyapunov approach for all criteria results using $X \in \mathbb{R}^{(n+n_K)\times(n+n_K)}$ with $X = X^{\top} > 0$. Without the convention it is not possible to apply the upcoming transformation, which would lead to bilinear matrix inequalities (BMI) where the determination of a global optimal solution can not be guaranteed[Det01]. Unfortunately, this introduces extra conservatism to the problem as it forms an artificial coupling between the specifications for the benefit of better solubility. Furthermore, dependent on the channel, there are several auxiliary variables such as W, α or γ.
Additionally to this matrix variable there is the controller parameterization A_K, B_K, C_K, D_K which has to be determined. From the former derivations it can easily be seen that multiplications of these objective variables occur, for example in the form of $A_{\mathrm{cl}}^{\top}X + XA_{\mathrm{cl}}$. Actually this results in nonlinear terms and of course no LMI condition.
Therefore it is necessary to transform the problems into a linear relation. In terms of matrix inequalities it is desired to keep the inertia of the descriptive matrix when transforming. For a quadratic matrix M it is defined by:

$$\mathrm{inertia}(M) := \begin{pmatrix} \#\{\lambda \in \mathrm{eig}(M) \,|\, \mathrm{Re}(\lambda) > 0\} \\ \#\{\lambda \in \mathrm{eig}(M) \,|\, \mathrm{Re}(\lambda) < 0\} \\ \#\{\lambda \in \mathrm{eig}(M) \,|\, \mathrm{Re}(\lambda) = 0\} \end{pmatrix}.$$

Tesis publicada con autorización del autor
No olvide citar esta tesis

For a symmetric positive definite matrix this means to maintain positive definiteness after applying an inertia preserving transform. This technique is often used in LMI related control theory because it keeps up the desired property and thus the inequality relation.
Originally inertia-preserving matrices have been investigated in [BS91] where the application to hermitian and symmetric matrices was made clear. This corresponds to the quadratic forms in LMI theory.

3.3.1 Derivation idea

To introduce the necessary transformation the problem is separated into several steps. First the Lyapunov variable $X = X^\top$ shall be partitioned into a system and controller part in the following way:

$$X =: \begin{pmatrix} P & N \\ N^\top & \bar{P} \end{pmatrix}, \quad X^{-1} =: \begin{pmatrix} Q & M \\ M^\top & \bar{Q} \end{pmatrix}$$

where new matrix variables $P = P^\top, M, Q = Q^\top, N$ are introduced, whereas $\bar{P}, \bar{Q}$ do not play an important role. Thus the original symmetry is maintained. The proposed structure holds the following relation:

$$I = XX^{-1} = \begin{pmatrix} PQ + NM^\top & PM + N\bar{Q} \\ N^\top Q + \bar{P}M^\top & \bar{P}\bar{Q} + N^\top M \end{pmatrix} \Rightarrow \begin{cases} PQ + NM^\top = I \\ PM + N\bar{Q} = 0 \\ N^\top Q + \bar{P}M^\top = 0 \end{cases} \tag{3.3}$$

which needs X to be invertible, coming from the requirement of $X \overset{!}{>} 0$. Now consider the nonlinear term:

$$XA_{\mathrm{cl}} = \begin{pmatrix} P & N \\ N^\top & \bar{P} \end{pmatrix} \begin{pmatrix} A + B_u D_K C_y & B_u C_K \\ B_K C_y & A_K \end{pmatrix}$$

The idea is to make use of the identity result just shown in Equation (3.3). This motivates the proposed transformation matrix T:

$$T := \begin{pmatrix} Q & I \\ M^\top & 0 \end{pmatrix} \quad \Rightarrow \quad XT = \begin{pmatrix} PQ + NM^\top & P \\ N^\top Q + \bar{P}M^\top & N^\top \end{pmatrix} = \begin{pmatrix} I & P \\ 0 & N^\top \end{pmatrix}.$$

Tesis publicada con autorización del autor
No olvide citar esta tesis

Then the transposed transformation matrix is multiplied from the left-hand side:

$$A_{\mathrm{cl}}T = \begin{pmatrix} (A + B_u D_K C_y)Q + B_u C_K M^\top & A + B_u D_K C_y \\ B_K C_y Q + A_K M^\top & B_K C_y \end{pmatrix} .$$

Finally it is applied to the whole expression:

$$T^\top X A_{\mathrm{cl}} T = \begin{pmatrix} I & 0 \\ P & N \end{pmatrix} \begin{pmatrix} (A + B_u D_K C_y)Q + B_u C_K M^\top & A + B_u D_K C_y \\ B_K C_y Q + A_K M^\top & B_K C_y \end{pmatrix}$$

$$= \begin{pmatrix} AQ + B_u(D_K C_y Q + C_K M^\top) & A + B_u D_K C_y \\ P(A + B_u D_K C_y)Q + P B_u C_K M^\top + N B_K C_y Q + N A_K M^\top & PA + (P B_u D_K + N B_K) C_y \end{pmatrix}$$

$$=: \begin{pmatrix} A\mathbf{Q} + B_u \hat{\mathbf{C}} & A + B_u \hat{\mathbf{D}} C_y \\ \hat{\mathbf{A}} & \mathbf{P}A + \hat{\mathbf{B}} C_y \end{pmatrix}$$

where the following substitutions have been made:

$$\begin{aligned} \hat{\mathbf{A}} &= \mathbf{P}(A + B_u D_K C_y)\mathbf{Q} + \mathbf{P} B_u C_K M^\top + N B_K C_y \mathbf{Q} + N A_K M^\top , \\ \hat{\mathbf{B}} &= \mathbf{P} B_u D_K + N B_K , \\ \hat{\mathbf{C}} &= D_K C_y \mathbf{Q} + C_K M^\top , \\ \hat{\mathbf{D}} &= D_K . \end{aligned}$$

The introduction of new variables through substitution of nonlinear terms is common technique within the LMI framework. In this case linear inequalities are obtained with the new optimization variables $P, Q, \hat{A}, \hat{B}, \hat{C}, \hat{D}$ (marked bold). For the sill remaining unknown matrices, especially the controller matrices, a system of equations has to be solved which is shown in Section 3.4.
Other nonlinear terms and transform multiplications occurring in the control specifications for a particular channel j are:

$$T^\top X B^j_{\mathrm{cl}} = \begin{pmatrix} I & 0 \\ P & N \end{pmatrix} \begin{pmatrix} B_j + B_u D_K F_j \\ B_K F_j \end{pmatrix} = \begin{pmatrix} B_j + B_u \hat{\mathbf{D}} F_j \\ \mathbf{P} B_j + \hat{\mathbf{B}} F_j \end{pmatrix}$$

$$C^j_{\mathrm{cl}} T = \begin{pmatrix} C_j + E_j D_K C_y & E_j C_K \end{pmatrix} \begin{pmatrix} Q & I \\ M^\top & 0 \end{pmatrix} = \begin{pmatrix} C_j \mathbf{Q} + E_j \hat{\mathbf{C}} & C_j + E_j \hat{\mathbf{D}} C_y \end{pmatrix}$$

$$T^\top X T = \begin{pmatrix} I & 0 \\ P & N \end{pmatrix} \begin{pmatrix} Q & I \\ M^\top & 0 \end{pmatrix} = \begin{pmatrix} \mathbf{Q} & I \\ I & \mathbf{P} \end{pmatrix}$$

Tesis publicada con autorización del autor
No olvide citar esta tesis

Now all preliminaries for formulating an LMI optimization problem for the closed-loop system are made.

3.3.2 Application to control specifications

The actual transformation matrix applied to the symmetric structured inequalities has the form $\bar{T} := \mathrm{diag}(T, I)$. This is then used to transform the nonlinear matrix inequalities in the manner $\bar{T}^\top F(x)\bar{T} > 0$, which maintains the inertia. As a general requirement arising from $X > 0$, the first LMI:

$$\begin{pmatrix} \mathbf{Q} & I \\ I & \mathbf{P} \end{pmatrix} > 0 \tag{3.4}$$

must hold. Without extensive derivations the following LMIs are stated with respect to the considered design specifications from [SGC97]:

- **Internal stability:**

$$\begin{pmatrix} A\mathbf{Q} + B_u\hat{\mathbf{C}} + \mathbf{Q}A^\top + \hat{\mathbf{C}}^\top B_u^\top & \hat{\mathbf{A}}^\top + (A + B_u\hat{\mathbf{D}}C_y) \\ \hat{\mathbf{A}} + (A + B_u\hat{\mathbf{D}}C_y)^\top & \mathbf{P}A + \hat{\mathbf{B}}C_y + A^\top\mathbf{P} + C_y^\top\hat{\mathbf{B}}^\top \end{pmatrix} < 0$$

- **Generalized $\mathbf{H}_2$ performance:** $\min \alpha$ s.t. $\alpha > 0$,

$$\begin{pmatrix} A\mathbf{Q} + B_u\hat{\mathbf{C}} + \mathbf{Q}A^\top + \hat{\mathbf{C}}^\top B_u^\top & \hat{\mathbf{A}}^\top + (A + B_u\hat{\mathbf{D}}C_y) & B_j + B_u\hat{\mathbf{D}}F_j \\ \hat{\mathbf{A}} + (A + B_u\hat{\mathbf{D}}C_y)^\top & \mathbf{P}A + \hat{\mathbf{B}}C_y + A^\top\mathbf{P} + C_y^\top\hat{\mathbf{B}}^\top & \mathbf{P}B_j + \hat{\mathbf{B}}F_j \\ (B_j + B_u\hat{\mathbf{D}}F_j)^\top & (\mathbf{P}B_j + \hat{\mathbf{B}}F_j)^\top & -I \end{pmatrix} < 0\,,$$

$$\begin{pmatrix} \mathbf{Q} & I & (C_j\mathbf{Q} + E_j\hat{\mathbf{C}})^\top \\ I & \mathbf{P} & (C_j + E_j\hat{\mathbf{D}}C_y)^\top \\ C_j\mathbf{Q} + E_j\hat{\mathbf{C}} & C_j + E_j\hat{\mathbf{D}}C_y & \alpha I \end{pmatrix} > 0\,, \quad D_j + E_j\hat{\mathbf{D}}F_j = 0$$

- **Suboptimal $\mathbf{H}_\infty$ performance:** $\gamma > 0$,

$$\begin{pmatrix} A\mathbf{Q} + B_u\hat{\mathbf{C}} + \mathbf{Q}A^\top + \hat{\mathbf{C}}^\top B_u^\top & \hat{\mathbf{A}}^\top + (A + B_u\hat{\mathbf{D}}C_y) & * & * \\ \hat{\mathbf{A}} + (A + B_u\hat{\mathbf{D}}C_y)^\top & \mathbf{P}A + \hat{\mathbf{B}}C_y + A^\top\mathbf{P} + C_y^\top\hat{\mathbf{B}}^\top & * & * \\ (B_j + B_u\hat{\mathbf{D}}F_j)^\top & (\mathbf{P}B_j + \hat{\mathbf{B}}F_j)^\top & -\gamma I & * \\ C_j\mathbf{Q} + E_j\hat{\mathbf{C}} & C_j + E_j\hat{\mathbf{D}}C_y & D_j + E_j\hat{\mathbf{D}}F_j & -\gamma I \end{pmatrix} < 0$$

Tesis publicada con autorización del autor
No olvide citar esta tesis

- **Passivity:**

$$\begin{pmatrix} -\text{"}- & -\text{"}- & (B_j + B_u\hat{\mathbf{D}}F_j) - (C_j\mathbf{Q} + E_j\hat{\mathbf{C}})^\top \\ -\text{"}- & -\text{"}- & (\mathbf{P}B_j + \hat{\mathbf{B}}F_j) - (C_j + E_j\hat{\mathbf{D}}C_y)^\top \\ * & * & -(D_j + E_j\hat{\mathbf{D}}F_j) - (D_j + E_j\hat{\mathbf{D}}F_j)^\top \end{pmatrix} < 0$$

- **Robust stability:** for $\Delta \in \mathbf{\Delta}$

$$\begin{pmatrix} A\mathbf{Q} + B_u\hat{\mathbf{C}} + \mathbf{Q}A^\top + \hat{\mathbf{C}}^\top B_u^\top & \hat{\mathbf{A}}^\top + (A + B_u\hat{\mathbf{D}}C_y) & * & * \\ \hat{\mathbf{A}} + (A + B_u\hat{\mathbf{D}}C_y)^\top & \mathbf{P}A + \hat{\mathbf{B}}C_y + A^\top\mathbf{P} + C_y^\top\hat{\mathbf{B}}^\top & * & * \\ (B_j + B_u\hat{\mathbf{D}}F_j)^\top & (\mathbf{P}B_j + \hat{\mathbf{B}}F_j)^\top & -I & * \\ C_j\mathbf{Q} + E_j\hat{\mathbf{C}} & C_j + E_j\hat{\mathbf{D}}C_y & D_j + E_j\hat{\mathbf{D}}F_j & -I \end{pmatrix} < 0$$

With this catalog of applicable LMI constraints an SDP based optimization algorithm can be utilized for finding a common controller parameterization fulfilling all desired objectives (if feasible).

3.4 Multi-objective controller synthesis

Considering the closed-loop system containing a dynamic control structure based on output feedback and an additional channel distinction for performance objective characterization described by LMIs, the actual synthesis of the controller can be realized. Here, the main conclusion to the design algorithm is given and practical implementation issues shall be discussed.

3.4.1 Optimization procedure

After specifying the control objectives and linearizing the matrix inequalities an SDP optimization problem has to be solved for obtaining the required matrix variables $P, Q, \hat{A}, \hat{B}, \hat{C}, \hat{D}$. First, one has to define the appropriate cost function J to be minimized, $\min J(\ldots)$ s.t. LMIs. There are the following proposition for adequate choices:

- **One-sided control:** The most direct way for the upper framework is to use just one functional dependent on one of the optimization characteristics. This could be $J := \alpha$ for minimizing the generalized H_2 norm or $J := \gamma$ for obtaining the optimal H_∞ solution. Note that a SDP cost function has to be linear. Thus, a positiveness condition has to be included and no commonly used quadratic functions are allowed.

Tesis publicada con autorización del autor
No olvide citar esta tesis

The one-sided approach is useful in cases where one specific objective is really of major interest. However, this often leads to significant negative effects at other aspects, making it impossible to be realized. This holds inn particular if the control effort is not included.

- **Mixed characteristics:** To prevent such an unbalanced consideration a more weighted cost function can be selected. As an example $J := c_1\alpha + c_2\gamma$ with coefficients c_1, c_2 to be depict dependent on the desired penalizing effect. Here, the tuning can be an issue while giving additional degrees of freedom.
  Additionally one could add the trace of the auxiliary matrix for a conventional H_2 performance or introduce passivity indexes which have not be introduced in this work.

- **Preprocessing:** Like in the case of suboptimal H_∞ control, where the optimal value close to a borderline eventual would have lead to unsophisticated behavior, often a predefined choice of characteristic variables is made. This can happen based on knowledge about the system and related signals or by preprocessing. In fact, computing these values using the optimal framework gives an idea about the range or lower limitation on bounds like α and γ. Then a nearly optimal constant is depicted.
  Practically speaking, there are a lot of tests, synthesis attempts and test simulations involved in finding optimization parameters for the desired performance.

- **Numerical conditioning:** An alternative to strict cost formulations, eventually being numerically critical, is to consider the conditioning of the Lyapunov variable separation. Reconsider the constraint (3.4) emerging from the linearization with a slight modification:
  $$\begin{pmatrix} \mathbf{Q} & tI \\ tI & \mathbf{P} \end{pmatrix} > 0$$
  where $t \geq 1$ represents an additional optimization variable. This is equivalent to $t^2 I - PQ < 0$ and thus maximizing the value t results in a well-conditioned result as proposed by [SGC97].
  Of course this could also be included into a mixed cost function approach.
  In [Det01] the following extra step for a reasonable synthesis is proposed. Minimize b subject to:
  $$Q < bI\,,\; P < bI\,,\; \begin{pmatrix} bI & \hat{C} \\ \hat{C}^\top & bI \end{pmatrix} > 0\,,\; \begin{pmatrix} bI & \hat{D} \\ \hat{D}^\top & bI \end{pmatrix} > 0\,.$$

Tesis publicada con autorización del autor
No olvide citar esta tesis

This assures the norms of the matrix variables to be forced into a reasonable numerical range.

After choosing the appropriate type of cost characterization a numerical solving procedure has to be set up. In [BV09] a collection of the most important basics on algorithms with respect to convex optimization and SDPs in particular are presented. The main advantage of linear optimization problems subject to LMI constraints is the development of efficient interior point methods twenty years ago.
The work [WB00] introduced a algorithm framework for solving SDPs based on the works just mentioned. This resulted the MATLAB toolbox cvx [CVX12] which was used for the investigation during this work. It has the advantage of intuitive problem formulation and comprehensive output of data about the numerical procedure.
Recently an approach towards an exterior point algorithm for solving the mixed H_2/H_∞ problem has been presented [YYE15]. Although it just faces the state-feedback design, the work is capable of treating a nonlinear matrix inequality case. The idea could be an interesting way of avoiding the conservatism introduced by common methods.
Note that the solution to the mixed-objective robust control synthesis is computed offline in contrast to other optimal approaches. The result is a dynamical system which can be implemented easily while fulfilling all design specifications. This allows several iterations of the same optimization setup with slide changes and for example enabling mixed integer problems to be solved conventionally. Thus high complexity formulations become manageable.

3.4.2 Controller reconstruction

In the former Section 3.3 it is shown how to obtain linear inequality constraints for the respective design objectives. The idea is based on the substitution of nonlinear terms which have to be related back to the controller realization A_K, B_K, C_K, D_K after solving an SDP for $P, Q, \hat{A}, \hat{B}, \hat{C}, \hat{D}$.
First the common Lyapunov variable X shall be reconstructed by using the relation (3.3) implying:

$$NM^\top = I - PQ\,.$$

From the LMI condition (3.4) using the Schur complement $P > 0$ and $Q - P^{-1} > 0$ can be concluded, leading to $I - PQ < 0$ invertible This guarantees the upper equation in $N, M \in \mathbb{R}^{n \times n_K}$ always to be solvable, though not necessarily unique. The easiest choice of the controller order is to be equal to the order of the augmented system $n_K := n$, because it makes N and M square matrices and simplifies the system of

Tesis publicada con autorización del autor
No olvide citar esta tesis

equations. Then, due to the infinite number of solutions, one matrix can be chosen nonsingular and the other determined easily. For example:

$$M := I \quad \Rightarrow \quad N = I - PQ\,. \tag{3.5}$$

The interesting question occurs whether a more sophisticated usage of these additional degrees of freedom can be made, e.g. an extra optimization step. It is important to find nonsingular matrices N and M.
Now it is possible to recover the parameterization for the controller $K(s)$ (or $\tilde{K}(s)$ respectively) from the substitute definition:

$$\begin{aligned} D_K &= \hat{\mathbf{D}}\,, \\ C_K &= \left(\hat{\mathbf{C}} - \hat{\mathbf{D}} C_y \mathbf{Q}\right) M^{-\top}\,, \\ B_K &= N^{-1}\left(\hat{\mathbf{B}} - \mathbf{P} B_u \hat{\mathbf{D}}\right)\,, \\ A_K &= N^{-1}\Big(\hat{\mathbf{A}} - \mathbf{P}(A + B_u D_K C_y)\mathbf{Q} - \mathbf{P} B_u C_K M^{\top} - N B_K C_y \mathbf{Q}\Big) M^{-\top}\,. \end{aligned}$$

For this way of of direct solution it is important that N and M are invertible. In [SGC97] it is stated that this treatment does not introduce any additional conservatism to the problem.

3.4.3 Problem solubility

Especially in relation to AREs certain assumptions on the system have to be made, guaranteeing an analytical solution. Unfortunately, in optimization based numerical approaches this aspect is often left to the pure feasibility determination of the algorithm without offering an insight on the origin of the bad conditions. Therefore, some criteria in connection with the mixed $\mathrm{H}_2/\mathrm{H}_\infty$ control developed in [DZGB94] shall be stated.
A output-feedback design for the plant $P(s) = \left[\begin{array}{c|ccc} A & B_2 & B_\infty & B_u \\ \hline C_z & 0 & 0 & D_{zu} \\ C_y & D_{y2} & D_{y\infty} & 0 \end{array}\right]$ is considered.
The following assumptions have to be made:

(A1) (A, B_u) stabilizable and (A, C_y) detectable

(A2) $\mathrm{rank}_c\,(D_{zu})$ full with $\left[D_{zu} \,|\, D_{zu}^{\perp}\right]$ unitary (orthonormal basis)

(A3) $\mathrm{rank}_r\,(D_{y2})$ full with $R_0 := D_{y2} D_{y2}^{\top} > 0$ and $R_1 := D_{y\infty} D_{y\infty}^{\top} > 0$

Tesis publicada con autorización del autor
No olvide citar esta tesis

$$\textbf{(A4)}\ \operatorname{rank}_c \begin{bmatrix} A - j\omega I & B_u \\ C_z & D_{zu} \end{bmatrix} \text{ full } \forall \omega \in \mathbb{R}$$

$$\textbf{(A5)}\ \operatorname{rank}_r \begin{bmatrix} A - j\omega I & B_2 \\ C_y & D_{y2} \end{bmatrix} \text{ full } \forall \omega \in \mathbb{R}$$

Mainly, the solubility is related to the corresponding H_∞ problem. The first assumption is crucial for stabilizing a system by output-feedback in general. Condition 2 guarantees the control action to be included into the objective output, whereas the second part is of technical interest. Assumption (A3) is important for the solution of the H_2 part to be nonsingular. The last two points, considering different Rosenbrock matrices, are necessary for the corresponding Riccati equation to have a stabilizing solution.
In this work $D_{z\infty} \neq 0$ is permitted but was so far not considered to be included into the assumptions for an analytic solution. But nevertheless, clearly $D_{z2} = 0$ has to be guaranteed for obtaining a finite dimensional solution. For simplicity the system must not have a control-measurement feedthrough $D_{yu} = 0$, which in case could be enforced by integral action.

The numerical aspects of obtaining a feasible optimization problem have been investigated in [Det01]. It turns out that after exceeding a certain number of decision variables the available LMI solvers suffer of handling the problem form coming from the linearization approach. Therefor, a variable elimination idea has been established, capable of dealing with high dimensional problems at the expense of the loss of generality.

3.4.4 Model extensions and reducing conservatism

A common disadvantage of robust control design, such as H_∞ synthesis, is the augmentation of the controller dimension. So far the control system is required to have the same order as the considered system. This also includes the states of selected input and output filters, which for too many signals can grow in number quiet rapidly.
Another huge increase of controller states occurs in case of nominal regulation from part 3.2.5. It adds twice the dimension of the tracked input signal as it is part of the extended system to be stabilized as well as part of the controller realization in form of the internal model.
One approach to reduce the system order of the controller $K(s)$ is sketched in [SGC97]. Assume the control dimension to be less than the system dimension, thus $n_K < n$.

Tesis publicada con autorización del autor
No olvide citar esta tesis

With $k := n - n_K$ this results in the matrix variable adaption $N, M \in \mathbb{R}^{n\times(n-k)}$, where full column rank is assumed. Thus, for the transformation matrix $T \in \mathbb{R}^{(2n-k)\times 2n}$, introduced in Section 3.3, holds $\dim\Big(\ker(T)\Big) = k$. This leads to all characteristic multiplication terms, like $T^\top X A_{\mathrm{cl}} X$, to be zero on this subspace, which results in nonstrict LMIs at the end. In [Boy94] the impact of strict feasibility and conversion to strict LMIs is discussed. Generally, an investigation on a unique solution A_K, B_K, C_K, D_K of dimension $n - k$ has to be made in the particular case.
Another possibility is to use more general tools on model reduction, like intensively explained in [DP05], in beforehand to the controller synthesis. As the extended plant could possibly be of large dimension, a lower dimensional approximation can be found and used for designing $K(s)$. This can for example be done by canceling out unobservable or controllable system parts while keeping a similar input-output behavior, measured by an H_∞ norm error.

Beside the supposedly high dimensional solution there is the frequently mentioned problem of conservatism in connection with LMI based control procedures. The thesis [Det01] is dealing with LMI framework introduced by Carsten Scherer and concentrates on the application, practicability and implementation of the approach. This also includes reducing the conservatism introduced by one common Lyapunov variable for all specifications. In general the solution to the corresponding ARE X_0 forms the least conservative "bound" (in a symmetric matrix definiteness way) on matrices X fulfilling the respective ARI. For example considering the Lyapunov equation:

$$\forall X_0 : A^\top X_0 + X_0 A + Q = 0 \quad \Rightarrow \quad X_0 < X \ , \forall X : A^\top X + X A + Q < 0 \, .$$

The idea is to introduce a scaling between two Lyapunov variables of the form $X_2 = \beta X_1$ with the scalar β. Thus, the conservative common Lyapunov assumption is weakened significantly. Obviously this forms another nonlinearity and does no make direct SDP optimization possible. In that work, an extra line search algorithm over β is proposed. Although computationally expensive, the offline calculation for such multi-objective controllers, as already discussed, allows to realize this without too much additional effort.

Tesis publicada con autorización del autor
No olvide citar esta tesis

4 Flexible Robot Arm

The aim of this work is to design a controller for a flexible robot arm structure which basically is represented by a partial differential equation (PDE). It is desired to examine the structural properties of such an infinite dimensional system and the opportunities of robust control techniques in this context. This shall be compared to the work from [METH96] and their results.
Therefore, an LTI model is proposed based on reasonable assumptions which can be used for the robust control synthesis. Different configurations regarding included damping effects and the sensor concept are presented whose influence on the resulting performance is investigated.
All the tests and validation steps are done by simulation using MATLAB Simulink. Although there are no experimental results to varify characteristic effects, different order models are used for simulation and control design. Utilizing a higher order representation for the real system as for the control design, allows it to observe the influence of the simplifications made and eventually leads to undesired vibrations.

4.1 Modeling & simulation

First, an adequate system model has to be obtained that can be utilized for the control scheme and implemented. As one of the most detailed and profound works on obtaining and analyzing a distributed parameter model for the robot arm, [Kan90] forms the basis of this modeling process. In general this is performed in two steps: by using the Hamilton principle a comprehensive nonlinear system of differential equation is generated which then is made manageable by linearization and modal analysis.
In terms of partial differential equations it is not as straight forward to solve these numerically in comparison to ordinary differential equations. Therefore, the modal analysis is no just necessary for the control methodology, but also crucial for the simulative realization of the system.

Tesis publicada con autorización del autor
No olvide citar esta tesis

4.1.1 Beam equation derivation

There are several approaches for modeling such a flexible beam. The two most frequently used ones are the Timoshenko and the Euler-Bernoulli beam, which are both presented here. The difference between these descriptions depends on the accuracy required.
Generally, mechanical systems in robotics are often modeled by the Lagrange framework [DL15]. The idea can be derived from the Hamilton principle of virtual displacement which is used here directly obtain the model equations.

System setup

For this work, basically, the simplest case of an one-link flexible robot arm is considered. The system sketch with all important characteristics is shown in Figure 4.1. For

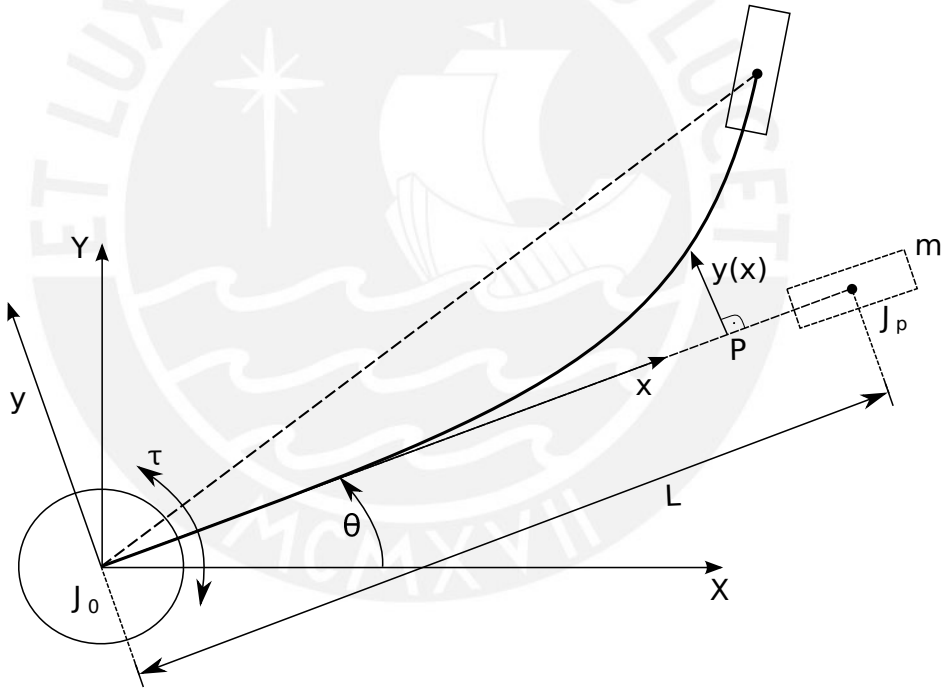

Figure 4.1: Structural scheme of one-link flexible arm with virtual displacement

the control purpose the torque $u(t) = \tau(t)$, generated by an electrical DC motor, is utilized for controlling the system. An important, and for rigid robotic systems most significant, state is the rotation angle $\theta(t)$. Usually, this determines uniquely the end-effector position. However, in the flexible case, the additional beam deformation $y(x,t)$ with respect to equilibrium line is included into the model.
The important geometric dimensions are the arm length L, load mass m, load inertia

Tesis publicada con autorización del autor
No olvide citar esta tesis

J_p and the hub inertia J_0. Furthermore, there are the material properties such as the density ρ, the cross-section area A, the elasticity measure Young modulus E and the cross-section inertia I.
For converting between the global coordinates (X, Y) and the generalized coordinates (x, y) the following simple kinematic relation can be found:

$$P(X,Y) = \begin{pmatrix} x\cos(\theta(t)) - w(L,t)\sin(\theta(t)) \\ x\sin(\theta(t)) + w(L,t)\cos(\theta(t)) \end{pmatrix} .$$

The deflection $y(x,t)$ is caused by bending $w(x,t)$ and shear $s(x,t)$ with the following slope description:

$$y'(x,t) = w(x,t) + s(x,t) .$$

Because of the cramped beam there are boundary conditions $y(0,t) = y'(0,t) = 0$. Typical parameter sets are given in Table 4.1. The values have been taken from the

Symbol	Meaning	Value	Unit
E	Young modulus	$1.96 \cdot 10^{11}$	$[N/m^2]$
I	cross-section inertia	$2.08 \cdot 10^{-12}$	$[m^4]$
A	cross-section area	$25 \cdot 10^{-6}$	$[m^2]$
L	arm length	0.25	$[m]$
T_h	link thickness	$1 \cdot 10^{-3}$	$[m]$
ρ	density	$10.667 \cdot 10^3$	$[kg/m^3]$
m	payload mass	0.2	$[kg]$
J_0	hub inertia	$1 \cdot 10^{-3}$	$[kg\,m^2]$

Table 4.1: System parameters for slewing arm model

experimental setup in [METH96].

Kinetic & potential energy

Now physical energy considerations are applied for obtaining a model in terms of differential equations. Thus, all the different energy types have to be expressed.
The kinetic energy contains three parts $T = T_1 + T_2 + T_3$. First, an auxiliary calculation is performed:

$$\dot{X} = -x\dot{\theta}\sin(\theta) - \dot{y}\sin(\theta) - y\dot{\theta}\cos(\theta)$$
$$\dot{Y} = x\dot{\theta}\cos(\theta) + \dot{y}\cos(\theta) - y\dot{\theta}\sin(\theta)$$

Tesis publicada con autorización del autor
No olvide citar esta tesis

which leads to:

$$\begin{aligned}\dot{X}^2+\dot{Y}^2 &= \sin^2(\theta)\left(x^2\dot{\theta}^2+\dot{y}^2+2x\dot{\theta}\dot{y}+y^2\dot{\theta}^2\right)+\cos^2(\theta)\left(x^2\dot{\theta}^2+\dot{y}^2+2x\dot{\theta}\dot{y}+y^2\dot{\theta}^2\right)\\ &\quad+\cos(\theta)\sin(\theta)\left(2xy\dot{\theta}^2+2y\dot{y}\dot{\theta}-2x\dot{\theta}^2y-2\dot{y}y\dot{\theta}\right)\\ &= x^2\dot{\theta}^2+\dot{y}^2+2x\dot{\theta}\dot{y}+y^2\dot{\theta}^2\end{aligned}$$

In the following the arguments are mainly left out for convenience, thus $y=y(x,t), w=w(x,t), s=s(x,t), \theta=\theta(t)$. The link energy itself contains of a translatory and a rotatory part which are integrals over the arm curve:

$$\begin{aligned}2T_1 &= \rho A\int_0^L\left(\dot{X}^2+\dot{Y}^2\right)dx+\rho I\int_0^L\left(\dot{w}(x,t)+\dot{\theta}(t)\right)^2dx\\ &= \rho A\int_0^L\left(\dot{\theta}^2y^2+x^2\dot{\theta}^2+2x\dot{\theta}\dot{y}+\dot{y}^2\right)dx+\rho I\int_0^L\left(\dot{w}(x,t)+\dot{\theta}(t)\right)^2dx\,.\end{aligned}$$

As hub is fixed, there is just a rotation energy component:

$$2T_2=J_0\dot{\theta}(t)^2\,.$$

For the payload, a distinction between translation and rotation is made with respect to its center of mass:

$$\begin{aligned}2T_3 &= m\left[\dot{X}^2+\dot{Y}^2\right]_{x=L}+J_P\left(\dot{w}(L,t)+\dot{\theta}\right)^2\\ &= m\left(\dot{\theta}^2y(L,t)^2+x^2\dot{\theta}^2+2x\dot{\theta}\dot{y}(L,t)+\dot{y}(L,t)^2\right)+J_P\left(\dot{w}(L,t)+\dot{\theta}\right)^2.\end{aligned}$$

Here, no gravitational influence is considered. That just leaves the potential energy component due to elastic deflection:

$$2V=EI\int_0^L(w')^2dx+kGA\int_0^L s^2dx\,,$$

where additional parameters, k $[-]$ a factor dependent on the cross-section shape and G $[N/m^2]$ the modulus of elasticity in shear, are introduced which will be dropped later.
Lastly, the work done by the applied input torque is given in form the virtual work:

$$\delta W=u(t)\delta\theta\,,$$

where δ denotes the variation operator explained in the following part.

Tesis publicada con autorización del autor
No olvide citar esta tesis

Hamilton principle

The Lagrange formalism and Hamilton's principle of virtual displacement are frequently used for the analysis of mechanical systems. In the following the general concept is introduced and applied to the flexible robot arm.
Therefor a revision of the variation concept and virtual displacement idea is made. In [Bed85] a comprehensive explanation regarding the subject of applying Hamilton principle is given, especially in connection with continuum mechanics. Variational calculus is based on the minimization of a certain integral defined subject to the considered problem. Here it is desired that the integral

$$I = \int_{t_1}^{t_2} (T - U + W) dt$$

to be minimized in the interval $[t_1, t_2] = [0, t]$. With the generalized coordinates $q_k(t)$ describing the system state an admissible comparison motion (comparison function) is defined:

$$q_k^*(t, \epsilon) := q_k(t) + \epsilon \eta_k(t)\,,$$

where $\eta_k \in \mathcal{C}^2([t_1, t_2])$ an arbitrary functions fulfilling $\eta_k(t_1) = \eta_k(t_2) = 0$. The principle of Hamilton now states that the upper integral value is stationary when $q_k^*(t, \epsilon) = q_k(t)$, which leads to the optimality condition:

$$\left[\frac{\partial I^*(\epsilon)}{\partial \epsilon}\right]_{\epsilon=0} \stackrel{!}{=} 0\,.$$

This motivates the notation of the variaton operater with respect to the comparison function in the following way:

$$\delta(\cdot) \equiv \left[\frac{\partial}{\partial \epsilon}(\cdot)^*\right]_{\epsilon=0}\,,$$

which obviously implies $\delta q_k = \eta_k$. Then the final variational condition can be formulated as:

$$\boxed{\int_{t_1}^{t_2} \delta(T - V + W) dt \stackrel{!}{=} 0}\,.$$

Some important relations for $T = T(q_k, \dot{q}_k), V = V(q_k)$ are:

- $\delta T = \frac{\partial T}{\partial q_k}\delta q_k + \frac{\partial T}{\partial \dot{q}_k}\delta \dot{q}_k$,
- $\delta V = \frac{\partial V}{\partial q_k}\delta q_k$,

Tesis publicada con autorización del autor
No olvide citar esta tesis

- $\delta W = Q_k\,\delta q_k$ with Q_k the generalized forces.

From the approach also the Lagrange method can be derived within a few more steps.

Now, the Hamilton technique of virtual displacement shall be applied to the flexible arm system whose energy have been characterized yet. To prepare the final calculation, first the term $s = y' - w$ is substituted into V and the variation operator δ is applied to the energy terms.

$$\begin{aligned}
\delta T_1 &= \rho A \int_0^L \left(\dot\theta y^2 + x^2\dot\theta + x\dot y\right) dx\delta\,\dot\theta + \rho A \int_0^L \dot\theta^2 y\,\delta y\,dx + \rho A \int_0^L \left(x\dot\theta + \dot y\right)\delta\dot y\,dx \\
&\quad + \rho I \int_0^L \left(\dot w + \dot\theta\right)\left(\delta\dot w + \delta\dot\theta\right) dx\,, \\
\delta T_2 &= J_0\dot\theta\,\delta\dot\theta\,, \\
\delta T_3 &= \left[m\left(\dot\theta y^2 + x^2\dot\theta + x\dot y\right)\delta\dot\theta + m\dot\theta^2 y\,\delta y + m\left(x\dot\theta + \dot y\right)\delta\dot y + J_P\left(\dot w + \dot\theta\right)\left(\delta\dot w + \delta\dot\theta\right)\right]_{x=L}\,, \\
\delta V &= EI\int_0^L w'\,\delta w' dx + kGA\int_0^L (y' - w)(\delta y' - \delta w) dx\,, \\
\delta W &= u\,\delta\theta\,.
\end{aligned}$$

The following auxiliary calculations help to put the problem into the proposed form. Consider the integral:

$$\int_{t_1}^{t_2}\left[A\,\delta\theta + \int_0^L B\,\delta y dx + \int_0^L C\,\delta w dx + D\,\delta y(L) + E\,\delta w(L)\right] dt \stackrel{!}{=} 0\,.$$

Because of the variations being able to take any values, the coefficients must all be zero, thus:

$$A, B, C, D, E \stackrel{!}{=} 0\,.$$

Using the original variation condition with the arbitrary closed time interval c:

$$\int_c \delta(T_1 + T_2 + T_3 - V + W) dt \stackrel{!}{=} 0$$

and taking the partial integral of terms containing time derivatives of $\delta\theta, \delta y, \delta w, \delta y(L), \delta w(L)$, a comparison to the upper form can be made. Examplarily the relation can be found by using:

$$\int_c f(y, \dot y, \theta, \dot\theta, \ldots)\delta\dot\theta\,dt = f\,\delta\theta\,\Big|_c - \int_c \dot f\,\delta\theta\,dt \stackrel{\delta\theta(\partial c)=0}{=} -\int_c \dot f\,\delta\theta\,dt\,.$$

Tesis publicada con autorización del autor
No olvide citar esta tesis

This then results in five equations containing an ODE, two PDEs and two boundary conditions (BC). Plugging in leads to:
(A)$\rightarrow \delta\theta$:

$$\ddot{\theta}\left(\left(\rho I L + \frac{L^3}{3}\rho A + J_0 + J_P + mL^2\right) + \rho A\int_0^L y^2 dx + my(L)^2\right)$$
$$+2\dot{\theta}\left(\rho A\int_0^L y\dot{y}\,dx + my(L)\dot{y}(L)\right) + \left(\rho A\int_0^L x\ddot{y}\,dx + mL\ddot{y}(L)\right)$$
$$+\left(\rho I\int_0^L \ddot{w}\,dx + J_p\ddot{w}(L)\right) = u$$

(B)$\rightarrow \int \delta y$:

$$kGA\Big(y'' - w'\Big) - \rho A\Big(x\ddot{\theta} + \ddot{y} - y\dot{\theta}^2\Big) = 0$$

(C)$\rightarrow \int \delta w$:

$$EI\,w'' + kGA(y' - w) - \rho I(\ddot{w} + \ddot{\theta}) = 0$$

(D)$\rightarrow \delta y(L)$:

$$m\Big(L\ddot{\theta} + \ddot{y}(L) - \dot{\theta}^2 y(L)\Big) + kGA\Big(y'(L) - w(L)\Big) = 0$$

(E)$\rightarrow \delta w(L)$:

$$J_P\Big(\ddot{w}(L) + \ddot{\theta}\Big) + EI\,w'(L) = 0$$

Remember the fixed beam boundary conditions $y(0,t) = y'(0,t) = 0$ or $w(0,t) = 0$ respectively, which have been used for partial integration over terms containing $\delta y'$ and $\delta w'$.
These ordinary equations, partial equations and boundary conditions describe the robot arm considering deformation under few physical assumptions. This quiet complicated mathematical model is called *Timoshenko* beam model.

Simplifications

The model shall be used for simulation and control design purposes. To handle the distributed parameter model in an easier way some simplifications have to be performed to allow analytical as well as numerical considerations.
First the effect of shearing and the rotation energy of the beam shall be neglected. This seems reasonable for arms with a small cross-section area and with relative stiff material, for which the shearing strain does not have to be taken into account. That means using the relations:

Tesis publicada con autorización del autor
No olvide citar esta tesis

- $s \equiv 0 \Rightarrow y' = w$,
- $kGA \int_0^L s^2 dx \equiv 0$ (term in potential energy V),
- results in (C)-equation terms to be substituted into (B)- and (D)-equation.

With help of that the much shorter nonlinear system of equations:

$$\begin{aligned}
&\ddot{\theta}\left(\left(\frac{L^3}{3}\rho A + J_0 + J_P + mL^2\right) + \rho A\int_0^L y^2 dx + my(L)^2\right)\\
&+ 2\dot{\theta}\left(\rho A\int_0^L y\dot{y}\,dx + my(L)\dot{y}(L)\right) + \left(\rho A\int_0^L x\ddot{y}\,dx + mL\ddot{y}(L)\right) = u\\
&EI\,y'''' + \rho A\Big(x\ddot{\theta} + \ddot{y} - y\dot{\theta}^2\Big) = 0\\
&EI\,y(L)''' - m\Big(L\ddot{\theta} + \ddot{y}(L) - \dot{\theta}^2 y(L)\Big) = 0\\
&y''(L) = 0
\end{aligned}$$

is found. This model is referred to as the *Euler-Bernoulli* beam.
To apply linear system theory methods the nonlinear system equations are linearized around the operational point of small deflection and angular velocity, thus $w, y, \dot{\theta} << 1$. Due to that higher order terms disappear and the following linear model of the flexible robot arm is obtained:

$$J\,\ddot{\theta}(t) + \rho A\int_0^L x\ddot{y}(x,t)\,dx + mL\ddot{y}(L,t) = u(t)\,, \tag{4.1}$$

$$EI\,y(x,t)'''' + \rho A\Big(x\ddot{\theta}(t) + \ddot{y}(x,t)\Big) = 0\,, \tag{4.2}$$

with the total inertia $J = (\rho AL^3/3 + J_0 + J_P + mL^2)$ subject to the BCs:

$$\begin{aligned}
&y(0,t) = y'(0,t) = 0\,,\\
&y''(L,t) = 0\,,\\
&EI\,y(L,t)''' - m\Big(L\ddot{\theta}(t) + \ddot{y}(L,t)\Big) = 0\,.
\end{aligned}$$

This is the common linear model used for the flexible arm, well investigated in the literature [DL15], although sometimes treated with a different BC ansatz. Now a modal analysis can be performed for analyzing the solution structure of the distributed parameter model and designing an adequate control procedure.
Sometimes a simpler version of the 1st dynamic equation of the linear representation can be found without an integral term. First the 2nd dynamic equation is multiplied

Tesis publicada con autorización del autor
No olvide citar esta tesis

by x and then integrated with respect to x over the interval $[0, L]$:

$$\rho A \int_0^L x\ddot{y}\, dx = -EI \int_0^L xy''''dx - \rho A \int_0^L x^2\, dx\, \ddot{\theta}$$
$$= -EI\, xy''' \Big|_0^L + EI\Big(y''(L) - y''(0)\Big) - \frac{\rho A L^3}{3}\, \ddot{\theta}\,.$$

Now plugging in the BCs leads to:

$$\rho A \int_0^L x\ddot{y}\, dx = -mL\Big(L\ddot{\theta}(t) + \ddot{y}(L,t)\Big) - EI\, y''(0) - \frac{\rho A L^3}{3}\, \ddot{\theta}\,.$$

Then the integral term in the 1st equation can be replaced which leads, due to cancalations, to the much simpler version of Equation (4.1):

$$(J_0 + J_P)\, \ddot{\theta}(t) - EI\, y''(0,t) = u(t)\,. \tag{4.3}$$

Depending on which system of equations seems more adequate for the current purpose, this or the original version of the linear system can be used.

4.1.2 Modal analysis

In the previous part a linear distributed parameter model has been developed. For being able to simulate the system and to design a controller it is crucial to know the form of the solution. Especially for the PDE case this is not as obvious as for ODEs. This investigation results in an infinite dimensional ODE which is approximated in terms of a finite representation.
For the flexible robot arm there are two approaches to tackle this problem [BO88]. Choosing the ansatz function for the separation of variables is part of the modeling procedure itself and depends on which effects are wanted to be investigated on.
In the following part the notation changes slightly due to common literature conventions. For the bending deformation y the variable w is used instead. Reconsider the system structure shown in Figure 4.2 adapted to the new circumstances. To summarize possible configurations used in literature to characterize the BCs, Table 4.2 presents the most significant examples. It is desired to use a solution procedure which is capable of handling arbitrary BC selections.
For the demonstrations in the following part a normalized, and thus dimensionless, system is utilized. This leaves the parameters mentioned in Table 4.1 to be treated as 1 and without dimension. Therefore, a qualitative analysis of the modeling approaches

Tesis publicada con autorización del autor
No olvide citar esta tesis

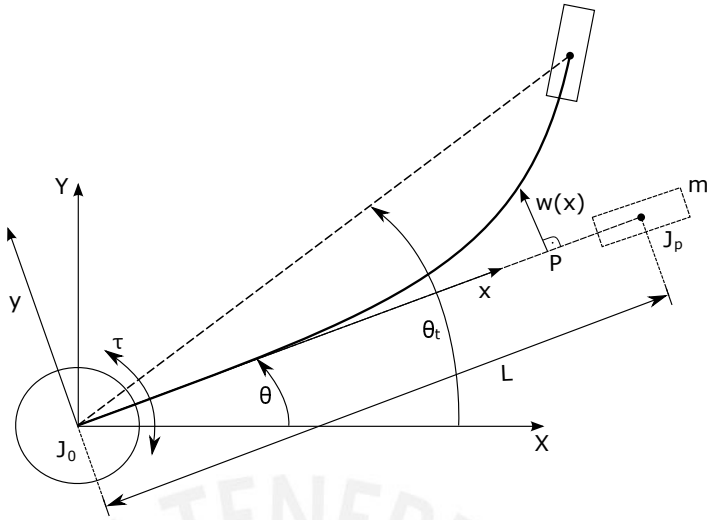

Figure 4.2: Flexible robot arm sketch for modal analysis

	Source	Boundary conditions	Interpretation
(BC1)	[METH96]	$w(0,t) = w'(0,t) = 0$	cramped beam
		$w''(L,t) = 0$	neglected shear
		$EI\, w'''(L,t) = m\Big(L\ddot{\theta}(t) + \ddot{w}(L,t)\Big)$	balance of shear forces at tip
(BC2)	[DL15]	$w(0,t) = 0$	fixed beam
		$EI\, w''(0,t) = J_0\Big(\ddot{\theta}(t) + \ddot{w}'(0,t)\Big) - u(t)$	balance of moments at base
		$EI\, w''(L,t) = -J_P\Big(\ddot{\theta}(t) + \ddot{w}'(L,t)\Big)$	balance of moments at tip
		$EI\, w'''(L,t) = m_p\Big(L\ddot{\theta}(t) + \ddot{w}(L,t)\Big)$	balance of shear forces at tip
(BC3)	[BO88]	$w(0,t) = w'(0,t) = 0$	cramped beam
		$w''(L,t) = w'''(L,t) = 0$	simplicity

Table 4.2: Possible boundary configurations

is performed.

Constrained mode method

The first ansatz is based on the initial assumption of a constrained hub $\ddot{\theta} \equiv 0$ without actuation $u(t) = 0$ [Kan90]. Under this condition, from (4.2) the system takes the form:

$$w''''(x,t) + \frac{A\rho}{EI}\, \ddot{w}(x,t) = 0\,, \tag{4.4}$$

which is a characterized as one linear partial differential equation of 4th order. Because of the linearity the well known separation of variables can be performed in the following

Tesis publicada con autorización del autor
No olvide citar esta tesis

manner:

$$w(x,t) =: \phi(x)q(t) \quad \Rightarrow \quad \frac{EI}{A\rho}\frac{\phi''''(x)}{\phi(x)} = -\frac{\ddot{q}(t)}{q(t)} \quad \stackrel{!}{=} \quad \text{const.} =: \omega^2 \,.$$

Choosing a strictly positive coefficient ω^2 is related to expected form of solutions. Thus, the dynamic equations become:

$$\ddot{q}(t) + \omega^2 q(t) = 0 \,, \tag{4.5}$$

$$\phi''''(x) - \frac{A\rho}{EI}\omega^2\,\phi(x) = 0 \,. \tag{4.6}$$

For determining the infinite eigenfrequencies, the BCs have to be included into the solving process. This results in an eigenfunction problem. The Equation (4.6) forms a boundary value problem (BVP) of fourth order with the general solution:

$$\begin{aligned}\phi(x) &= A\sin(\beta x) + B\cos(\beta x) + C\sinh(\beta x) + D\cosh(\beta x) \\ &= A\sin(\beta x) + B\cos(\beta x) + \left(\frac{C}{2} + \frac{D}{2}\right) e^{\beta x} + \left(-\frac{C}{2} + \frac{D}{2}\right) e^{-\beta x}\end{aligned}$$

with the eigenvalue $\beta^4 := \frac{A\rho}{EI}\omega^2$. Plugging the general solution into any BCs leads to a system of equations of the following form with the parameter vector $P = [A, B, C, D]^\top$:

$$\mathcal{A}(\beta)P = 0 \quad \Leftrightarrow \quad P \in \ker\Big(\mathcal{A}(\beta)\Big)$$

with the characteristic matrix $\mathcal{A}(\beta)$. This leads to the so-called *transcendental equation*:

$$\boxed{\det\Big(\mathcal{A}(\beta)\Big) \stackrel{!}{=} 0}, \tag{4.7}$$

which has to be solved for an infinite number of transcendental roots β_i and corresponding parameter set basis P_i. Note that Equation (4.7) has no polynomial form an is highly nonlinear, thus can only be solved numerically. In Figure 4.3 the respective eigenvalue solutions are plotted for several iterations. The comparison between the distinct BCs shows slight differences. In the following the results are generated just for (BC1) from Table 4.2. Generally, there seems to be a constant difference between to eigenvalues $\Delta\beta_i = \beta_{i+1} - \beta_i$ as expected. Although, there are some exceptions, these are considered to be numerical inaccuracies.

Now, for every eigenvalue β_i a solution ϕ_i can be calculated by determining $\ker\Big(\mathcal{A}(\beta_i)\Big)$. It has to be mentioned that this task is numerically challenging because of high powers of β_i appearing due two second and third order derivatives. This conditions the ma-

Tesis publicada con autorización del autor
No olvide citar esta tesis

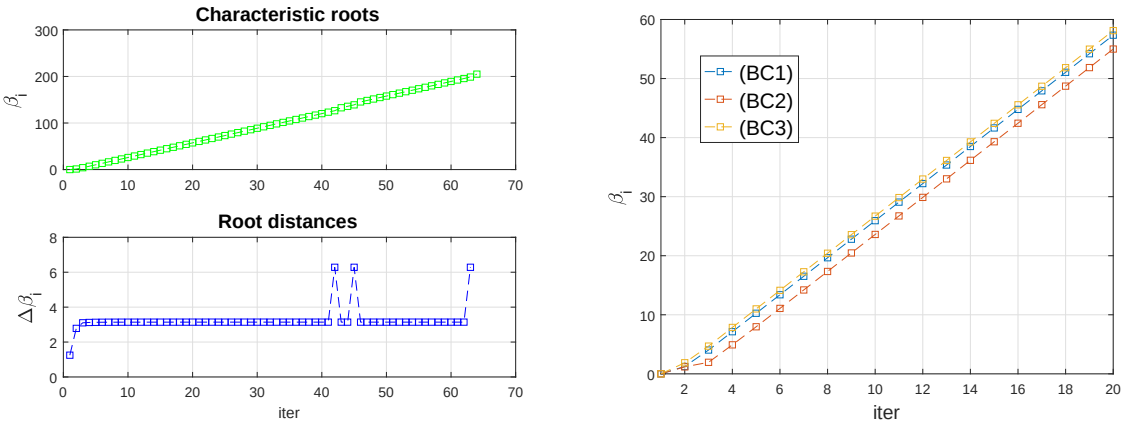

(a) Eigenvalues for (BC1) (b) Root comparison for different BCs

Figure 4.3: Transcendental roots in constrained mode

trix $\mathcal{A}$ very bad which is handled by row-wise normalization effectively. In the works mentioned in Table 4.2 analytic solutions are given.
Note that these solutions are not unique due to $\dim\ker\left(\mathcal{A}(\beta_i)\right) = 1$ and could be chosen in an arbitrary manner. Here, they are normalized such that

$$\|\phi_i\|^2_{L_2(0,L)} = \langle\phi_i, \phi_i\rangle_{L_2(0,L)} = \int_0^L \phi_i(x)^2 dx = 1$$

and a orthonormal function basis is obtained due to the orthogonality $\langle\phi_i, \phi_j\rangle = 0$ for $i \neq j$. The first few, most significant eigenmodes are illustrated in Figure 4.4. Thus

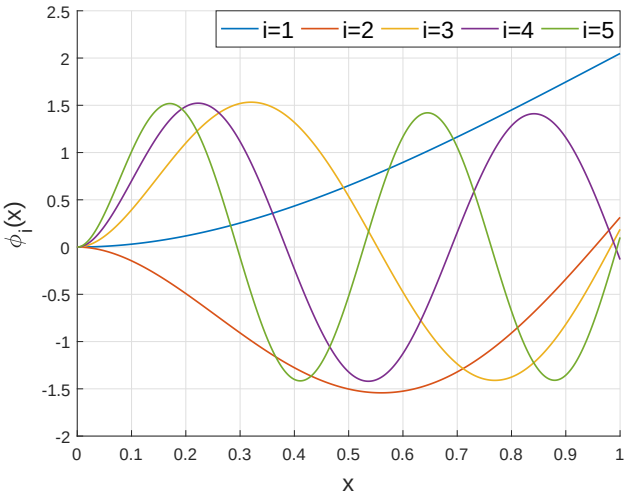

Figure 4.4: Eigenfunction examples $\phi_i(x)$ for constrained mode

Tesis publicada con autorización del autor
No olvide citar esta tesis

the solution of (4.4) can be represented as the infinite sum

$$w(x,t) = \sum_{i=1}^{\infty} \phi_i(x) q_i(t) \tag{4.8}$$

with respect to the characteristic eigenvalues-eigenfrequency relation $\omega_i = \sqrt{\frac{EI}{A\rho}}\,\beta_i^2$. Now, a solution for the non-homogeneous system shall be constructed. Therefor the approach is plugged into the original linear equations. Substituting the deformation form (4.8) into the dynamic equation (4.1) leads to:

$$\begin{aligned} & J\ddot{\theta}(t) + A\rho \sum_{i=1}^{\infty} \int_0^L x\phi_i(x)dx\, \ddot{q}_i(t) + mL \sum_{i=1}^{\infty} \phi_i(L)\ddot{q}_i(t) = u(t) \\ \Rightarrow \quad & J\ddot{\theta}(t) - \sum_{i=1}^{\infty} \omega_i^2 \left(A\rho \int_0^L x\phi_i(x)dx + mL\,\phi_i(L) \right) q_i(t) = u(t)\,. \end{aligned}$$

Here, equation (4.3) can also be used as an alternative to (4.1), which yet includes (BC1) for simplifications. Nevertheless, a similar system structure is generated.
Plugging the infinite sum for $w(x,t)$ into the PDE 4.2 and modulating the equation with $\phi_j, j \in \{1,2,\ldots\}$ over $[0,L]$ using the orthonormality yields:

$$\begin{aligned} & \sum_{i=1}^{\infty} \phi_i''''(x) q_i(t) + A\rho\, x\ddot{\theta}(t) + A\rho \sum_{i=1}^{\infty} \phi_i(x)\ddot{q}_i(t) = 0 \\ \Rightarrow \quad & \frac{A\rho}{EI}\,\omega_j^2\, q_j(t) + A\rho \int_0^L x\phi_j(x)dx\, \ddot{\theta}(t) + A\rho\, \ddot{q}_j(t) = 0\,. \end{aligned}$$

With substituting the coefficients, which can be determined by the knowledge of the eigenfunctions ϕ_i, into constants a_i, b, c_i, d_i the infinite dimensional ODE describing the dynamics has the following form:

$$\begin{aligned} & \ddot{\theta}(t) - \sum_{i=1}^{\infty} a_i q_i(t) = b\,u(t) \\ & \ddot{q}_j(t) + c_j q_j(t) + d_j \ddot{\theta}(t) = 0\,, \quad j \in \{1,2,\ldots\}\,. \end{aligned}$$

The simulation is performed for finite approximation of order N with the respective state vector:

$$z = [\theta\,,\, \dot{\theta}\,,\, q_1\,,\, \dot{q}_1\,,\, \ldots\,,\, q_N\,,\, \dot{q}_N]^\top\,.$$

Tesis publicada con autorización del autor
No olvide citar esta tesis

where the system dynamics in LTI matrix form $\dot{x} = Ax + Bu$ are given by:

$$A = \begin{pmatrix} 0 & 1 & 0 & 0 & \cdots & 0 & 0 \\ 0 & 0 & a_1 & 0 & \cdots & a_N & 0 \\ 0 & 0 & 0 & 1 & \cdots & 0 & 0 \\ 0 & 0 & -(c_1 + d_1 a_1) & 0 & \cdots & -d_1 a_N & \\ \vdots & \vdots & \vdots & \vdots & \ddots & \vdots & \vdots \\ 0 & 0 & 0 & 0 & \cdots & 0 & 1 \\ 0 & 0 & -d_N a_1 & 0 & \cdots & -(c_N + d_N a_N) & 0 \end{pmatrix}, \quad B = \begin{pmatrix} 0 \\ b \\ 0 \\ -d_1 b \\ \vdots \\ 0 \\ -d_N b \end{pmatrix}.$$

Simulating this finite dimensional approximation of the original system with an excitation of the form $u(t) = U \sin(\omega_u t)$ leads to the results presented in Figure 4.5 where the first four mode trajectories are plotted. One can see that the amplitude range highly

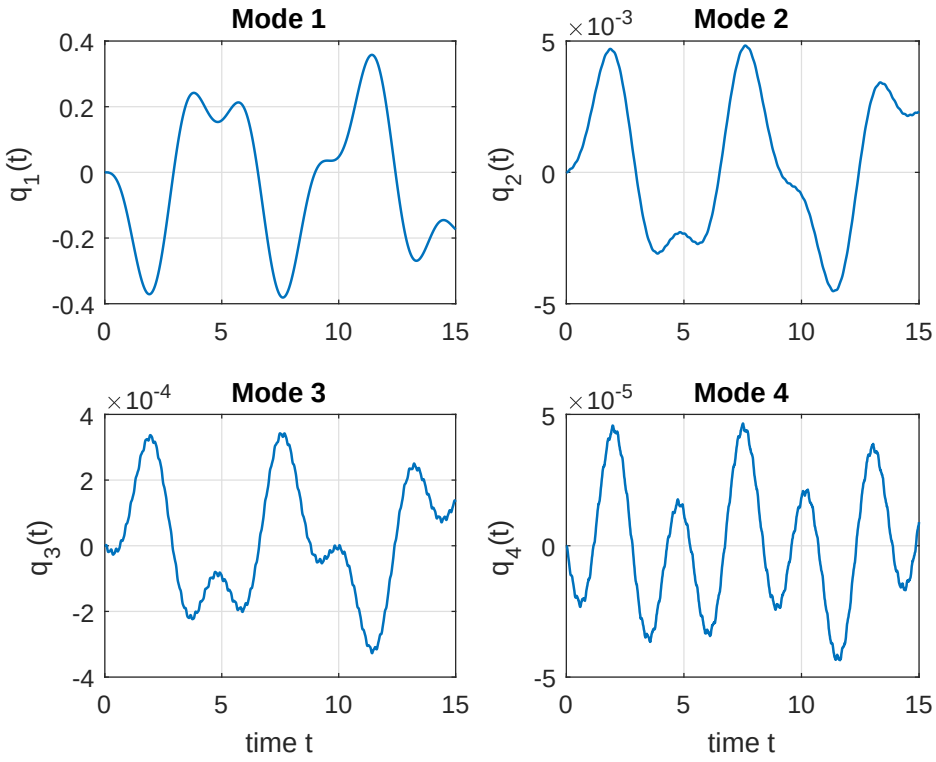

Figure 4.5: Mode solution examples $q_i(t)$ for constrained mode

decreases with the mode order. This loss of impact is evident for the approximation idea to leave higher mode components out. Another important observation is that because of the vastly coupled system dynamics each mode graph contains of several frequency components beside the excitation and its own eigenfrequency.

Tesis publicada con autorización del autor
No olvide citar esta tesis

Finally, the deformation can be simulated using the relation:

$$w(x,t) = \sum_{i=1}^{\infty} \phi_i(x) q_i(t) \approx \sum_{i=1}^{N} \phi_i(x) q_i(t)$$

resulting in the three dimensional plot from Figure 4.6. Some of the BCs, such as the

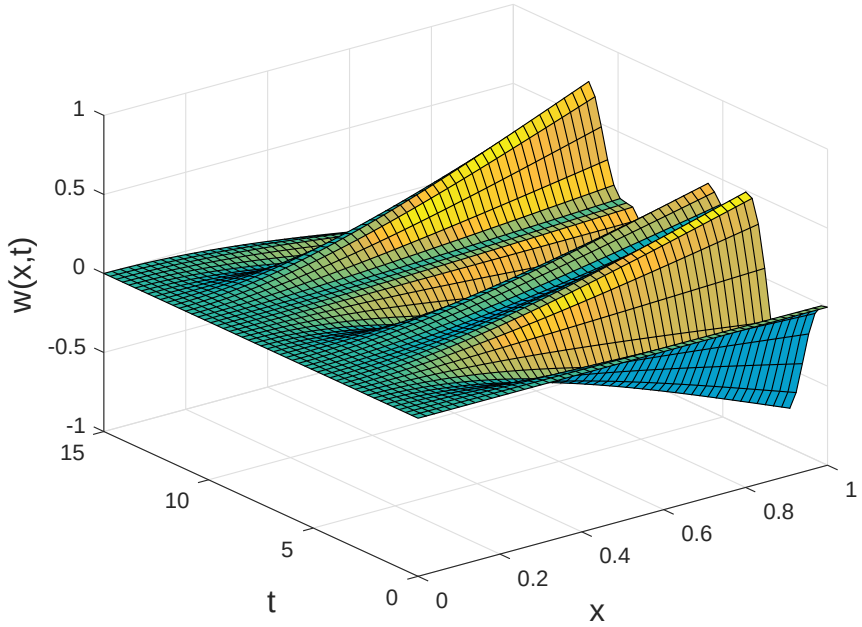

Figure 4.6: Resulting bending deformation $w(x,t)$ in constrained mode

crimped beam condition, can easily be recognized to be fulfilled. For referring these results directly to the flexible arm structure, the basic kinematic relation $(X,Y) = \left[x\cos(\theta(t)) - w(x,t)\sin(\theta(t))\,,\; x\sin(\theta(t)) + w(x,t)\cos(\theta(t))\right]$ is applied.
Overall, the constrained mode assumption is relatively strong but leads to simple precalculations due to the assumption of no direct effect of the deformation on the rotational hub. This can be interpreted as the result if a high hub inertia. On the other hand, a lots of couplings in the system dynamics with respect to the mode states are generated. Accordingly, the system gets complicated and stiff for large scale, thus hard to simulate. Therefore, this approach is hard to validate and not often used.

Unconstrained mode method

In comparison to the former approach, the unconstrained mode method does not rely on the fixed hub assumption. Though, the procedure is based on analog ideas. Sim-

Tesis publicada con autorización del autor
No olvide citar esta tesis

ilarly, the homogeneous system is considered first. The following ansatz for the state variables is made:

$$\begin{aligned}\theta(t) =& \eta(t) + \gamma\, q(t)\,,\\ w(x,t) =& \phi(x) q(t)\,.\end{aligned}$$

The basic assumption is a direct influence of the mode component q on the rotational angle θ. This introduces an extra degree of freedom in form of the parameter γ. It is chosen such that:

$$J\gamma + A\rho \int_0^L x\phi(x)dx + mL\,\phi(L) = 0\,,$$

which ensures the moment caused by deformation to vanish. Consequently, plugging this into (4.1) yields:

$$J\ddot{\eta}(t) + \left[J\gamma + A\rho \int_0^L x\phi(x)dx + mL\,\phi(L)\right] \ddot{q}(t) = u(t)$$

and thus, also considering (4.2) one gets:

$$\begin{aligned} J\ddot{\eta}(t) &= 0\,,\\ EI\,\phi''''(x)q(t) + A\rho\left(x\ddot{\eta}(t) + (\gamma x + \phi(x))\,\ddot{q}(x,t)\right) &= 0\,.\end{aligned}$$

Applying again the separation of variables principle holds:

$$\Rightarrow \quad \frac{EI}{A\rho}\,\frac{\phi''''(x)}{\gamma x + \phi(x)} = -\frac{\ddot{q}(t)}{q(t)} \quad \stackrel{!}{=} \quad \text{const.} =: \omega^2\,.$$

To obtain a homogeneous problem formulation the new variable $\Phi(x) := \phi(x) + \gamma x$ is substituted into this relation and the following characteristic ODEs are found:

$$\ddot{q}(t) + \omega^2 q(t) = 0\,, \tag{4.9}$$

$$\Phi''''(x) - \frac{A\rho}{EI}\,\omega^2\,\Phi(x) = 0\,, \tag{4.10}$$

where the BVP is adjusted for the (BC1) from Table 4.2:

$$\begin{aligned}&\Phi(0) = \Phi''(L) = 0\,,\\ &\Phi'(0) = \gamma\,,\\ &\Phi'''(L) = -\frac{m\omega^2}{EI}\,\Phi(L)\,.\end{aligned}$$

Tesis publicada con autorización del autor
No olvide citar esta tesis

The 3rd BC shall be reformulated independently of the auxiliary parameter γ. Therefore first, the new spatial variable Φ shall be related to γ with:

$$\begin{aligned} J\gamma &= -A\rho\int_0^L x\Big(\Phi(x)-\gamma x\Big)dx - mL\left(\Phi(L)-\gamma L\right) \\ &= -A\rho\int_0^L x\Phi(x)dx + A\rho\frac{L^3}{3}\gamma - mL\Phi(L) + mL^2\gamma \end{aligned} \tag{4.11}$$

$$\begin{aligned} \Rightarrow \quad (J_0+J_P)\,\gamma &= -\frac{EI}{\omega^2}\int_0^L x\,\Phi''''(x)dx - mL\Phi(L) \\ &= -\frac{EI}{\omega^2}\Big(x\Phi'''(x)\,\Big|_0^L - \int_0^L \Phi'''(x)dx\Big) - mL\Phi(L) \\ &= -\frac{EI}{\omega^2}\Big(L\Phi'''(L) - \Phi''(L) + \Phi''(0)\Big) - mL\Phi(L) \\ &\overset{BC}{=} -\frac{EI}{\omega^2}\Big(-\frac{mL\omega^2}{EI}\,\Phi(L) + \Phi''(0)\Big) - mL\Phi(L) \\ &= -\frac{EI}{\omega^2}\,\Phi''(0) \end{aligned} \tag{4.12}$$

Thus, the third BC can be stated easily as:

$$\frac{EI}{J_0+J_P}\,\Phi''(0) + \omega^2\Phi'(0) = 0\,.$$

which is referred to as (BC1'). Now, a homogeneous BVP has to be solved, similarly as for the constrained mode method with slightly changed BCs. The function ansatz again is:

$$\Phi(x) = A\sin(\beta x) + B\cos(\beta x) + C\sinh(\beta x) + D\cosh(\beta x)\,,$$

where $\beta^4 := \frac{A\rho}{EI}\,\omega^2$ the eigenvalue. Then the transcendental equation $\det\Big(\mathcal{A}(\beta)\Big) = 0$ is obtained by plugging this form into the (BC1'). The characteristic roots β_i are obtained as presented in Figure 4.3. With the same $L_2(0,L)$ normalization, but in this case of the respective auxiliary eigenfunctions Φ_i, where the eigenmodes shown in sub-figure 4.7 (a) are obtained. To relate these solutions back to the original eigenfunctions the coefficients γ_i are computed, either by using directly the definition (4.11) or the much simpler form (4.12). Those eigenmodes can be seen in sub-figure 4.7 (b).
Then the general solutions have the infinite sum representations:

$$w(x,t) = \sum_{i=1}^{\infty}\phi_i(x)q_i(t)\,, \quad \theta(t) = \eta(t) + \sum_{i=1}^{\infty}\gamma_i q_i(t)$$

Tesis publicada con autorización del autor
No olvide citar esta tesis

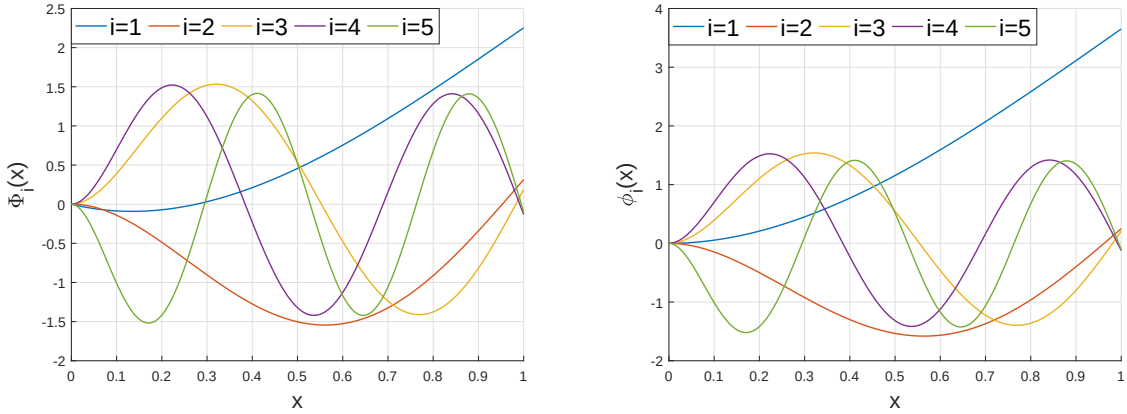

(a) Auxiliary eigenfunctions $\Phi_i(x)$ (normalized) (b) Original eigenfunctions $\phi_i(x) = \Phi_i(x) - \gamma_i x$

Figure 4.7: Eigenfunction examples for unconstrained mode method

with the eigenvalue-eigenfrequency pairing $\omega_i = \sqrt{\frac{EI}{A\rho}}\,\beta_i^2$. Thus, the non-homogeneous dynamic system formed by (4.1) and (4.2) is considered again with the new solution forms.

Plugging the solution into the first equation and using the property of γ_i leads to:

$$\begin{aligned} & J\ddot{\eta}(t) + \sum_{i=1}^{\infty}\left[J\gamma_i + A\rho\int_0^L x\phi_i(x)dx + mL\,\phi_i(L)\right]\ddot{q}_i(t) = u(t)\,, \\ \Rightarrow\quad & J\ddot{\eta}(t) = u(t)\,, \end{aligned}$$

and for second dynamic relation one obtains:

$$\begin{aligned} & EI\sum_{i=1}^{\infty}\phi_i''''(x)q_i(t) + A\rho\sum_{i=1}^{\infty}\Big(\gamma_i x + \phi_i(x)\Big)\ddot{q}_i(t) + A\rho\, x\ddot{\eta}(t) = 0\,, \\ \Rightarrow\quad & \sum_{i=1}^{\infty}\omega_i^2\Big(\gamma_i x + \phi_i(x)\Big)q_i(t) + \sum_{i=1}^{\infty}\Big(\gamma_i x + \phi_i(x)\Big)\ddot{q}_i(t) = -\frac{x}{J}\,u(t)\,, \\ \Leftrightarrow\quad & \sum_{i=1}^{\infty}\Phi_i(x)\Big(\ddot{q}_i(t) + \omega_i^2 q_i(t)\Big) = -\frac{x}{J}\,u(t)\,. \end{aligned}$$

Modulating the relation with Φ_j with respect to x over $[0, L]$ and using the orthonormality of the auxiliary eigenfunction $\langle\Phi_i, \Phi_j\rangle = 0\,\forall i \neq j$, $\langle\Phi_i, \Phi_i\rangle = 1$, as well as the definition of γ_j, the following relation is derived $\forall j \in \{1, 2, \ldots\}$:

$$\ddot{q}_j(t) + \omega_j^2 q_j(t) = -\frac{1}{J}\int_0^L x\,\Phi_j(x)dx\,u(t) = \underbrace{-\frac{1}{JA\rho}\left(\frac{EI}{\omega_j^2}\Phi_j''(0) + mL\Phi_j(L)\right)}_{=:k_j}u(t)\,.$$

Tesis publicada con autorización del autor
No olvide citar esta tesis

For realization purposes, a finite approximization of order N is performed resulting in the following states:

$$z = [\eta\,,\,\dot{\eta}\,,\,q_1\,,\,\dot{q}_1\,,\,\ldots\,,\,q_N\,,\,\dot{q}_N]^\top$$

with the LTI system state space representation:

$$A = \begin{pmatrix} 0 & 1 & 0 & 0 & \cdots & 0 & 0 \\ 0 & 0 & 0 & 0 & \cdots & 0 & 0 \\ 0 & 0 & 0 & 1 & \cdots & 0 & 0 \\ 0 & 0 & -\omega_1^2 & 0 & \cdots & 0 & \\ \vdots & \vdots & \vdots & \vdots & \ddots & \vdots & \vdots \\ 0 & 0 & 0 & 0 & \cdots & 0 & 1 \\ 0 & 0 & 0 & 0 & \cdots & -\omega_N^2 & 0 \end{pmatrix}, \quad B = \begin{pmatrix} 0 \\ 1/J \\ 0 \\ k_1 \\ \vdots \\ 0 \\ k_N \end{pmatrix}. \tag{4.13}$$

Now, there are no dynamic couplings between the modes, except for the common control input. Solving this ODE system for an excitation signal $u(t) = U\sin(\omega_u t)$ generates the trajectories presented in Figure 4.8. In this case one clearly notes that

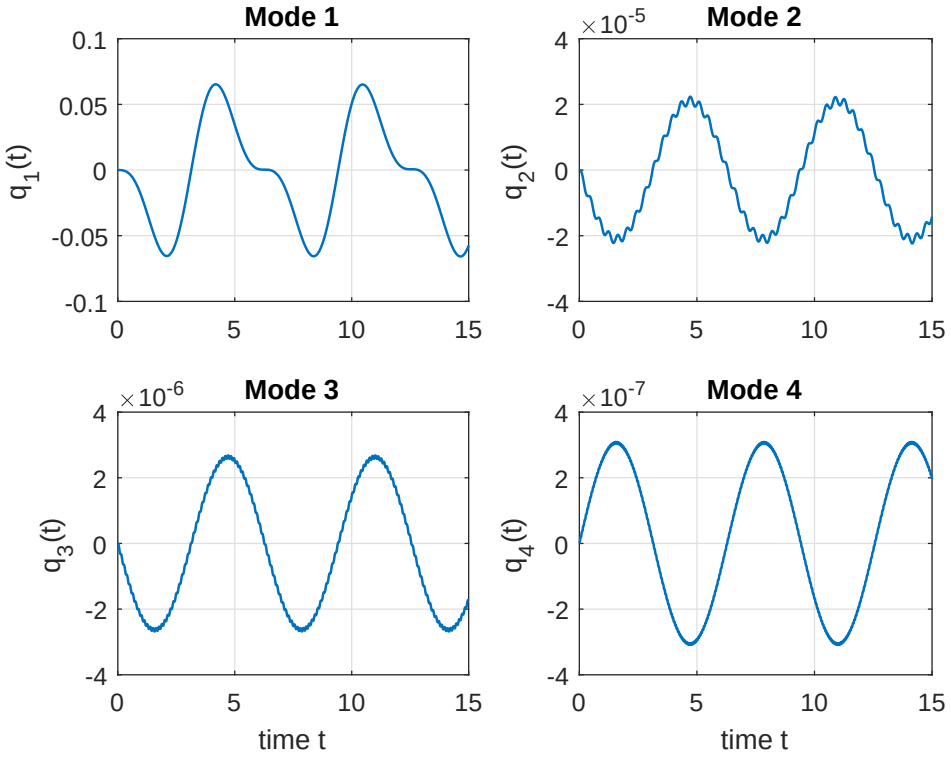

Figure 4.8: Mode solution examples $q_i(t)$ for unconstrained mode

Tesis publicada con autorización del autor
No olvide citar esta tesis

each mode just contains of the excitation frequency and its eigencomponent due to the uncoupled linear dynamical blocks in matrix A. As in the former subject, the high frequency modes lie in a small scale range.
With these numeric solutions the total deformation:

$$w(x,t) = \sum_{i=1}^{\infty} \phi_i(x) q_i(t) \approx \sum_{i=1}^{N} \phi_i(x) q_i(t)$$

can be computed, which has been realized in Figure 4.9. Notably, the constraints due

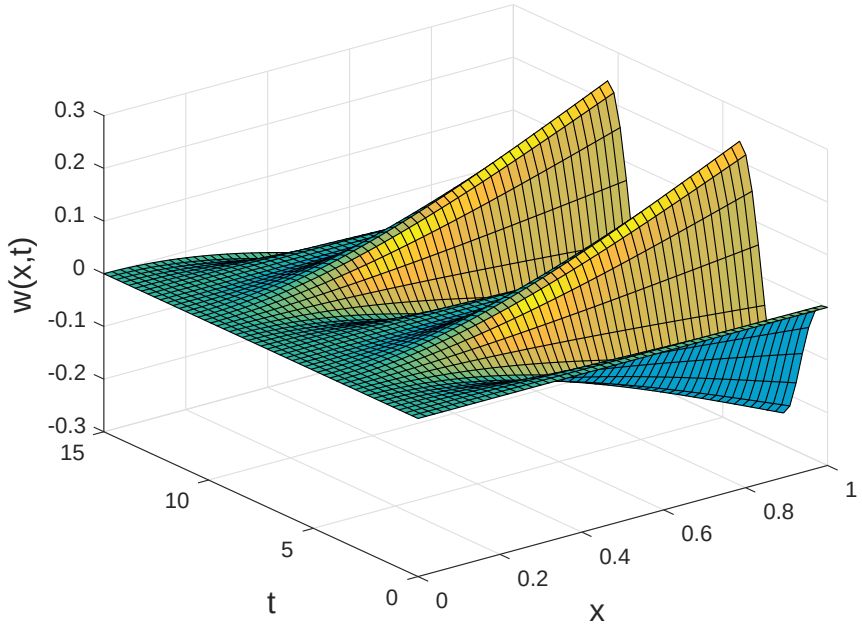

Figure 4.9: Resulting bending deformation $w(x,t)$ in unconstrained mode

to the BCs are valid. This time, the oscillation shape is more harmonic in comparison to Figure 4.6 because of the much simpler system of dynamic equations. The relation to the flexible arm structure is done by calculating the rotational angle:

$$\theta(t) = \eta(t) + \sum_{i=1}^{\infty} \gamma_i q_i(t) \approx \eta(t) + \sum_{i=1}^{N} \gamma_i q_i(t)$$

and utilizing again $(X,Y) = \Big[x\cos(\theta(t)) - w(x,t)\sin(\theta(t))\,,\; x\sin(\theta(t)) + w(x,t)\cos(\theta(t))\Big]$.
The unconstrained mode method is based on the more general assumption of a direct influence of the elastic deformation modes q_i on the rigid body motion represented by the rotational angle θ [BO88]. After difficult pre-considerations, a relatively simple

Tesis publicada con autorización del autor
No olvide citar esta tesis

model structure is obtained with purely decoupled mode dynamics, forming oscillatory blocks in the matrix A. This allows an efficient time simulation even for high model order.
This approach is most frequently used in the literature seems more reasonable than the constrained mode one. Therefore, it shall be selected as the utilized system structure in this work for simulation and control design based on (BC1).

Dynamic extensions

In [METH96] several extensions for the flexible robot arm model are mentioned. The arm is rotated by a DC motor and the respective back-electromotive force shall be included into the modelling approach. Consider the input law for the torque:

$$u(t) = \frac{K_t}{R_a}\left(v(t) - K_e\dot{\theta}(t)\right)$$

where K_t the torque constant, R_a the internal resistance and K_e the electromotive constant. Additionally the viscosity on the motor shaft/spindle $D\dot{\eta}$ and on arm and payload $2\zeta_i\omega_i\dot{q}_i$ shall be included.
For the unconstrained mode flexible arm model, plugging these extension in holds:

$$J\ddot{\eta}(t) + \left(\frac{K_tK_e}{R_a} + D\right)\dot{\eta}(t) + \frac{K_tK_e}{R_a}\sum_{i=1}^{\infty}\gamma_i q_i(t) = \frac{K_t}{R_a}\,v(t)$$
$$\ddot{q}_j(t) + \left(\frac{K_tK_e}{R_a}\sum_{i=1}^{\infty}\gamma_i\dot{q}_i(t) + 2\zeta_j\omega_j\,\dot{q}_j(t)\right) + \omega_j^2 q_j = k_j\frac{K_t}{R_a}\,v(t)\,.$$

Including the motor model and damping considers multiple effects of practical interest. Nevertheless, it introduces lots of couplings which can lead to problem and it remains unclear how to choose the mode damping factors ζ_i.
In several works, such as [Kan90] and [DL15], the extension to multiple link structures is explained. A similar approach to the Hamilton principle with additional rotational transformations can be used to obtain a higher order set of ODEs, PDEs and BCs. This seems very interesting for application issues, but goes too far in terms of this work, which is interested in investigating basic effects.

4.1.3 Validation

The obtained mathematical model is tested under realistic circumstances and evaluated for practical use. There is no available experimental data and thus the validation has to

Tesis publicada con autorización del autor
No olvide citar esta tesis

be done by reason. This includes to use the real parameterization and tryout different excitation scenarios.

Realistic parameter setting

After the qualitative demonstrations during the modal analysis, a quantitative evaluation of the model is performed. In order to do so, the parameters from the experiment in [METH96], which are shown in Table 4.1, are plugged into the linear model from (4.1) and (4.2). Based on that the modal approximation procedure generates an LTI system representation. In the following, again a sine wave signal $u(t) = U\sin(t)$ with $U = 0.05Nm$ (corresponds to $1V$ for the DC motor from the article) excites the system.

First, the constrained mode method is shown to be inappropriate for this system. In Figure 4.10 (a) the respective modes $q_i(t)$ and (b) the resulting deformation $w(x,t)$ are illustrated. The caused bending due to the vibrations is clearly negligibly small,

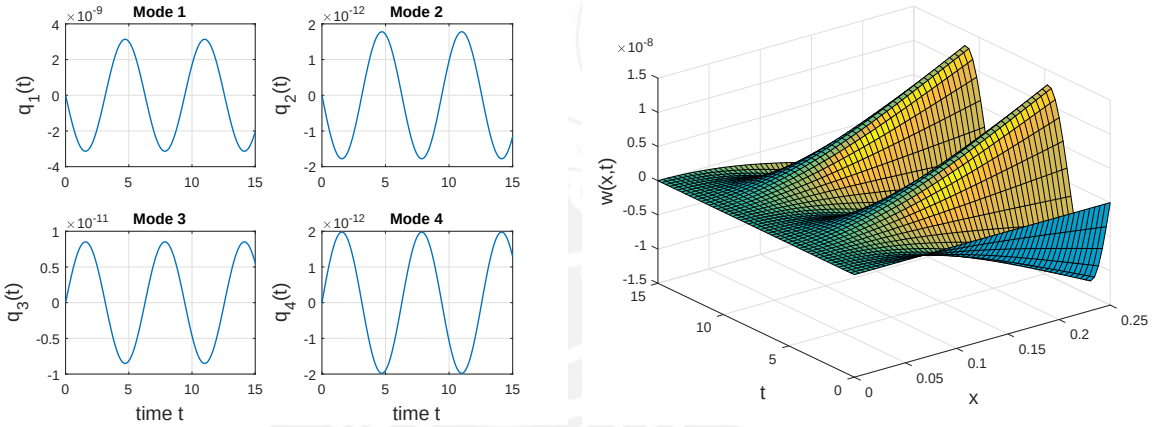

(a) Eigenmodes (b) Deformation

Figure 4.10: Constrained mode results for real system parameters

as the peak deformation is in the range of 10^{-8}. Remember that the constrained mode approach requires idealistically a very large hub inertia J_0, which is no given in this case. Thus, it does not serve for investigations on vibrations here.

That is why for this work, only unconstrained mode model has been implemented. As before, the BVP related to the spatial boundary conditions has to be solved. In Figure 4.11 the auxiliary and original eigenfunctions are plotted for the first five modes. Of course, the auxiliary functions have been normalized $\|\Phi\|_{L_2(0,L)} = 1$. Note that this time, the first mode ϕ_1 has an significant impact. To get an impression of the eigendynamics, Table 4.3 lists the corresponding eigenfrequencies ω_i for the first seven modes,

Tesis publicada con autorización del autor
No olvide citar esta tesis

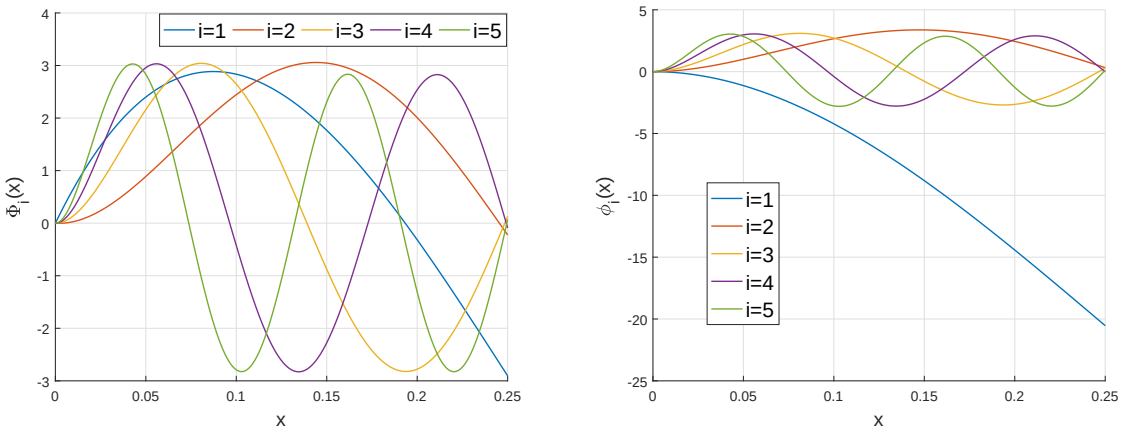

(a) Auxiliary eigenfunctions $\Phi_i(x)$ (b) Original eigenfunctions $\phi_i(x)$

Figure 4.11: Unconstrained mode eigenfunction constellations for real parameters

which are obtained by solving the transcendental equation (4.7). The high frequencies

Mode number i	1	2	3	4	5	6	7
Eigenfrequency $\omega_i\,[rad/s]$	52.7	316.2	996.5	$2.1 \cdot 10^3$	$3.5 \cdot 10^3$	$5.4 \cdot 10^3$	$7.6 \cdot 10^3$

Table 4.3: Eigenfrequencies ω_i of real flexible arm (unconstrained mode)

in the unnormalized case are likely to lead to stiff systems and cause numerical issues. Thus, stiff solvers are recommended when implementing a system of higher order. With respect to these characteristics, the time-dependent eigenmodes q_i are calculated by solving the ODE system (4.13). They are presented in Figure 4.12. The entire trajectories are shown in (a). In comparison to Figure 4.10 (a), the scale lies within a realistic margin. Most notably, the excitation frequency can be recognized. The zoom in part (b) demonstrates the vibrations due to the respective eigenfrequency. Note the different range of the time axes.

By combining the spatial eigenfunctions $\phi_i(x)$ and time-domain eigenmodes $q_i(t)$, the deformation $w(x,t)$ can be calculated. The deformation plot from Figure 4.13 confirms the reasonability of the unconstrained approach. With a peak bending deformation of around $3cm$, a significant impact of the flexibility on the actual robot arm is expected. Still, the deformation is small enough to give admission to the model. This can be observed more clearly when considering Figure 4.14. It presents the flexible arm working space in global coordinates (X, Y) and the position at the end of simulation time $t = 15s$. The equilibrium arm position, which forms the reference for the local x axis, is marked by a dashed line. A noticeable bending is observed considering the elastic

Tesis publicada con autorización del autor
No olvide citar esta tesis

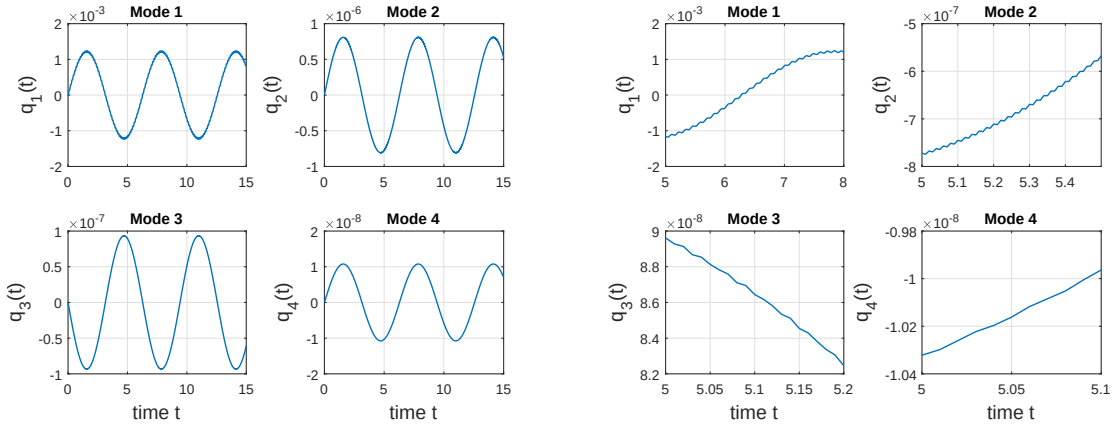

(a) Eigenmodes $q_i(t)$ (b) Zoom showing eigenfrequency-oscillations

Figure 4.12: Unconstrained mode eigenmodes for real parameters

arm, which is sampled in blue. Such a result is comprehensible for the applied torque dimension.

In direct comparison to the referenced work [METH96] one can state, that similar results are obtained. The eigenfrequencies correspond and the transfer behavior is just slightly different, because of the considered damping. Here, no damping shall be included because of simplicity and to investigate the oscillatory effects directly.

Excitation scenarios

Additionally, the obtained system is examined for different test scenarios. The excitation signals simulate real practical conditions, as well as difficult circumstances, which probably harm the system security.

The first scenario starts with a linearly rising torque applied to the system for the first few seconds. This is sufficiently smooth for not exciting any oscillations in the first place, which can be observed in Figure 4.15. Two different mode plots can are presented. In (a), the input torque is kept constant with $u(t) = 0.04Nm \, \forall t \geq 10s$ instead of continuing to rise linearly. This leads to a steady deformation, which is illustrated in Figure 4.16. There, the steady state bending is presented for the entire flexible arm structure.

In opposite to that, Figure 4.15 (b) demonstrates what happens in case of a sudden break after accelerating. This leaves the modes in a new initial state without excitation, which causes them to oscillate with their eigenfrequency. Such a vibratory behavior is undesired and thus, unsteady input signals should be avoided. In terms of the validation, this reflects the sensitive character of undamped system.

Tesis publicada con autorización del autor
No olvide citar esta tesis

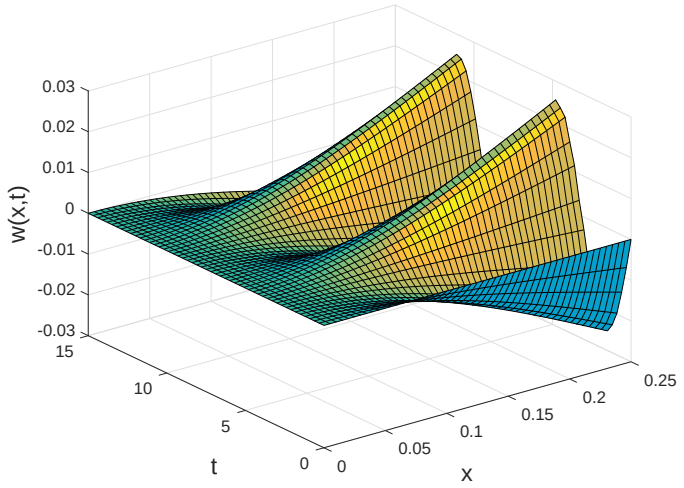

Figure 4.13: Bending deformation $w(x,t)$ for unconstrained mode with real parameters

To take a closer look at the decoupled homogeneous system dynamics, the is excited by initializing the mode states $q_{0,i} \neq 0$. The results are presented in Figure 4.17. As expected, similar eigendynamics are observed in (a). The relatively large frequency values shown in Table 4.3 result in rapidly oscillating bending deformation as seen in subfigure (b).
When dealing with undamped systems of second order, resonances can cause large problems resulting in a destabilization. The infinite dimensional nature of the real system leads to an infinite number of resonance frequencies that occur as large peaks in the bode plot. In Figure 4.18 the deformation plots for a resonance excitation with the first two eigenfrequencies are presented. In both cases an unstably growing amplitude can be noticed. The first mode resonance in (a) is causing larger deformation as (b), while both are excited with the same amplitude.
The observed reactions towards the proposed excitation signals show that the oscillation behavior appears, that is desired to be investigated in a control context. Furthermore, a realistic scaling with respect to the physical parameterization can be observed.

Parameter variations

A brief demonstration on the variation of one important parameter is made to complete the validation considerations. The elasticity of the flexible arm is significantly influenced by the Young modulus E. It represents the structural stiffness against rotation due to bending. Figure 4.19 shows a comparison between the trajectories of the

Tesis publicada con autorización del autor
No olvide citar esta tesis

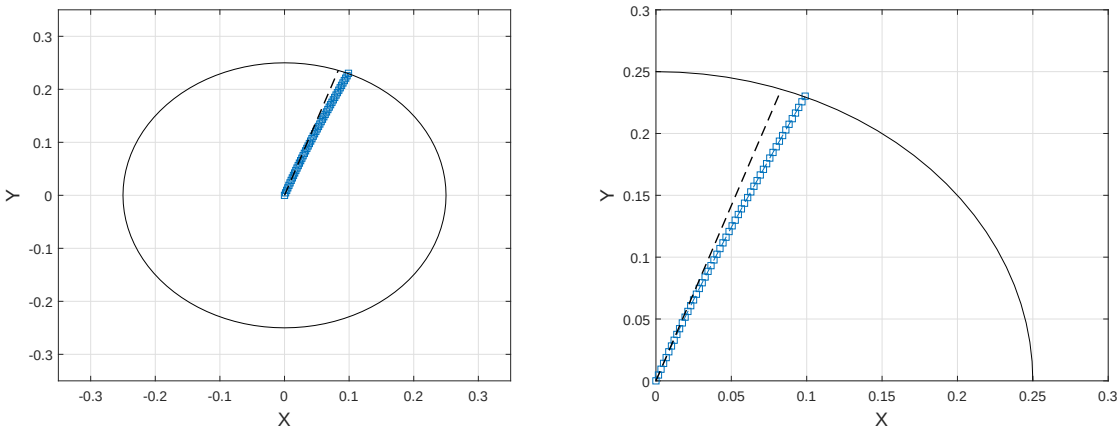

(a) Entire working space (b) End-position quadrant

Figure 4.14: Flexible arm structure in unconstrained mode after excitation

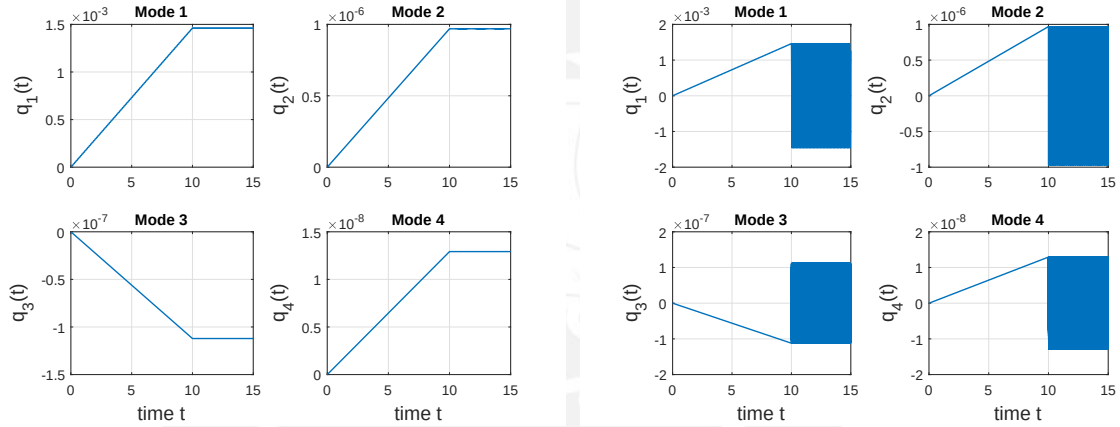

(a) Constant torque after acceleration (b) Sudden break after acceleration

Figure 4.15: Eigenmodes for different acceleration scenarios

mode $q_i(t)$ for different values of E. It is easy to notice that decreasing the modulus E leads to less stiffness and stronger vibrations of the first mode. Beside the increased amplification of the excitation signal, the eigenmodes become more significant as well. This forms another evidence for the accuracy of the mathematical model.

4.2 Control analysis & objectives

In anticipation of Chapter 5, some control characteristics of the flexible robot arm shall be discussed. It is pointed out that there is a very close related to the modeling process in terms of robust control, as it forms the basis for the robustness and uncertainty analysis.

Tesis publicada con autorización del autor
No olvide citar esta tesis

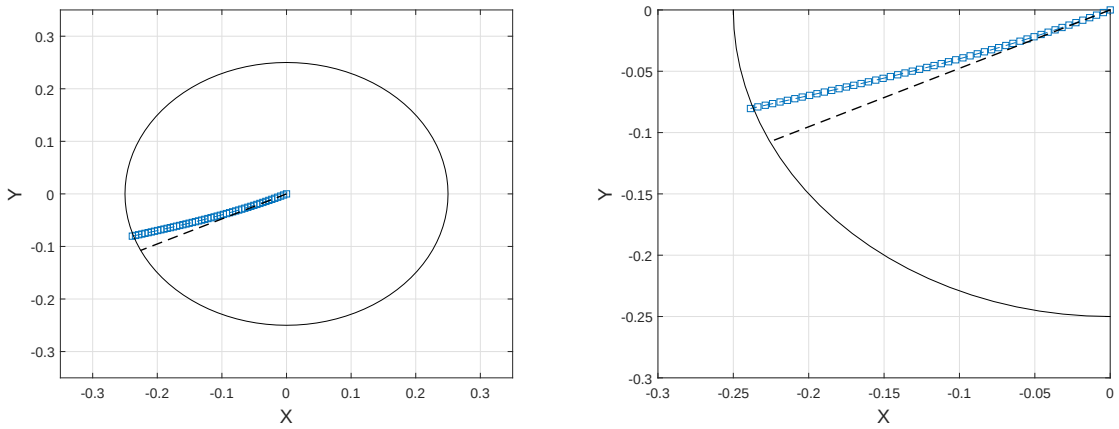

(a) Entire working space (b) End-position quadrant

Figure 4.16: Flexible arm structure after constant torque applied smoothly

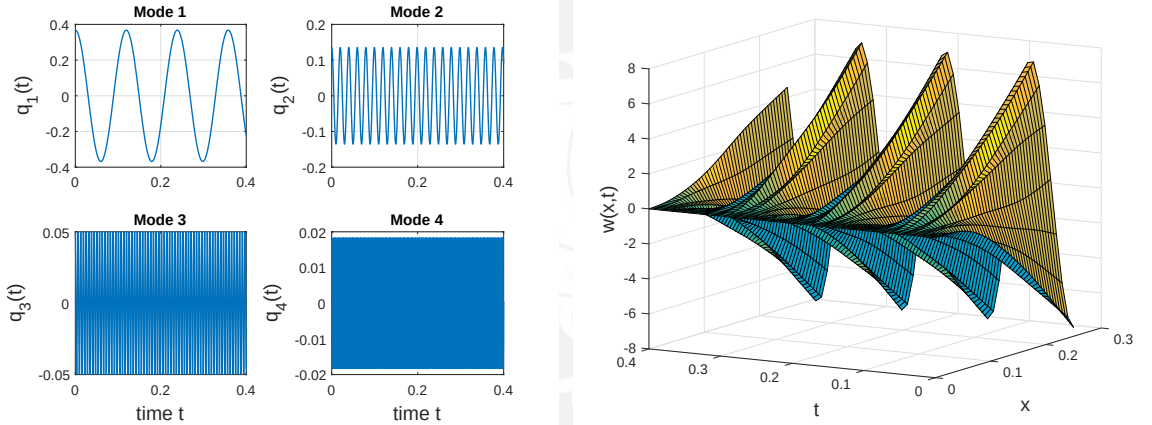

(a) Respective decoupled eigendynamics (b) Deformation from different start position

Figure 4.17: Excitation by non-zero initial state z_0

Therefor, the different system configurations shall be examined in terms of system theoretic characteristics. Then, dependent on these results, the control tasks shall be formulated more detailed. This is accompanied by specifying the possible sensor concepts and formulating related optimization problems, as they are not strictly predefined in this work.

4.2.1 Controllability & observability

The central system properties for a more sophisticated controller synthesis are controllability and observability. This is especially interesting to be characterized for an arbitrary order system of dimension N. For the following investigation consider the

Tesis publicada con autorización del autor
No olvide citar esta tesis

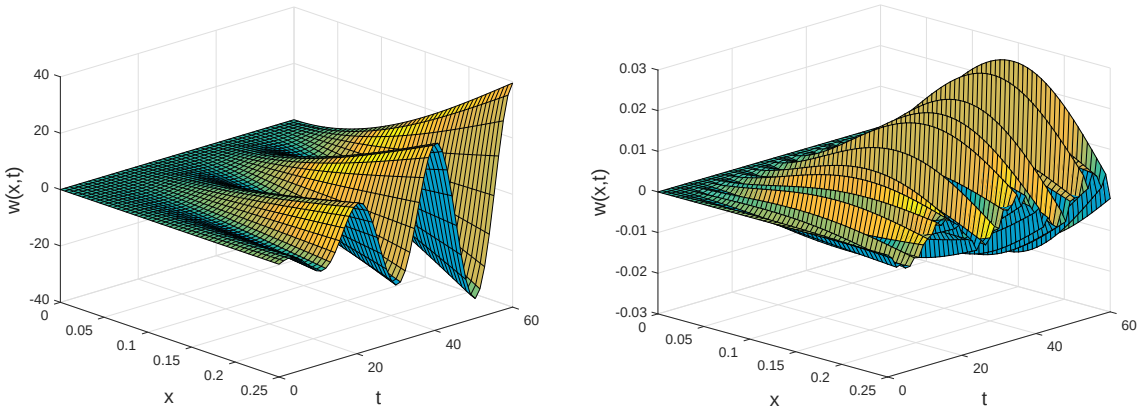

(a) $u(t) = U\sin(\omega_1 t)$ (b) $u(t) = U\sin(\omega_2 t)$

Figure 4.18: Deformation evolution in resonance cases

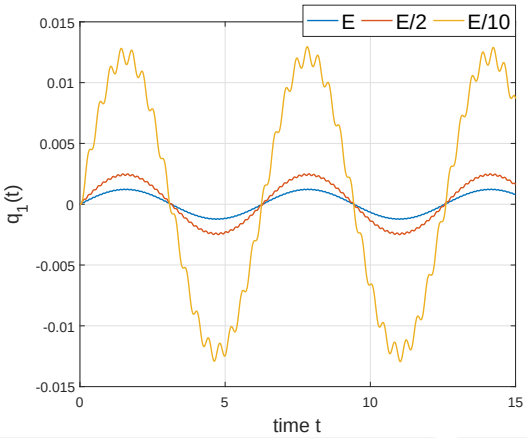

Figure 4.19: Parameter variation effect of E on mode $q_1(t)$

dynamic matrices for the unconstrained mode method from (4.13) with its state vector z containing a finite number of modes q_i.

Controllability

A system is said to be controllable if the controllability matrix

$$\mathcal{C} = \left[B, AB, A^2B, \ldots, A^{2N+1}B\right]$$

Tesis publicada con autorización del autor
No olvide citar esta tesis

has full rank $2(N+1)$. Because of the sparse structure and the special pairing with the control channels the following symbolic expression for $\mathcal{C}$ is determined:

$$\mathcal{C} = \begin{pmatrix} 0 & 1 & 0 & 0 & 0 & 0 & \cdots \\ 1 & 0 & 0 & 0 & 0 & 0 & \cdots \\ 0 & k_1 & 0 & -k_1 w_1^2 & 0 & k_1 w_1^4 & \cdots \\ k_1 & 0 & -k_1 w_1^2 & 0 & k_1 w_1^4 & 0 & \cdots \\ 0 & k_2 & 0 & -k_2 w_2^2 & 0 & k_2 w_2^4 & \cdots \\ k_2 & 0 & -k_2 w_2^2 & 0 & k_2 w_2^4 & 0 & \cdots \\ \vdots & \vdots & \vdots & \vdots & \vdots & \vdots & \ddots \end{pmatrix}.$$

That knowledge is used to calculate the determinant of the controllability matrix. Applying the Laplace expansion for determinants leads to the expression:

$$\det(\mathcal{C}) = (-1)^{N-1} \left(\prod_{i=1}^{N} k_i \omega_i^2 \prod_{j=i+1}^{N} (-1)^j \big(\omega_i - \omega_j\big)\big(\omega_i + \omega_j\big) \right)^2 .$$

The following important conclusions can be draw from that formula:

- The system is always observable under reasonable conditions.
- It is uncontrollable in case $\exists i \neq j : \omega_i = \pm\omega_j$. The eigenfunction analysis has shown that there can only be distinct eigenvalues.
- If there is not enough control impact, that means $\exists i : k_i = 0$, the system naturally becomes uncontrollable. By construction of these coefficients dependent on the eigenfunctions this is also not likely to happen.
- Problematic from a numerical perspective are the highly different scalings ω_i which leads to unreasonable for higher order systems.

With these considerations, the controllability is assured for reasonable system conditions.

Observability

Clearly the observability depends on the choice of the system output y. At the beginning, just one basic sensor is considered. For the hub rotation a potentiometer is used

Tesis publicada con autorización del autor
No olvide citar esta tesis

to measure the rotation angle θ resulting in the output relation:

$$y_1 = \theta(t) = \eta(t) + \sum_{i=1}^{N} \gamma_i q_i(t) = \underbrace{\left[1, 0, \gamma_1, 0, \ldots, \gamma_N, 0\right]}_{=:C_1} z\,.$$

Note that the parameter vector $\gamma = [\gamma_1, \ldots, \gamma_N]^\top$ plays the central role for observation. The system is said to be observable if the observability matrix:

$$\mathcal{O} = \begin{bmatrix} C \\ CA \\ CA^2 \\ \vdots \\ CA^{2N+1} \end{bmatrix}$$

has full rank $2(N+1)$. With a slight switch of channel pairings in comparison to the controllability case, the matrix can be stated as:

$$\mathcal{O} = \begin{pmatrix} 1 & 0 & \gamma_1 & 0 & \gamma_2 & 0 & \gamma_3 & 0 & \cdots \\ 0 & 1 & 0 & \gamma_1 & 0 & \gamma_2 & 0 & \gamma_3 & \cdots \\ 0 & 0 & -\gamma_1\omega_1^2 & 0 & -\gamma_2\omega_2^2 & 0 & -\gamma_3\omega_3^2 & 0 & \cdots \\ 0 & 0 & 0 & -\gamma_1\omega_1^2 & 0 & -\gamma_2\omega_2^2 & 0 & -\gamma_3\omega_3^2 & \cdots \\ 0 & 0 & \gamma_1\omega_1^4 & 0 & \gamma_2\omega_2^4 & 0 & \gamma_3\omega_3^4 & 0 & \cdots \\ 0 & 0 & 0 & \gamma_1\omega_1^4 & 0 & \gamma_2\omega_2^4 & 0 & \gamma_3\omega_3^4 & \cdots \\ 0 & 0 & -\gamma_1\omega_1^6 & 0 & -\gamma_2\omega_2^6 & 0 & -\gamma_3\omega_3^6 & 0 & \cdots \\ 0 & 0 & 0 & -\gamma_1\omega_1^6 & 0 & -\gamma_2\omega_2^6 & 0 & -\gamma_3\omega_3^6 & \cdots \\ \vdots & \vdots & \vdots & \vdots & \vdots & \vdots & \vdots & \vdots & \ddots \end{pmatrix}.$$

A dual structure to the first case is found, presented for higher order exemplary. Thus, the characteristic determinant is expressed analogously:

$$\det(\mathcal{O}) = \left(\prod_{i=1}^{N} \gamma_i \omega_i^2 \prod_{j=i+1}^{N} (-1)^j \Big(\omega_i - \omega_j\Big)\Big(\omega_i + \omega_j\Big) \right)^2 .$$

Similarly, the system is always observable under usual circumstances and with $\gamma_i \neq 0\,\forall i$. It suffers as well from bad numerical conditioning.

In total, it does not seem to be necessary to check the system for stabilizability nor detectability. In case of damping it is assured because of the asymptotically stable system dynamics.

Tesis publicada con autorización del autor
No olvide citar esta tesis

4.2.2 Optimal sensor concept

To extend the system configuration additional sensors shall be considered beside the potentiometer. On the actuator side it does not seem possible to add more degrees of freedom, but it is excepted to improve the performance with additional information about the system by extra measurement.

Strain gauge

In [METH96] finding the optimal sensor location of one strain gauge is part of the contribution. The strain measures the deformation acceleration in the following manner:

$$y_2 = -\frac{T_h}{2}\, w''(x,t) = -\frac{T_h}{2} \sum_{i=1}^{N} \phi_i''(x) q_i(t) = \underbrace{\left[0, 0, \mu_1(x), 0 \ldots, \mu_N(x)\right]}_{=:C_2} z$$

with the thickness T_h already mentioned in Table 4.1 an the substituted coefficients $\mu_j(x) := -\frac{T_h}{2}\, \phi_j''(x)$. The dependency on the position x can be used for optimizing the observability conditioning by choosing the optimal position x^* maximizing a certain measure.
In the upper work an observability Gramian based idea is proposed. There the PI norm is considered in the form:

$$PI = \left(\sum_{i=1}^{2(N+1)} \lambda_i \right) \left(\sum_{i=1}^{2(N+1)} \lambda_i \right)^{\frac{1}{2(N+1)}} ,$$

where $\lambda_i \in \mathrm{eig}(Q)$ with the Gramian Q being the solution to the Lyapunov equation $A^\top Q + QA + C^\top C = 0$. This characteristic value depends on $x \in [0, L]$ and is computed for several values such that a graph is obtained. Based on that, the article recommends a positioning close to the hub.
In this work, the extra information source shall be included into optimization procedure. The offline computation in connection with the LMI framework introduced in Chapter 3 gives the opportunity to build an external optimization loop. For sampled position values a mixed-integer problem is established.
In comparison to the referenced work a direct control performance measure can be utilized as a cost function. Thus, the whole closed-loop is taken into account and the optimal sensor location can be linked to a certain robust objective output. For example, focusing on the end-effector position could possibly result in a strain closer to end of arm. During the following Chapter 5 this idea is examined in detail.

Tesis publicada con autorización del autor
No olvide citar esta tesis

Gyroscope

Another promising measurement addition seems the determination of the angular velocity at the hub utilizing a gyro for example. The related measurement output is:

$$y_3 = \dot{\theta} = \dot{\eta}(t) + \sum_{i=1}^{N} \gamma_i \dot{q}_i(t) = \underbrace{\left[0, 1, 0, \gamma_1, \ldots, 0, \gamma_N\right]}_{=:C_3} z\,.$$

In comparison to y_1 all the velocity states have an impact on the output, but with the same set of coefficients. The motivation for using such a setup is the resulting relative degree of one with respect to this output. Non of the other two configurations holds this opportunity.
According to [BL07] this property is a requirement for applying passive control strategies. These fit perfectly into the robust control scheme and seem predestined for handling flexible structures. This interesting idea is followed up as well in the application chapter 5.
Still, one has to beware of increasing the system complexity and order too much. This aspect has to be kept in mind when adding various features at the same time. Another disadvantage in practice is that in general gyroscope data usually is noisier in comparison to the established sensors.

Tesis publicada con autorización del autor
No olvide citar esta tesis

5 Control Application

After presenting the multi-objective control framework in Chapter 3 and deriving an adequate mathematical model of the flexible robot arm in in Chapter 4, these aspects shall be combined here. The obtained system structure is converted to a general plant description with its respective objective channel specifications. Therefor, the given system properties are discussed and a characterization of external disturbances and internal uncertainties is performed.
Approximating a distributed parameter system and neglecting the high-frequency dynamics causes common problems. Undesirable vibrations may occur and could lead to spillover effects and even destabilization. The investigation from [Ver09] discusses these aspects and proposes a robust control technique for handling such inconveniences, like already motivated in this work. An interesting example is the application to vibration damping in buildings from [ALJB10].
First an analysis of the system structure with regards to performance objectives and the uncertain influences is made. Based on that, the implementation and different configurations of interest are examined in detail. Finally, the compound framework is tested and verified via simulation.

5.1 Problem formulation

The robust control structure has been introduced in Section 2.1 with the channel distinction in from Section 3.1. Now the model obtained from the unconstrained mode method in Section 4.1 is formulated in such a way that different objectives can be included.
With the dynamic matrices from (4.13) the $2(N+1)$ dimensional state vector:

$$x = [\eta\,,\ \dot{\eta}\,,\ q_1\,,\ \dot{q}_1\,,\ \ldots\,,\ q_N\,,\ \dot{q}_N]^T$$

is considered.

Tesis publicada con autorización del autor
No olvide citar esta tesis

5.1.1 Output & measurement

Possible measurement outputs have been discussed in 4.2. To express them in a common way consider the auxiliary state expressions:

$$\eta = \underbrace{[1, 0 \ldots, 0]}_{=c_1} x\,, \quad q = \begin{bmatrix} q_1 \\ \vdots \\ q_N \end{bmatrix} = \underbrace{\begin{pmatrix} 0 & 0 & 1 & 0 & \cdots & 0 & 0 \\ \vdots & \vdots & & & \ddots & & \\ 0 & 0 & 0 & 0 & \cdots & 1 & 0 \end{pmatrix}}_{=c_2} x\,.$$

Then, with the parameter vector $\gamma = [\gamma_1, \ldots, \gamma_N]$ the main measurement output, or control input respectively, has the tracking error form:

$$y = \theta - \theta^* = \eta + \sum_{i=1}^{N} \gamma_i q_i - \theta^* = \underbrace{\left(c_1 + \gamma\, c_2\right)}_{=C_y} x - r$$

with $r = \theta^*$ as the rotation angle reference value. Now the control objective outputs z shall be defined. First of all, it is desired that $\theta \to \theta^*$ and $q \to 0$ asymptotically as $t \to \infty$. Speaking, the rotation angle shall take its reference value without any bending vibrations in the end. This leads to the following objective output selection for state error:

$$\begin{pmatrix} z_1 \\ z_2 \end{pmatrix} := \begin{pmatrix} \theta - \theta* \\ q_1 \\ \vdots \\ q_N \end{pmatrix} = \begin{pmatrix} c_1 + \gamma c_2 \\ c_2 \end{pmatrix} x + \begin{pmatrix} -1 \\ 0 \\ \vdots \\ 0 \end{pmatrix} r\,.$$

Another important aspect for the performance of the control system is to include the control action u as an objective, thus $z_3 = u$. Furthermore, it is interesting to focus on the end-effector position as well because for robotics this is connected to the main task and possibly weights the deformation in a more significant way. Considering the bending at the end $w(L,t)$ to be relatively small the following holds:

$$\begin{aligned} z_3 &= \theta_t - \theta_t^* = \theta + \arcsin\left(\frac{w(L)}{L}\right) - \theta_t^* \approx \theta + \frac{w(L)}{L} - \theta_t^* \\ &= \eta + \sum_{i}^{N} \left(\gamma_i + \frac{\phi_i(L)}{L}\right) q_i - r = \left(c_1 + \left(\gamma + \frac{1}{L}\phi(L)\right) c_2\right) x - r \end{aligned}$$

The geometric relation is obtained from Figure 4.2 by the trigonometric equation $\sin(\theta_t - \theta) \approx \frac{w(L)}{L}$.

Tesis publicada con autorización del autor
No olvide citar esta tesis

There are still various options for objective definitions but these are the most important ones to be focused on in this work. The final nominal objective outputs take the compound structure:

$$\begin{pmatrix} z_1 \\ z_2 \\ z_3 \\ z_4 \end{pmatrix} = \left(\begin{array}{c} \theta - \theta^* \\ \hline q_1 \\ \vdots \\ q_N \\ \hline u \\ \hline \theta_t - \theta_t^* \end{array}\right) = \begin{pmatrix} c_1 + \gamma c_2 \\ c_2 \\ 0 \\ c_1 + \left(\gamma + \frac{1}{L}\phi(L)\right) c_2 \end{pmatrix} x + \begin{pmatrix} -1 \\ 0 \\ 0 \\ -1 \end{pmatrix} r + \begin{pmatrix} 0 \\ 0 \\ 1 \\ 0 \end{pmatrix} u = C_z x + D_{zr} r + D_{zu} u \,,$$

with $\phi(L) = [\phi_1(L), \ldots, \phi_N(L)]$.In analogy to that formulation consider the possible measurement outputs:

$$\begin{pmatrix} y_1 \\ y_2 \end{pmatrix} = \begin{pmatrix} \theta - \theta^* \\ -\frac{T_h}{2} w''(p) \end{pmatrix} = \begin{pmatrix} c_1 + \gamma c_2 \\ \mu(p) c_2 \end{pmatrix} + \begin{pmatrix} -1 \\ 0 \end{pmatrix} r = C_y x + D_{yr} r \,,$$

where $p \in (0, L)$ denotes the selected position of the strain gauge for y_2 and $\mu(p) := -\frac{T_h}{2} [\phi_1''(p), \ldots, \phi_N''(p)]$. For simplicity y_3 is not included yet. This forms an implementation goal for the end configuration dependent on the results obtained by the extensions.

5.1.2 Channel specification

After clarifying the possibilities of output configurations, the input signals and respective performance channels are explained. As they are linked to physical circumstances, the inputs are pretty much fixed in comparison with outputs. The external input vector w contains of:

$$w = \begin{pmatrix} r \\ d \end{pmatrix} \,,$$

where d is considered to be an external disturbance on the actuator sight, meaning $B_d = B_u$. In this work, no noise is considered for simplicity. Of course this would have been an interesting practical aspect. Thus, the system is expressed in the form Σ_{nom} from 2.3:

$$\begin{cases} \dot{x} = Ax + B_w w + B_u u \\ z = C_z x + D_{zw} w + D_{zu} u \\ y = C_y x + D_{yw} w \end{cases} .$$

Tesis publicada con autorización del autor
No olvide citar esta tesis

Now, the central nominal performance specifications introduced in Section 2.2 and expressed in terms of LMIs in Section 3.2 shall be formulated

- H_∞ performance: $d \rightarrow \Delta\theta = e$
  This reduces the impact of the external disturbance on the tracking error, which softens the worst case operation conditions.

- H_2 performance: $r \rightarrow u$
  For an efficient performance of the system the control action is taken into the H_2 channel. Thus, no external signal feedthrough is generated, avoiding complications with basic assumptions. Using the generalized H_2 concept gives the opportunity to include actuator constraints in a soft way and avoid saturation. This is due to the norm transfer behavior from energy (L_2) to amplitude (L_∞.)

- Passive transfer behavior: $d \rightarrow \dot{\theta}$?
  To include an adequate damped performance with certain intrinsic robustness passivity shall be induced. The passivation shall be related to the flexible mode states.

- Disturbance rejection: $\lim_{t\to\infty} \Delta\theta(t) = 0 \, \forall r, d$
  Of course, it is desired to track the reference signal and therefore solving the regulation problem for all external influences, if possible.

Then the channel-wise transfer functions of the general open-loop plant can be realized as:

$$P_\infty(s) = \left[\begin{array}{c|cc} A & B_\infty & B_u \\ \hline C_\infty & 0 & 0 \\ C_y & 0 & 0 \end{array}\right], P_2(s) = \left[\begin{array}{c|cc} A & 0 & B_u \\ \hline C_2 & 0 & D_{2u} \\ C_y & D_{y2} & 0 \end{array}\right], P_p(s) = \left[\begin{array}{c|cc} A & B_\infty & B_u \\ \hline C_p & D_p & D_{pu} \\ C_y & D_{yp} & 0 \end{array}\right].$$

Here, instead of the channel index j, like in Chapter 3, the explicit objective expression is used. The possibility of choosing arbitrary channel compositions also gives the opportunity to leave some out. That is why in the following, not always all configurations are considered if not useful.

5.1.3 Uncertainty modeling

To guarantee robustness of the closed-loop system, the uncertain structure related to that has to be modeled. An introduction on this topic has been given in Section 2.3. The general system here is considered to be uncertain in two ways:

Tesis publicada con autorización del autor
No olvide citar esta tesis

(a) During the modal analysis in Section 4.1 the high-frequency dynamics of order $N+1$ and higher has been neglected.

(b) Input and output parameters k andγ contain eigenfunction values. This heavily relies on the principle of separation of variables and thus on the linearity assumption. Further away from the operation point nonlinear effects influence these parameters.

Uncertainties are often characterized in the frequency domain. The corresponding system representation of the physical process is given by:

$$\begin{pmatrix} y_1 \\ y_2 \end{pmatrix} = \begin{pmatrix} \theta - \theta^* \\ -\frac{T_h}{2} w''(p) \end{pmatrix} = G_n(s)\, u\,,$$

where $G_n(s)$ denotes the nominal plant.

High-frequency component

The neglect of high frequency components can directly be seen considering the output form:

$$y_1 = \theta(t) - \theta^* = \eta(t) + \sum_{i=1}^{\infty} \gamma_i\, q_i(t) - \theta^* = \left(\eta(t) + \sum_{i=1}^{N} \gamma_i\, q_i(t) - \theta^*\right) + \sum_{j=N+1}^{\infty} \gamma_j\, q_j(t)$$

and similarly:

$$y_2 - \frac{T_h}{2} w''(p,t) = \sum_{i=1}^{\infty} \mu_i(p)\, q_i(t) = \left(\sum_{i=1}^{N} \mu_i(p)\, q_i(t)\right) + \sum_{j=N+1}^{\infty} \mu_j(p)\, q_j(t)\,.$$

From the decoupled mode dynamics one easily obtains the following transfer function representations:

$$q_i = \frac{k_i}{s^2 + w_i^2}\, u\,.$$

This allows to explicitly characterize the uncertainties in the way:

$$\Delta_1(s) = \sum_{i=N+1}^{\infty} \frac{k_i \gamma_i}{s^2 + w_i^2}\,, \quad \Delta_2(s) = \sum_{i=N+1}^{\infty} \frac{k_i \mu_i(p)}{s^2 + w_i^2}$$

Now, the aim is it to get the compound system into the form Σ_{rob} from (2.6). Therefor consider the block diagram from Figure 5.1. This can clearly be classified as an additive uncertainty, similar to the example in Figure 2.13. In state-space form one gets the

Tesis publicada con autorización del autor
No olvide citar esta tesis

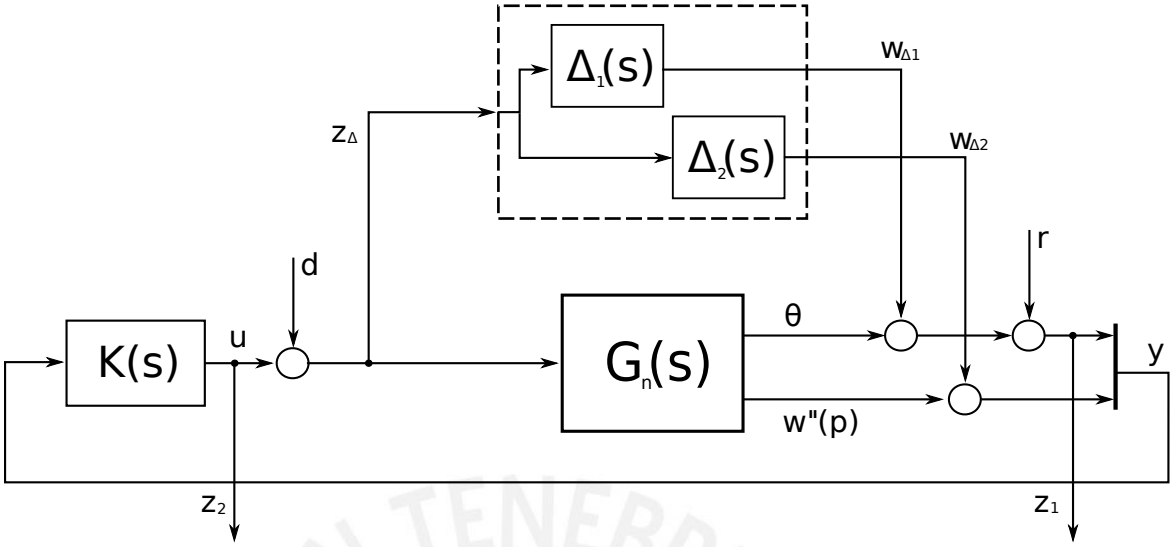

Figure 5.1: Block diagram with high-frequency uncertainties

realization adaption:

$$z_\Delta = C_\Delta x + D_{\Delta w} w + D_{\Delta u} u = \begin{pmatrix} 0 & 1 \end{pmatrix} w + 1u\,,$$

$$B_\Delta = \begin{pmatrix} 0 & 0 \\ 0 & 0 \end{pmatrix}\,,\; D_{y\Delta} = \begin{pmatrix} 1 & 0 \\ 0 & 1 \end{pmatrix}\,,\; D_{z\Delta} = \begin{pmatrix} 1 & 0 \\ 0 & 0 \end{pmatrix}\,.$$

These are needed for formulating the robust stability condition in terms of an LMI. A characterization of the uncertainties in terms of the description set $\mathbf{\Delta}$ defined in Section 2.3 can be done by performing a virtual experiment. Via a frequency domain identification (sweep for example) the bode plot of the uncertainty transfer functions ca be plotted. This is realized using the representations for $\Delta_1(s)$ and $\Delta_2(s)$ with a finite approximation order $N_\Delta > N$. In Figure 5.2 the respective magnitudes are plotted as the experiment outcome. This obviously shows the dilemma of the undamped system case as the magnitudes result to be unbounded. At the resonance frequency points it is impossible to guarantee robust stability because the H_∞ norm is not defined there. Therefore, the more realistic and practical model, proposed at the end of part 4.1.2, has to be considered. Note, that this changes the transfer function to take the form:

$$q_i = \frac{k_i}{s^2 + 2\zeta_i \omega_i s + w_i^2}\, u\,.$$

Figure 5.3 illustrates the same magnitude experiment over all frequencies ω for the damped system. Still there are the typical peaks in the oscillatory case, but dependent

Tesis publicada con autorización del autor
No olvide citar esta tesis

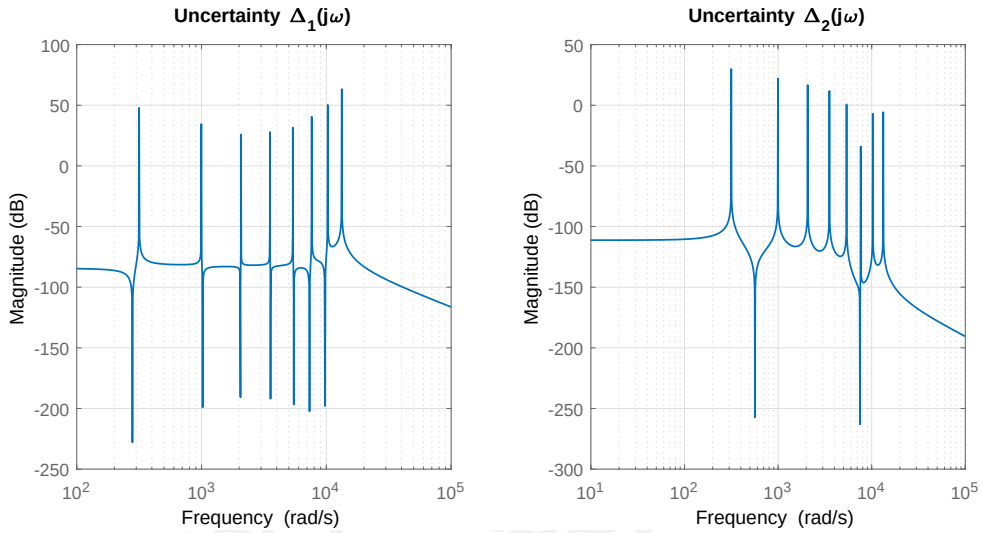

Figure 5.2: Magnitude plot of uncertainties without damping

on the choice of ζ_i these are more or less dominant. Here $\zeta_i = 0.1\,\forall i$ has been chosen. Notably, the disturbance on Δ_1 potentiometer side is much more significant.
For the framework it necessary to find an uncertainty normalization such that $\Delta \in \mathbf{\Delta}$ and thus $\|\Delta\|_\infty < 1$. To realize that, filters are designed based on the experimental knowledge. Because of the exemplary damping a low-pass characteristics is recommended. The filters can be selected as an PT1 function:

$$W_l(s) = \frac{K_l}{\tau_l s + 1}\,,\; l = 1, 2\,.$$

Here, it is proposed to choose the gain slightly higher than the maximum peaks from $|\Delta_l(j\omega)|$, in fact $K_l := 1.1\,\|\Delta_l\|_\infty$. The bandwidth has to be selected according to the expected low-pass behavior. Then the uncertainties can be expressed as $\Delta_l(s) = W_l(s)\bar{\Delta}_l$ with assuring $\bar{\Delta}_l \in \mathbf{\Delta}$.
Clearly, even in the virtual experiment modes were missing and to cover the expectations one should not be too accurate. A little bit of conservatism has to be taken into account for guaranteeing the much more important stability under all possible conditions.

Input parameters

Because of the occurrence of eigenfunction values in the input (and output) parameters a calculation error has to be taken into account. This results in a well structured

Tesis publicada con autorización del autor
No olvide citar esta tesis

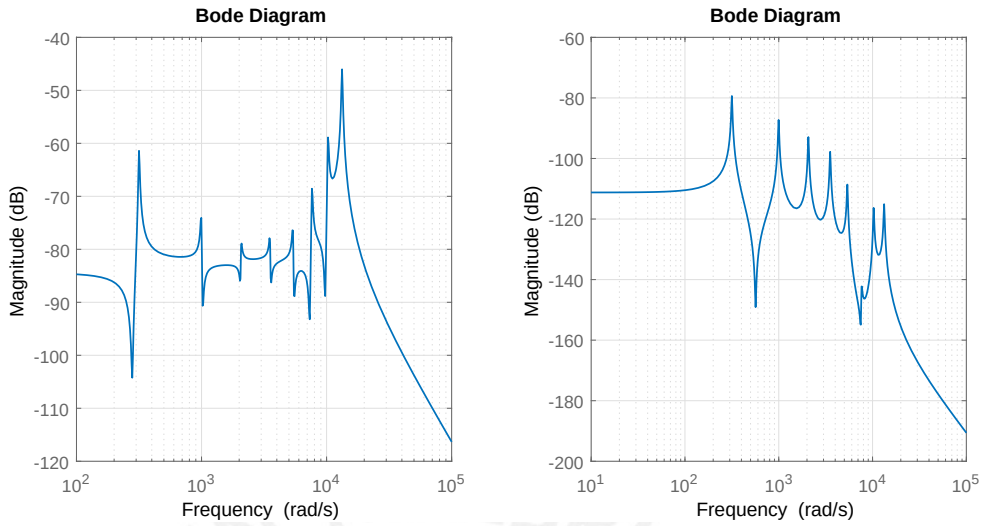

Figure 5.3: Magnitude plot of uncertainties with damping considered ($\zeta_i = 0.5$)

uncertainty model. As an example the flexible arm system input matrix has the form:

$$B_\Delta = \begin{pmatrix} 0 \\ 1/J + \delta_0 \\ 0 \\ k_1 + \delta_1 \\ \vdots \\ 0 \\ k_N + \delta_N \end{pmatrix} = \begin{pmatrix} 0 \\ 1/J \\ 0 \\ k_1 \\ \vdots \\ 0 \\ k_N \end{pmatrix} + \begin{pmatrix} 0 & 0 & \cdots & 0 \\ w_0 & 0 & \cdots & 0 \\ 0 & 0 & \cdots & 0 \\ 0 & w_1 & \cdots & 0 \\ \vdots & & \ddots & 0 \\ 0 & 0 & \cdots & 0 \\ 0 & 0 & \cdots & w_N \end{pmatrix} \begin{pmatrix} \delta_0 & & & \\ & \delta_1 & & \\ & & \ddots & \\ & & & \delta_N \end{pmatrix} = B + W\Delta\,,$$

with weight coefficients $w_i = 1$ in this case, which would later be adapted to guarantee $|\delta_i| < 1$ for normalization and can also be set dynamically for frequency weighting. This clearly leads a multiplicative uncertainty representation as shown in Figure 2.15. In this work there is a focus on the case of the high-frequency disturbances as they are considered to be more dominant. Nevertheless, there are interesting works done for uncertain parameters, especially in connection with LMIs [Sch00]. There, covering the uncertainty class with the use of multipliers enables the formulation fitting conditions and is even used in robust H_2 performance case.

Tesis publicada con autorización del autor
No olvide citar esta tesis

5.2 Simulation setup

After defining the control task and characterizing the model structure and considered influences, the conception for the control synthesis shall be developed. In the following the fundamental control structure from Figure 5.4 is derived and explained. It is based on the specifications announced in the previous section. The system contains

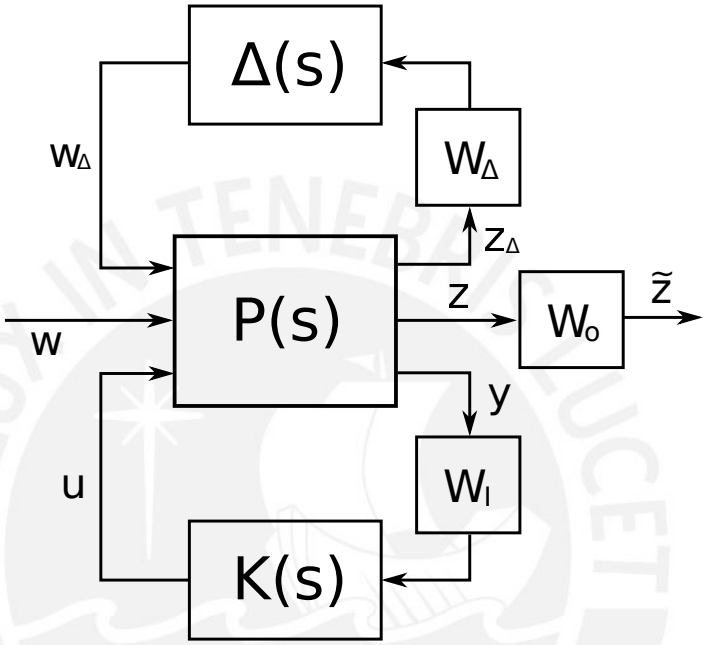

Figure 5.4: Control system setup with filters

of the three main components: the plant $P(s)$, defined by the physical model and the signal composition, the uncertainty $\Delta(s)$, the internal disturbance part which harms stability, and the controller, that shall be designed under the given circumstances and specifications. On the output side there are signal filters. It would also be possible to use input side filters which did not seem necessary here. Remember that the damped system description is used for more realistic results and easier uncertainty handling.

5.2.1 Objective definition & filters

Now, the tasks of the multi-objective control system are defined and their preliminaries have to be checked. A slide summery of the implemented LMI techniques from Chapter 3 is given.

Tesis publicada con autorización del autor
No olvide citar esta tesis

Internal stability

Most importantly the closed-loop system is required to be internally stable under all considered circumstances. For the nominal system this is done by fulfilling the corresponding Lyapunov inequality. The uncertainties due to the high-frequency components are included into the plant through its weighting filter $W_\Delta(s) := \mathrm{diag}(W_1(s), W_1(s))$. As the $\Delta \in \mathbf{\Delta}$ holds, the small gain theorem can be applied and H_∞ condition with $\gamma_{\mathbf{\Delta}} = 1$ is included.
Optimization with SDP can produce numerical problems if not programmed with discipline and caution. The reason for this is that solutions are searched for at the edge of the feasible region. It may results in destabilizing controllers. This is handled by conditioning of the Lyapunov variable and suboptimal test steps to not produce extreme solutions.

Reference tracking

The rotation angle θ shall follow the reference value r asymptotically. In Section 3.2 a nominal regulation procedure using the internal model principle was proposed. For the signal model $S = 0$ is taken because of a constant reference inputs $\dot{r} = 0$. In case of other signal classes this could be adapted. The first central requirement of $z_1 = y_1$ is fulfilled. Then the detectability condition for $\left(\begin{pmatrix} A & B_r \\ 0 & S \end{pmatrix}, \begin{pmatrix} C_{y_1} & D_{y_1 r} \end{pmatrix} \right)$ has to be checked. It is due to the integrator (or double integrator in the undamped case) characteristics of the η dynamics and the fact that r is not part of the dynamics that detectability is not given. Thus, the procedure is not applicable.
For solving the reference tracking problem the integrating system $W_I(s)$ is added to the measurement channel. It enables the selection of channels to be integrated. Here, the signal $\int y_1 dt$ is given into the controller whereas y_2 goes through directly.
Luckily, the external disturbance d is matched and can directly be compensated by the controller. This allows all states to be zero which leads to the desired results. Tests with disturbances attacking just in certain modes show that the aim of $\Delta\theta \to 0$ is reached while the whole arm keeps oscillating in pseudo-steady-state.

Performance

The great advantage of the mixed-objective robust control in comparison with the H_∞ controller developed in the reference work [METH96], is that a performance measure in a certain sense can be added. Pure H_∞ norm optimization tends to generate unsat-

Tesis publicada con autorización del autor
No olvide citar esta tesis

isfying control signals.
Here, the generalized H_2 norm optimization is used for this purpose. Beside good performance in the H_2 sense, in offers a soft amplitude bound. For a certain energy level of the reference signals a maximum absolute value which u does not pass, can be guaranteed. This convenient when dealing with actuator constraints.

Disturbance suppression

The impact of the external disturbance d on the error objective output shall be as small as possible. Sudden appearances of disturbance impulses must not harm the system safety. Thus, an H_∞ constraint is put on the channel and tried to be lowered in a sophisticated way.
On the one hand, this could prevent spatial constraints from being violated. It is also important for the model validity. As a linearization was performed, it is not desirable to leave the operating point too far. Nonlinear effects could occur and the controller would possibly not be prepared for that.

Passivation

It would be a nice property for the flexible system to expose a passive behavior. The injected damping would be able to give a certain robustness to the system with a natural and thus desirable performance. In [BL07] several passive and robust control approaches are applied to practical problems.
As a central requirement for passivation, the input-output relation has to have relative degree on. For that, using the output $\dot{\theta}$ has been proposed. Unfortunately, the LMI condition turns out to be unfeasible in all applied circumstances. Thus, this approach cannot be tested. It illustrates one of the problems for LMI procedures, that the assumptions needed for feasibility are unclear and the interpretation is left to the numerical solver.

5.2.2 Software framework

For solving the mixed-objective robust control problem a program has been implemented in Matlab to calculate the respective controller realization for a given plant definition and defined objectives. This includes to compose the system properly, check all central requirements, build up the optimization procedure, calculate the controller parameterization, evaluate the resulting performance and adjust the outcome iteratively. Then the controller is applied to the simulated system in Simulink. In Figure

Tesis publicada con autorización del autor
No olvide citar esta tesis

5.5 the implemented procedure is illustrated. For the convex optimization procedure

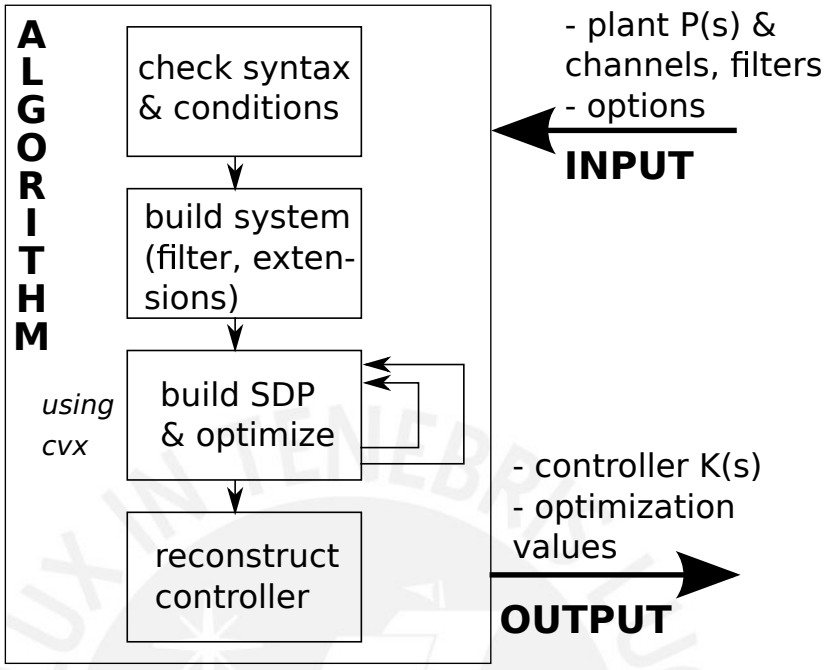

Figure 5.5: Software scheme for control synthesis

solving the SDP the Matlab toolbox *cvx* [CVX12] was chosen. The inner iteration loop refers to the subordinated optimization like finding the optimal strain gauge position. In the outer loop optimal values are determined, adapted and given into another optimization to find a sufficiently good combination of all objective bounds.
The output of the procedure is the controller $K(s)$ and characteristic values such as H_∞ gain γ, generalized H_2 gain α or the Lyapunov condition factor t.

5.3 Verification

Now, the procedure shall be executed for the different proposed scenarios. To evaluate the obtained controller two types of comparison controllers have been chosen. As a benchmark in industrial control PID controllers are by far the most frequently used. Here, $K_{\mathrm{PID}}(s)$ was designed for compensating the slowest dynamics and guaranteeing a certain phase margin. This form it can only be used for the SISO control case. The second referenced controller is based on H_2 norm optimization. In order to focus on the performance, just the control channel is considered. The standard Matlab function is used, which calculates $K_{H_2}(s)$ via an ARE approach.
The main emphasis of this work lies on the usage of the one-mode model as a basis for

Tesis publicada con autorización del autor
No olvide citar esta tesis

the controller design. As the multi-objective control framework already offers many degrees of freedom, an additional output filter W_0 has not been designed. Thus, the concrete tuning focus is more compact and comparability is ensured.

5.3.1 Nominal performance

The first step is to obtain a controller that is capable of fulfilling the formulated performance specifications in the nominal case. In order to do so, a mixed H_2/H_∞ design procedure is presented step by step. Within this procedure the LMI framework gives many opportunities for tuning.

The upcoming results are based on a common simulation patter. Every test scenarios is realized for $t \in [0s, 30s]$ with a constant reference $r = 1rad$ applied at $t = 2s$. After $t = 15s$ an additional constant disturbance signal of $d = 0.02Nm$ is given into the system. All controllers are examined towards their actuation performance, as well as their respective disturbance suppression. Note, that the real constraints on the input signal would be given by $u(t) \in [-0.5Nm, 0.5Nm]$ (equivalent to $[-10V, 10V]$).

At the beginning, the LMI based optimization is just searching for feasible solution that internally stabilizes the closed-loop. This is not expected to fulfill the specifications with regards to the reference tracking. Thus, an integrator $W_I(s)$ is used on the measurement signal $y_2 = \Delta\theta$. The improvement can be observed in Figure 5.6. Beside the reference tracking, the integrator leads to less mode oscillations and a more

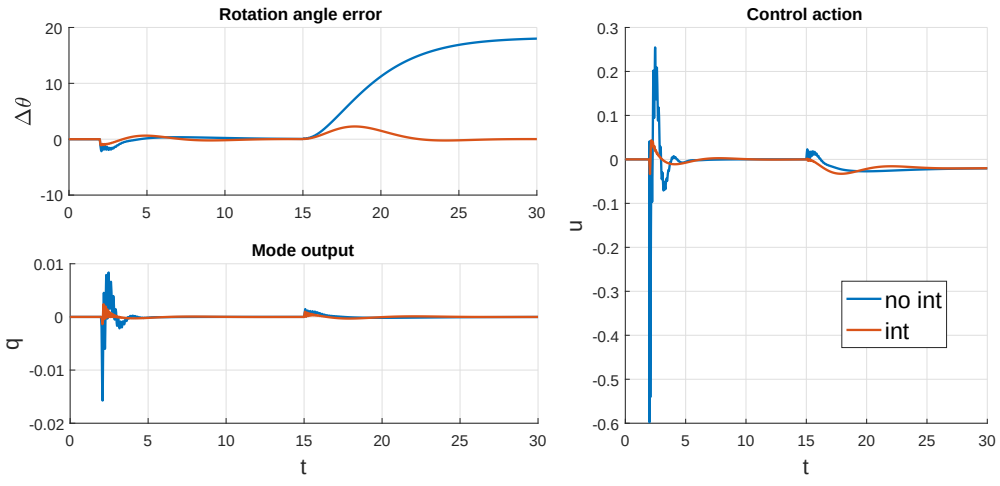

Figure 5.6: Impact of integrator inclusion

reasonable input signal. All of the following controllers include that integral part. The first performance channel shall be the H_∞ bound on the behavior between the distur-

Tesis publicada con autorización del autor
No olvide citar esta tesis

bance d and the output $z_\infty = z_1 = \Delta\theta$. When searching for the optimal H_∞ bound, $\gamma_{opt} = 0.1106$ is obtained. This, and values close to that limitation, are numerically bad conditioned and the obtained controllers do not stabilize the system internally. Thus, a suboptimal solution is preferred. In Figure 5.7 several system signals are presented for different H_∞ control constellations. In terms of suppressing the disturbance

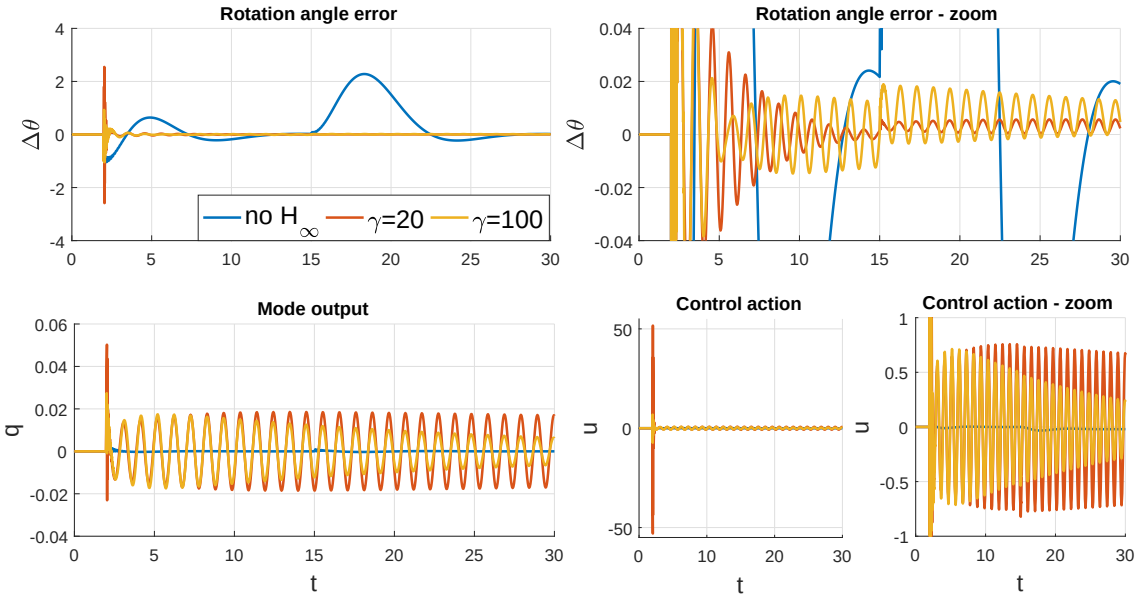

Figure 5.7: Evaluate H_∞ control performance with $z_\infty = \Delta\theta$

a large improvement is obtained. This comes with the cost of large oscillations in the mode state. The rude actuation in the H_∞ sense causes vibrations in all states and requires unreasonable large input signals. Widening the bound γ results in decaying oscillations, which are still unsatisfying. Furthermore, the reference tracking fails and a small steady state error remains.

The strong deformations caused by that motivate a change in the objective output. For comparison, the H_∞ channel is modified to concentrate on the mode trajectory $q(t)$ by setting $z_\infty = z_2 = q$. Correspondingly, the optimal bound would be $\gamma_{opt} = 0.1158$, which again causes numerical problems. Then, the respective suboptimal performance comparison is illustrated in Figure 5.8. By changing the objective, the vibrations could be reduced, but not significantly. The positive effects are that the reference overshoot is avoided and the desired reference value is tracked, except for some oscillations. In comparison to the control signal peak, shown in Figure 5.7, the new actuation got closer to realistic circumstances. The error peak due to the disturbance, is still relatively small and acceptable. Especially the aspect of no remaining offset in the tracking

Tesis publicada con autorización del autor
No olvide citar esta tesis

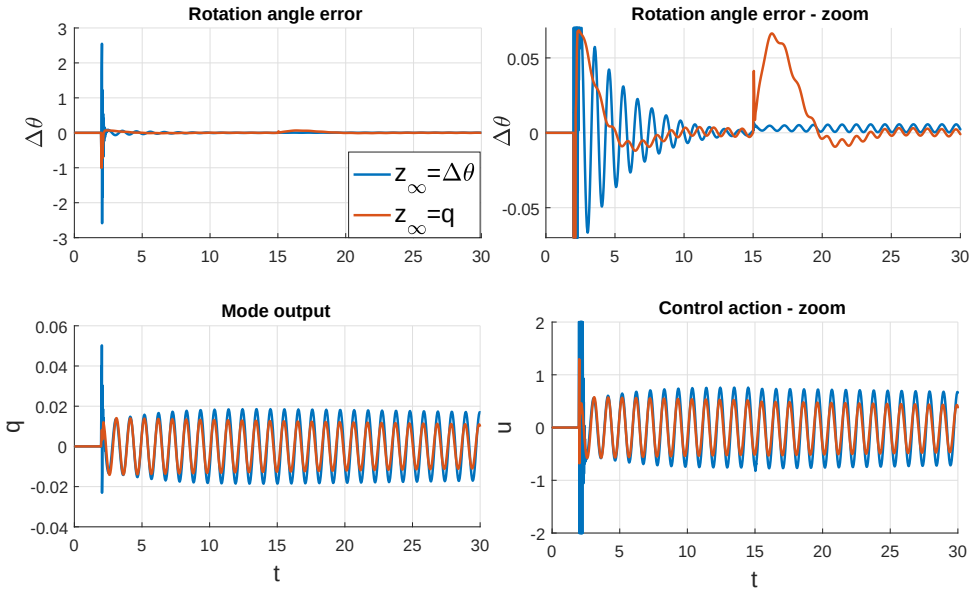

Figure 5.8: Comparing H_∞ objectives with common $\gamma = 20$

error, turns the mode output into an interesting selection.

In order to avoid the undesired oscillations and to improve the performance with respect to the control signal, an H_2 component is added to the synthesis process. The generalized H_2 norm puts a soft peak bound $\sqrt{\alpha}$ on the input torque $u(t)$. A mixed H_2/H_∞ controller is designed for both z_∞ output cases. The respective behaviors are compared in the plots of Figure 5.9. For the first objective case using z_1, the configuration $(\gamma, \sqrt{\alpha}) = (10, 15)$ has been used and for the second case with z_2 the bounds $(\gamma, \sqrt{\alpha}) = (5, 30)$ have been applied. Very distinct controllers are obtained. The one, which focuses on the deformation mode, results in excellent vibration avoidance, no remaining tracking error and very efficient control effort. On the other side, the error focused approach suppresses the disturbance very good and reacts a lot faster. Both approaches represent one extreme in the objective choice. One has to select whether the suppression of oscillations or external disturbances are of more importance. A combination could be selected to find a compromise.

In order to get impression of the obtained performance, the common comparison controllers shall be applied. Figure 5.10 illustrates their resulting closed-loop trajectories. The PID and conventional H_2 approaches represent two extreme solutions as well. On the one hand, the benchmark PID controller obtains a fast reaction, good disturbance rejection and perfect reference tracking. On the other hand, the deformation peaks are that large, that that the model validity could be doubted, and the control signal is

Tesis publicada con autorización del autor
No olvide citar esta tesis

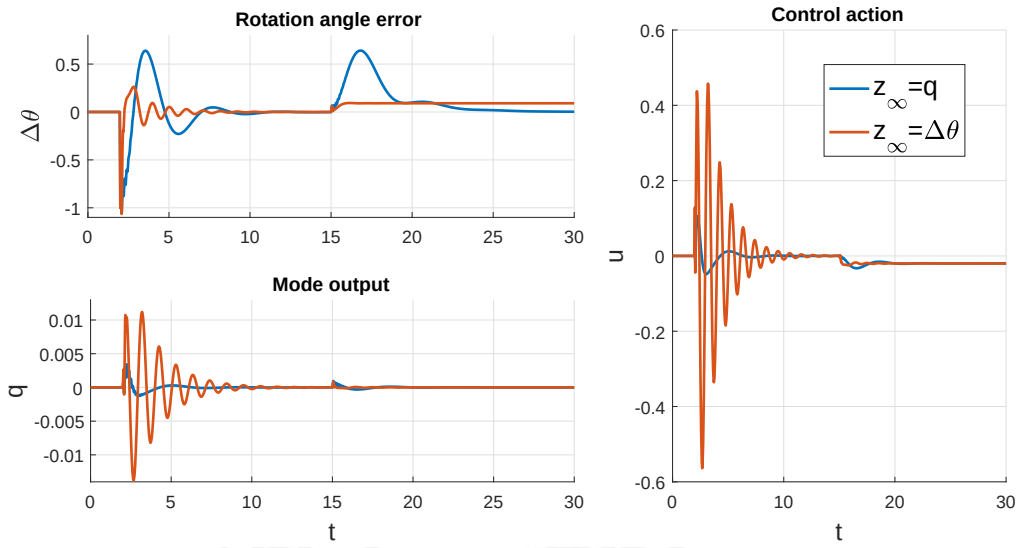

Figure 5.9: Performance of mixed H_2/H_∞ controllers with different objectives

totally out of range. There is the danger of a wind-up effect. The H_2 controller with focus on the actuation signal, obtains reasonable results, although a permanent reference deviation can be notified and the mode oscillations are also high in amplitude.
All four presented control concepts are put together in Figure 5.11, which directly compares the rotation angle errors. One may note that the disturbance focused H_2/H_∞ and the H_2 controllers are very similar in their overall behavior. The PID controller represents an idealistic and unrealistic setting because of the bad input signal performance, despite of demonstrating the best reference tracking results. In order to avoid oscillatory effects, such as the spillover effect, the mode focused mixed H_2/H_∞ controller is recommended, although its reference reaction could be improved.
The multi-objective robust control method offers so many degrees of freedom, that a lot more combinations are available. Thus, a lot more performance investigation could be done.

5.3.2 Measurement extension

In the paper from [METH96] the optimal positioning of a strain gauge for delivering extra measurement information has been discussed. For a selected position $p \in [0, L]$ and just considering the model including one mode, the additional output becomes:

$$y_2 = -\frac{T_h}{2} w''(p) = -\frac{T_h}{2} \phi''(p)\, q = \begin{pmatrix} 0 & 0 & -\frac{T_h}{2}\phi''(p) & 0 \end{pmatrix} z\,,$$

Tesis publicada con autorización del autor
No olvide citar esta tesis

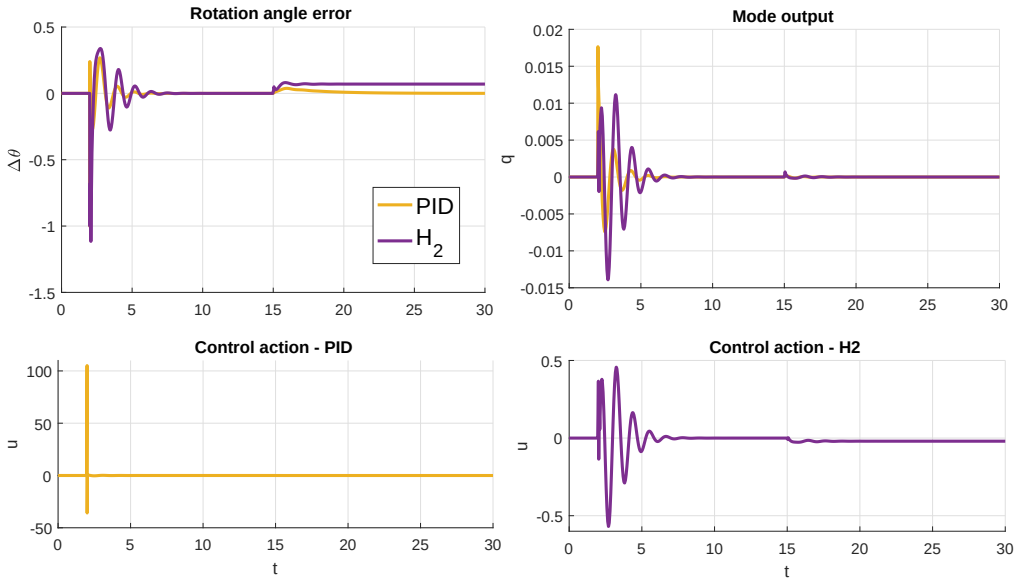

Figure 5.10: PID and H_2 comparison controller results

and thus provides additional information on the mode state q. First, the influence on the closed-loop behavior is evaluated. In order to do so, the mixed H_2/H_∞ controller with respect to the H_∞ objective output $z_\infty = q$ is considered. Figure 5.12 compares the results for the system with and without additional information. One may note, that the system response to the reference becomes much slower. This is accompanied by small mode deflections and low input amplitudes. This illustrates, that a whole new controller synthesis has to be made for rearranged system. It can not be expected, that simply giving additional information into the control system, automatically results in better performance measures for all specifications.

Here, the position is chosen very close to the hub. Nevertheless, changing the strain location does not lead to significant changes of the system response. The superordinated optimization procedure confirms this impression. A discrete sampling over the set of possible positions has been performed with the aim to minimize a certain cost characterization. In this case, $J := \alpha$ is chosen and a optimization of the generalized H_2 norm has been related to the sensor location. The result can be seen in Figure 5.13 (a). Note that the difference between the respective cost values is not that high and thus, no significant differences resulting from the choice of location can be expected. In the referenced article, the optimal position has to be close to the hub. This corresponds to the results made here, where a minimum lies in the first quarter of the arm length. It is not surprising that the amount of information seems to be related

Tesis publicada con autorización del autor
No olvide citar esta tesis

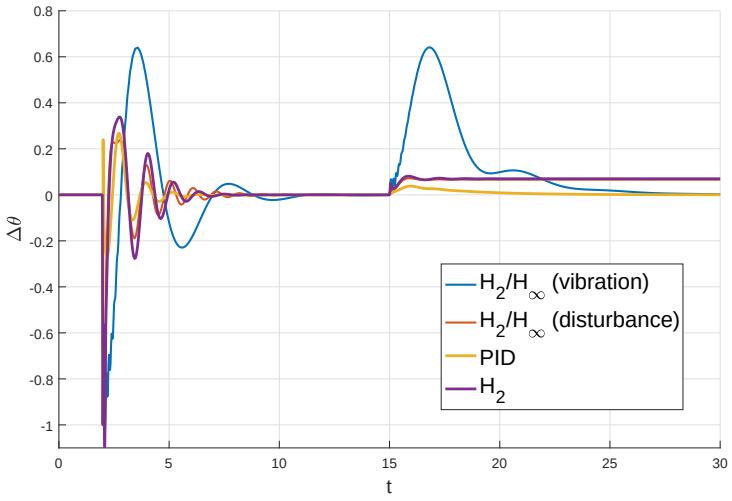

Figure 5.11: Tracking error comparison of multi-objective and test controllers

to weighting factor $\phi''(p)$, whose absolute value is bigger for positions close to the hub and tends to zero when it gets closer to the end-effector (BC).

5.3.3 Robustness discussion

The robustness analysis in terms of stability and performance makes sense in connection to the damped system, for which the uncertainties con be modeled appropriately. In this work, mainly the undamped system is investigated because of the more significant oscillation behavior. The corresponding resonances make it impossible to capture the uncertainty class of the neglected dynamics.

Thus, robust control synthesis would be another extensive topic, which cannot be covered here. Nevertheless, many preparatory has been done. At the first place, the robustness characterization becomes a lot easier when just considering one measurement output y_1. This results in a one-dimensional uncertainty structure, which does not require additional scaling and could be treated by the conventional small gain theorem without introducing too much conservatism.

The uncertainty structure due to the finite dimensional approximation of the distributed system was the inspiration for applying robust control techniques to this kind of problem.

Another critical issue in robust and optimal control is fragility, which was introduced by [KB97]. Basically, this refers to the fact, that optimal controllers often operate close to the boundary of feasibility. This holds especially for linear convex optimiza-

Tesis publicada con autorización del autor
No olvide citar esta tesis

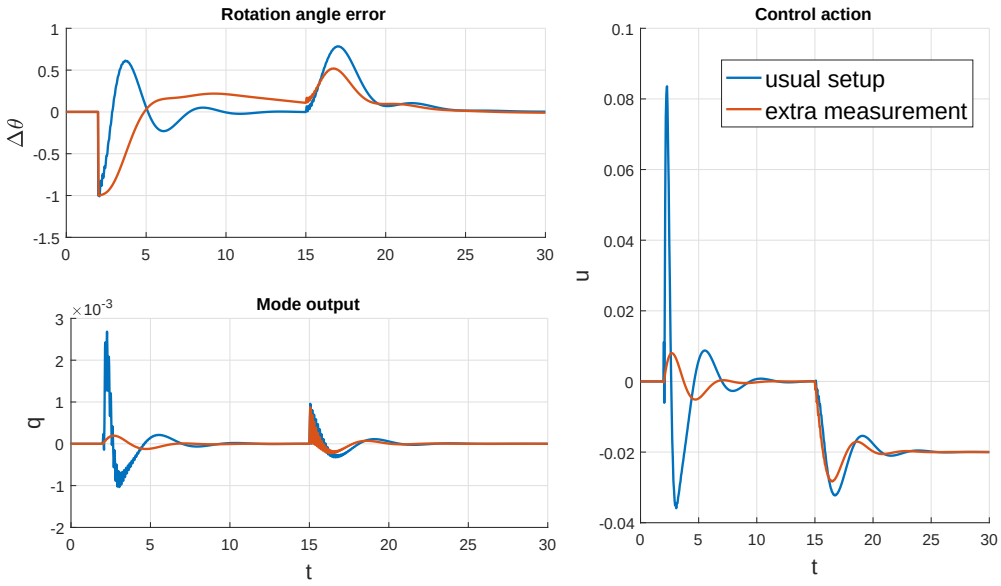

Figure 5.12: Performance change due to measurement extension

tion problems. It results in very low phase or gain margins, which make the system very sensitive to small changes of the controller parameters. Table 5.1 presents the resulting stability margins for the proposed controller approaches. Some of the con-

Controller	Gain margin (abs)	Phase margin (deg)
integrator	0.36	29.0
H_∞ with $z_\infty = z_1$	1.05	1.76
H_∞ with $z_\infty = z_2$	7.25	63.89
H_2/H_∞ with $z_\infty = z_1$	4.08	36.69
H_2/H_∞ with $z_\infty = z_2$	0.26	26.9
PID	0.027	42.2
H_2	4.42	27.6

Table 5.1: Stability margins for fragility characterization

trollers, such as the H_∞ with respect to $\Delta\theta$, have very low margins which does not leave much space for variations. Often, this characterization is forgotten because of the immediate composition of the whole system. This information about the internal connection is lost then. Thus, the sensibility of the obtained controllers towards their own parameter changes has to be taken care of.

Tesis publicada con autorización del autor
No olvide citar esta tesis

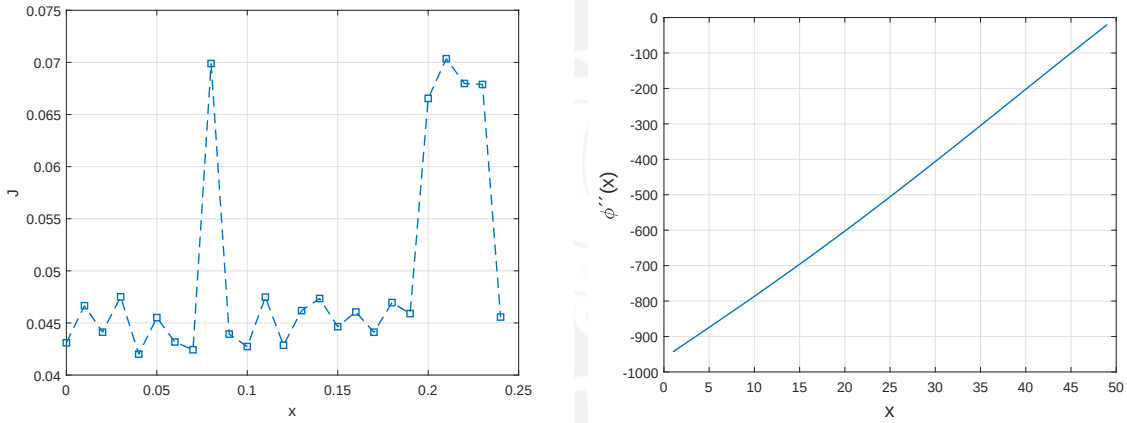

(a) Spatial optimization sampling (b) Weighting coefficient $\phi''(p)$

Figure 5.13: Indicators for optimization of sensor location

Tesis publicada con autorización del autor
No olvide citar esta tesis

6 Conclusion

This work deals with the multi-objective controller synthesis the distributed parameter system of a flexible robot arm. The control design is based on LMI characterizations, which can be converted to an SDP and solved by convex optimization techniques. The article [METH96] served as a reference example for robust control of such an elastic structure.
In order to realize an appropriate design method, the work contains of an extensive part on theoretical background. This includes the basic nomenclature and theorems of robust control, the characterization of internal stability and nominal performance, a catalog of LMI conditions and the basic idea behind them. An extensive derivation documentation on the mathematical modeling of the flexible robot arm is given. The profound theoretical basis is complemented by simulations and the validation of the flexible arm experiment. No real measurement data was available.
At the end, the control design methods are applied to the system structure and its defined performance specifications. The obtained controllers are compared between each other, as well as to some benchmark controllers.

6.1 Contribution & discussion

The field of robust control is one of the most extensively documented in control theory. This work provides an useful collection of fundamental background on the formulation and solution of robust design problems. It serves as a comprehensive introduction to the area without requiring a lot of knowledge on the topic in beforehand. The material collection and explanation forms a core work in this thesis.
Based on the common theoretical part, one of the modern directions in robust control is introduced in detail. The LMI based optimization approach for solving multi-objective control problems offers many opportunities and degrees of freedom to tune the controller more precisely. A further advantage of this method are the availability of efficient numerical methods for solving the convex optimization programs. However, this procedure introduces conservatism to the problem, which may result in unsophis-

Tesis publicada con autorización del autor
No olvide citar esta tesis

ticated performances. Another issue is the numerical conditioning of the obtained solutions. It remains a matter of investigation, how to apply this method to practical tasks.

Exemplary for the class of infinite dimensional systems, an one-link slewing robot arm forms the focus of this work. The derivation of an adequate system model include the application of the Hamilton principle, as well as a simplification for small deformations and a modal analysis. It is demonstrated that the constrained mode method does not serve for the purposes of this investigation, but that the unconstrained approach delivers reasonable results to be worked with. Although the infinite eigenfrequencies play an important role for the system behavior, it can be seen that an approximation with including one mode, is sufficient for describing the main system behavior. That is why such a model is used for the control synthesis. The model can be extended in several ways. Here, the undamped model used exclusively, because it is predestined for investigations on the severe effects of elasticity and vibrations.

In the last chapter, all this preliminary work is put together to design an appropriate controller for the flexible arm. For the realization, a software framework is created, that is able of performing the presented design steps for arbitrary systems. This is combined with the output of the modal analysis algorithm and the obtained eigenfunctions. In the resulting control evaluation a compromise between the several control objectives of reference tracking, good control performance, disturbance compensation and robustness has to be made. The proposed mixed H_2/H_∞ controllers demonstrate the extremes between vibration rejection and the suppression of external perturbations. It is shown that an extra measurement using a strain gauge does not improve the performance noticeably.

In total, this thesis forms a comprehensive literature study on robust control techniques and typical modeling process for flexible structures and infinite dimensional systems. It requires the implementation of a program framework that includes the flexible formulation and solution of mixed-objective robust control problems as an SDP on the one side. On the other side, the approximative simulation of an infinite dimensional system with the use of an automatic procedure is realized. A comparison with common sources is made for reproducing their results.

Throughout this work, many ideas and possible procedures have been proposed. The passivity control approach could not be realized due to the unfeasibility of the related optimization problem. Nevertheless, the combination between passive and robust techniques seems promising for flexible structures. Neither could the nominal regulation be realized, which utilizes the internal model principle. This appeared because of the

Tesis publicada con autorización del autor
No olvide citar esta tesis

lack of detectability of the reference.

6.2 Further work

After setting up many so many directions to go, this work can only be understood as a starting point for further application related investigations. The most important step would be to complete the robustness considerations. Including robust performance for structured uncertainties into the design algorithm, can be large extension of the control framework. Approaches like [Sch00], published beside other useful ideas in [EN00a], lead to useful LMI conditions on robust H_2 performance. The extension of the proposed uncertainty modeling relates directly to the infinite dimensional structure and could deliver an alternative approach towards classical PDE control.
For checking the validity of the results not just by reason, an experiment with a real robot arm is recommended. This is also due to the lack of presented results in the considered literature. Additionally, numerical considerations regarding sensitive algorithms utilized have to be continued. This affects the modal analysis, as well as the convex programming.
A prior intention of this thesis was the comparison of structured robust control approaches to common methods for distributed systems. There is an interesting work from [JZ12], which deals with infinite dimensional systems in a port-hamiltonian context. This relates again to the idea of using passivation control and its connection to robust design [BL07].
Beside all these open questions, the controller tuning can be continued. Especially including weighting filters could improve the current results. One has to beware of obtaining too many degrees of freedom, as they may leave the task confusing and unstructured. Another interesting remaining task, is the verification of the designed controllers, based on a low order model, to a higher order system, which could not be covered here.

Tesis publicada con autorización del autor
No olvide citar esta tesis

Bibliography

[ALJB10] Abreu, G.L.C.M. de ; Lopes Jr., V. ; Brennan, M.J.: Mixed H_2/H_∞ control of a two-floors building model using the linear matrix inequality approach. In: *ABCM Symposium Series in Mechatronics* 4 (2010), S. 198–207

[Bed85] Bedford, A.: *Research notes in mathematics*. Bd. 139: *Hamilton's principle in continuum mechanics*. Pitman Advanced Publishing Program, 1985

[BL07] Bao, Jie ; Lee, Peter L.: *Process control: The passive systems approach*. Springer, 2007 (Advances in industrial control)

[BO88] Barbieri, Enrique ; Özgüner, Ümit: Unconstrained and Constrained Mode Expansions for a Flexible Slewing Link. In: *Journal of Dynamic Systems, Measurement, and Control* 110 (1988), S. 416–421

[Boy94] Boyd, Stephen P.: *SIAM studies in applied mathematics*. Bd. vol. 15: *Linear matrix inequalities in system and control theory*. Society for Industrial and Applied Mathematics (SIAM 3600 Market Street Floor 6 Philadelphia PA 19104), 1994

[BS91] Berman, Abraham ; Shasha, Dafna: Inertia-Preserving Matrices. In: *SIAM Journal on Matrix Analysis and Applications* 12 (1991), Nr. 2, S. 209–219

[BV09] Boyd, Stephen ; Vandenberghe, Lieven: *Convex optimization*. 7. printing with corrections. Cambridge Univ. Press, 2009

[CVX12] CVX Research Inc.: *CVX: Matlab Software for Disciplined Convex Programming*. 2012. – `http://cvxr.com/cvx/`, visited 17.04.2017

[Det01] Dettori, Marco: *LMI techniques for control with application to a Compact Disc player mechanism*, Technische Universiteit Delft, Diss., 2001

Tesis publicada con autorización del autor
No olvide citar esta tesis

[DL15] De Luca, Alessandro: Flexible Robots. In: *Encyclopedia of Systems and Control*. 2015

[DP05] Dullerud, Geir E. ; Paganini, Fernando: *Texts in applied mathematic*. Bd. 36: *A course in robust control theory: A convex approach*. 2., corr. printing. Springer, 2005

[DZGB94] Doyle, J. ; Zhou, K. ; Glover, K. ; Bodenheimer, B.: Mixed H_2 and H_∞ performance objectives. II. Optimal control. In: *IEEE Transactions on Automatic Control* 39 (1994), Nr. 8, S. 1575–1587

[EN00a] El Ghaoui, Laurent (Hrsg.) ; Niculescu, Silviu-Iulian (Hrsg.): *Advances in design and control*. Bd. 2: *Advances in linear matrix inequality methods in control*. Society for Industrial and Applied Mathematics, 2000

[EN00b] El Ghaoui, Laurent ; Niculescu, Silviu-Iulian: Robust Decision Problems in Engineering: A Linear Matrix Inequality Approach. In: El Ghaoui, Laurent (Hrsg.) ; Niculescu, Silviu-Iulian (Hrsg.): *Advances in Linear Matrix Inequality Methods in Control*. Society for Industrial and Applied Mathematics, 2000, Kapitel 1, S. 3–37

[Fra76] Francis, Bruce A.: The linear multivariable regulator problem. In: *1976 IEEE Conference on Decision and Control including the 15th Symposium on Adaptive Processes*, 1976, S. 873–878

[JZ12] Jacob, Birgit ; Zwart, Hans J.: *Operator theory Linear operators & linear systems*. Bd. 223: *Linear Port-Hamiltonian systems on infinite-dimensional spaces*. Birkhäuser, 2012

[Kan90] Kanoh, Hideaki: Distributed Parameter Models of Flexible Robot Arms. In: *Avanced Robotics* 5 (1990), S. 87–99

[KB97] Keel, L. H. ; Bhattacharyya, S. P.: Robust, fragile, or optimal? In: *IEEE Transactions on Automatic Control* 42 (1997), Nr. 8, S. 1098–1105

[Kha02] Khalil, Hassan K.: *Nonlinear systems*. 3. ed. Prentice Hall, 2002

[KTLK86] Kanoh, H. ; Tzafestas, S. ; Lee, Ho G. ; Kalat, J.: Modelling and control of flexible robot arms. In: *1986 25th IEEE Conference on Decision and Control*, 1986, S. 1866–1870

Tesis publicada con autorización del autor
No olvide citar esta tesis

[METH96] Moran, A. M. ; Estiko, R. ; Tanaka, K. ; Hayase, M.: H_∞ Control of Flexible Arm Considering Motor Dynamics and Optimum Sensor Location. In: *Fourth international workshop on advanced motion control (IEEE - SICE)* (1996), S. 669–674

[Meu13] Meurer, Thomas: *Control of Higher-Dimensional PDEs: Flatness and Backstepping Designs*. Springer, 2013

[Meu16] Meurer, Thomas: *Regelung verteilt-parametrischer Systeme*. Skriptum zur Vorlesung an der Christian-Albrechts-Universität zu Kiel, 2016

[PRCF05] Payo, I. ; Ramos, F. ; Cortazar, O. D. ; Feliu, V.: Experimental Validation of Nonlinear Dynamic Models for Single-Link Very Flexible Arms. In: *Proceedings of the 44th IEEE Conference on Decision and Control*, 2005, S. 5304–5309

[Rai10] Raisch, Jörg: *Mehrgrössenregelung im Frequenzbereich*. Lecture Slides from TU Berlin, 2010

[Rod90] Rodriguez, Armando A.: *Control of infinite dimensional systems using finite dimensional techniques: a systematic approach*, Massachusetts Institute of Technology, Diss., 1990

[Rot93] Rotea, Mario A.: The generalized H_2 control problem. In: *Automatica (Journal of IFAC)* 29 (1993), S. 373–385

[SC96] Sooraksa, P. ; Chen, Guanrong: Mathematical modeling of a flexible robot arm. In: *IEEE International Conference on Control Applications*, 1996, S. 960–964

[Sch90] Scherer, Carsten: *The Riccati Inequality and State-Space H_∞-Optimal Control*, Universität Würzburg, Diss., 1990

[Sch00] Scherer, Carsten W.: Robust H_2 Control. In: El Ghaoui, Laurent (Hrsg.) ; Niculescu, Silviu-Iulian (Hrsg.): *Robust Mixed Control and Linear Parameter-Varying Control with Full Block Scalings*. Society for Industrial and Applied Mathematics, 2000, Kapitel 10, S. 187–207

[Sch01] Scherer, Carsten: *Theory of Robust Control*. Lecture Slides from Delft University of Technology, 2001

Tesis publicada con autorización del autor
No olvide citar esta tesis

[SGC97] Scherer, C. ; Gahinet, P. ; Chilali, M.: Multiobjective output-feedback control via LMI optimization. In: *IEEE Transactions on Automatic Control* 42 (1997), Nr. 7, S. 896–911

[SP01] Skogestad, Sigurd ; Postlethwaite, Ian: *Multivariable feedback control: Analysis and design*. Reprinted. Wiley, 2001

[SPS98] Sánchez-Peña, Ricardo S. ; Sznaier, Mario: *Robust systems theory and applications*. Wiley, 1998

[van96] van der Schaft, Arjan: *L 2-gain and passivity techniques in nonlinear control*. Bd. 218. Springer, 1996

[VB00] VanAntwerp, Jeremy G. ; Braatz, Richard D.: A tutorial on linear and bilinear matrix inequalities. In: *Journal of Process Control* 10 (2000), S. 363–385

[vDL86] van den Bossche, E. ; Dugard, L. ; Landau, I. D.: Modelling and Identification of a Flexible Arm. In: *American Control Conference*, 1986, S. 1611–1616

[Ver09] Verhoeven, S. L. H.: *Robust Control of Flexible Motion Systems: A Literature Study*. DCT Report at Dynamics and Control Technology Group, Eindhoven University of Technology, 2009

[WB00] Wu, Shao-Po ; Boyd, Stephen: sdpsol: A Parser/Solver for Semidefinite Programs with Matrix Structure. In: El Ghaoui, Laurent (Hrsg.) ; Niculescu, Silviu-Iulian (Hrsg.): *Advances in Linear Matrix Inequality Methods in Control*. Society for Industrial and Applied Mathematics, 2000, Kapitel 4, S. 79–91

[YHF00] Yang, Kyle Y. ; Hall, Steven R. ; Feron, Eric: Robust H_2 Control. In: El Ghaoui, Laurent (Hrsg.) ; Niculescu, Silviu-Iulian (Hrsg.): *Advances in Linear Matrix Inequality Methods in Control*. Society for Industrial and Applied Mathematics, 2000, Kapitel 8, S. 155–174

[Yos08] Yoshihiko, Miyasato: Model reference adaptive H_∞ control for flexible arms by finite dimensional controllers. In: *2008 47th IEEE Conference on Decision and Control*, 2008, S. 3257–3262

Tesis publicada con autorización del autor
No olvide citar esta tesis

[YYE15] Yuki, Imanishi ; Yasushi, Kami ; Eitaku, Nobuyama: An exterior-point approach to the mixed H_2/H_∞ control problem. In: *54th IEEE Conference on Decision and Control*, 2015, S. 1978–1982

[ZD98] Zhou, Kemin ; Doyle, John C.: *Essentials of robust control*. Prentice Hall, 1998

[ZDG96] Zhou, Kemin ; Doyle, John C. ; Glover, Keith: *Robust and optimal control*. Prentice Hall, 1996

[ZGBD94] Zhou, Kemin ; Glover, K. ; Bodenheimer, B. ; Doyle, J.: Mixed H_2 and H_∞ performance objectives. I. Robust performance analysis. In: *IEEE Transactions on Automatic Control* 39 (1994), Nr. 8, S. 1564–1574

Tesis publicada con autorización del autor
No olvide citar esta tesis

List of Figures

2.1 General system interconnections [ZD98] 7
2.2 Basic system structure with plant and controller 10
2.3 System structures with uncertainty 12
2.4 Standard feedback control loop 12
2.5 Mixed-sensitivity control loop and signal definition 13
2.6 Equivalent series interconnection of two systems 15
2.7 Parallel interconnection of two systems 16
2.8 Nonlinear system decomposition [DP05] 19
2.9 Control loop for stability considerations [Sch01] 24
2.10 General system $N(s)$ with separated uncertainty structure $\Delta(s)$ 38
2.11 Magnitude comparison of experimental plant $H(s)$ and system model $G(s)$ 40
2.12 Magnitude plots for uncertainty distribution 40
2.13 Closed loop interconnections with additive uncertainty 41
2.14 Closed loop system robust analysis for additive uncertainty 43
2.15 Closed loop interconnections with input multiplicative uncertainty . . . 46
2.16 Region of destabilizing parameters (contoured) 47
2.17 Inverse additive uncertainty structure from parametric uncertainties . . 50
2.18 Closed control loop structure with uncertainty $\Delta(s)$ 56

3.1 Mixed H_2/H_∞ system setup 63

4.1 Structural scheme of one-link flexible arm with virtual displacement . . 83
4.2 Flexible robot arm sketch for modal analysis 91
4.3 Transcendental roots in constrained mode 93
4.4 Eigenfunction examples $\phi_i(x)$ for constrained mode 93
4.5 Mode solution examples $q_i(t)$ for constrained mode 95
4.6 Resulting bending deformation $w(x,t)$ in constrained mode 96
4.7 Eigenfunction examples for unconstrained mode method 99
4.8 Mode solution examples $q_i(t)$ for unconstrained mode 100
4.9 Resulting bending deformation $w(x,t)$ in unconstrained mode 101

Tesis publicada con autorización del autor
No olvide citar esta tesis

4.10 Constrained mode results for real system parameters 103
4.11 Unconstrained mode eigenfunction constellations for real parameters . . 104
4.12 Unconstrained mode eigenmodes for real parameters 105
4.13 Bending deformation $w(x,t)$ for unconstrained mode with real parameters 106
4.14 Flexible arm structure in unconstrained mode after excitation 107
4.15 Eigenmodes for different acceleration scenarios 107
4.16 Flexible arm structure after constant torque applied smoothly 108
4.17 Excitation by non-zero initial state z_0 108
4.18 Deformation evolution in resonance cases 109
4.19 Parameter variation effect of E on mode $q_1(t)$ 109

5.1 Block diagram with high-frequency uncertainties 119
5.2 Magnitude plot of uncertainties without damping 120
5.3 Magnitude plot of uncertainties with damping considered ($\zeta_i = 0.5$) . . 121
5.4 Control system setup with filters 122
5.5 Software scheme for control synthesis 125
5.6 Impact of integrator inclusion 126
5.7 Evaluate H_∞ control performance with $z_\infty = \Delta\theta$ 127
5.8 Comparing H_∞ objectives with common $\gamma = 20$ 128
5.9 Performance of mixed H_2/H_∞ controllers with different objectives . . . 129
5.10 PID and H_2 comparison controller results 130
5.11 Tracking error comparison of multi-objective and test controllers 131
5.12 Performance change due to measurement extension 132
5.13 Indicators for optimization of sensor location 133

Tesis publicada con autorización del autor
No olvide citar esta tesis

List of Tables

2.1 Signal transmission and induced norms 27

4.1 System parameters for slewing arm model 84
4.2 Possible boundary configurations 91
4.3 Eigenfrequencies ω_i of real flexible arm (unconstrained mode) 104

5.1 Stability margins for fragility characterization 132

Tesis publicada con autorización del autor
No olvide citar esta tesis

Announcement

I, Matti Noack, hereby declare that this master thesis presented here is to the best of my knowledge and belief original and the result of my own investigations, unless otherwise acknowledged.

Formulations and ideas taken from other sources are cited as such.

This work has not been published and submitted, either in part or whole, for a degree at this or any other University.

Ilmenau, 03. 05. 2017 Matti Noack

Tesis publicada con autorización del autor
No olvide citar esta tesis